JOURNAL OF APPLIED PHYSICS

Vol. 30, No. 1 JANUARY, 1959

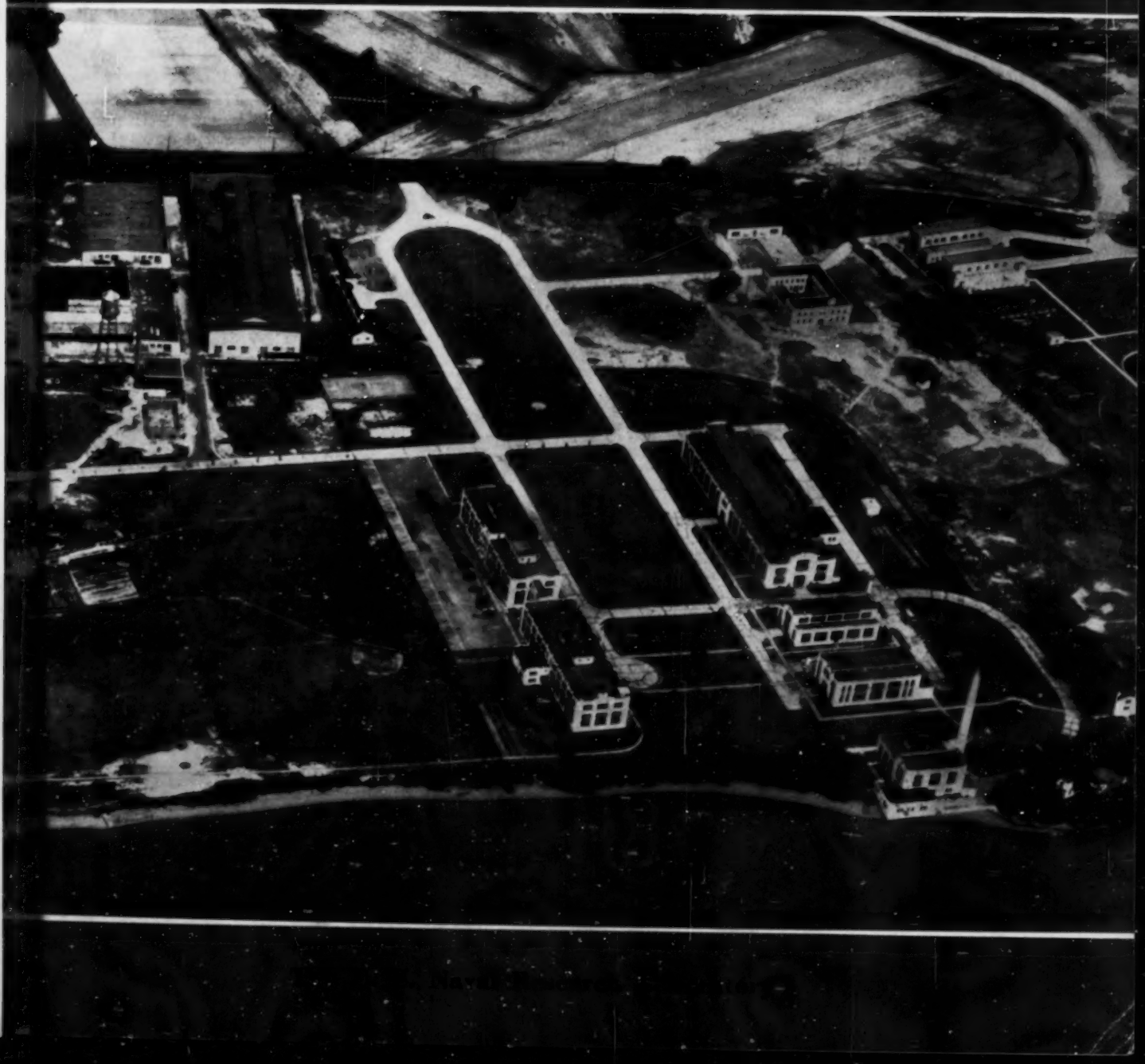

JOURNAL OF APPLIED

PHYSICS

JANUARY, 1939 Vol. 10, No. 1

In This Issue

		Page
Pure Physics Begets Applied Physics		3
U. S. Naval Research Laboratory	Ross Gunn	4
Resumés of Recent Research		11
Nobel Prize Goes to Enrico Fermi	S. A. Goudsmit	14

Contributed Original Research

Fine Grain Photographic Development	George Higgins	18
Letter to the Editor	Wm. Vaidya	26
Resonance Curve Method for the Absolute Measurement of Impedance at Frequencies of the Order 300 mc/Second	R. A. Chipman	27
On the Resonant Frequency of Closed Concentric Lines	W. W. Hansen	38
Studies in Lubrication. III. The Theory of the Thick Film Lubrication of a Complete Journal Bearing of Finite Length with Arbitrary Positions of the Lubricant Source	M. Muskat and F. Morgan	46
Structural Characteristics of Certain Silver Films	Sanford F. Essig	61
Electrical and Luminescent Properties of Phosphors Under Electron Bombardment	Wayne B. Nottingham	73
X-Ray Study of Menthol	S. S. Sidhu	83

In Every Issue

Here and There	16
Among Our Authors	17
Innovations in Instruments	vi
Advertising Index	xii

BOARD OF EDITORS

Elmer Hutchisson,
Editor

Associate Editors

R. M. Bozorth
D. W. Bronk
W. P. Davey
O. S. Duffendack
Saul Dushman
A. Stuart Hunter
C. H. Kunsman
J. T. Littleton
L. L. Nettleton
W. B. Nottingham
A. R. Olpin
John T. Tate

Publication of the American Institute of Physics

ADMINISTRATIVE STAFF

Henry A. Barton,
Director

Madeline M. Mitchell,
Publications Manager

William C. Copp,
Advertising Manager

GOVERNING BOARD

John T. Tate, *Chairman*
Karl T. Compton
E. C. Crittenden
Wheeler P. Davey
Homer L. Dodge
Harvey Fletcher
Arthur C. Hardy
Vern O. Knudsen
Melvin Mooney
Frederic Palmer, Jr.
R. L. Peek, Jr.
George B. Pegram
W. B. Rayton
F. K. Richtmyer
Wallace Waterfall

The Journal of Applied Physics, published monthly at Prince and Lemon Sts., Lancaster, Pa., is devoted to physics in its role as the science basic to other natural sciences and to the arts and industries. Previous to 1937 this publication was known as Physics. It aims to be of service not only in physical laboratories, but also in the laboratories of industrial, chemical, geological, geophysical, meteorological, radio, and similar concerns. The Journal of Applied Physics publishes editorials, news of physicists and reviews, as well as technical papers of applied physics.

SUBSCRIPTION PRICE

	U. S., Poss. and Canada	Foreign
To members of scientific societies	$5.00	$5.70
To all others	7.00	7.70

Manuscripts should be submitted to Elmer Hutchisson, Editor, University of Pittsburgh, Pittsburgh, Pennsylvania.

Changes of address, proofs, and complaints of failure to receive the Journal of Applied Physics should be addressed to the Publications Manager. New copies can be sent free only if notice of nondelivery is received within three months of date of issue.

Subscriptions and orders for back numbers should be addressed to Prince and Lemon Streets, Lancaster, Pa. or to the American Institute of Physics, 175 Fifth Avenue, New York, N. Y.

Advertising rates supplied on request. Orders, advertising copy and cuts should be sent to the American Institute of Physics.

Entered as second class matter at the Post Office at Lancaster, Pennsylvania, under the Act of March 3, 1897. Accepted for mailing at the special rate of postage provided for in the Act of February 28, 1925, authorized May 2, 1932.

Copyright 1939, by the American Institute of Physics.

50 v1
no.1-31
83

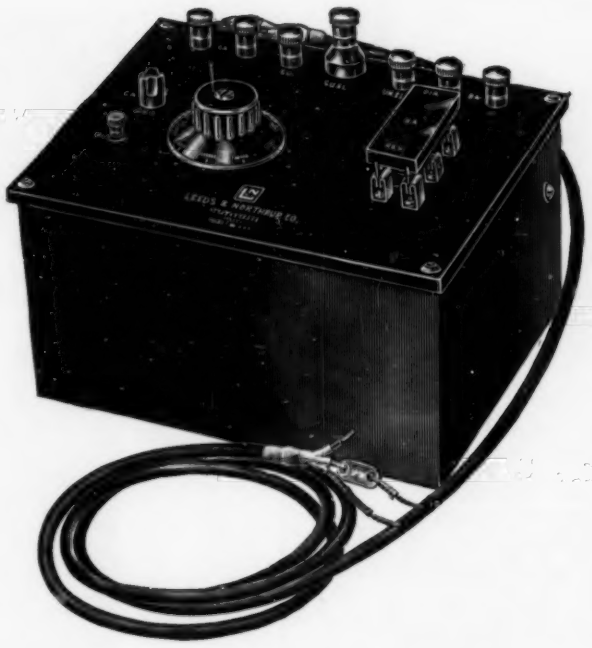

INSULATION-RESISTANCE TEST SET

GUARDED . . . FOR ACCURACY BY THE DIRECT-DEFLECTION METHOD

Entirely free from the effects of leakage currents, this Guarded Insulation-Resistance Test Set makes possible accurate insulation-resistance determinations with speed and convenience. It conforms to ASTM D257 Standard Methods of Test for Insulation Resistance of Electrical Insulating Materials.

All leakage currents are shunted around the galvanometer leaving only the current through the insulating material to cause the deflection. It is unnecessary to take any precautions to prevent leakage except to connect the guard circuits properly. It is even possible to measure with the test specimen in another room. Humidity has no effect except upon the dielectric under observation. The operator is protected from the high voltages used.

Battery and galvanometer reversing switches, calibrating resistors, Ayrton shunt and guard circuit are contained in the small, compact instrument case. A galvanometer with guard plate, a reading device and a battery complete the assembly.

Switches are designed to simplify operation and minimize calculation. Calibration of the galvanometer deflections is facilitated by the specially designed Ayrton shunt. Simply turning the shunt to a calibrating position automatically connects the circuit for calibration.

Write for Catalog E-54(1)

LEEDS & NORTHRUP COMPANY, 4978 STENTON AVE., PHILA., PA.

LEEDS & NORTHRUP

MEASURING INSTRUMENTS · TELEMETERS · AUTOMATIC CONTROLS · HEAT-TREATING FURNACES

Jrl Ad E-54-460(3)

LIGHT *without* GLARE

Polaroid* Illumination is the application to lighting of a scientific principle. It gives two advantages not obtained with ordinary illumination.

1. **Light without glare.** Polaroid Lighting provides glare-free illumination for all kinds of work and insures clear, effortless vision and minimum eye fatigue. All glare is gone —view is precise and easy—eye strain and fatigue are relieved.

2. **Sharp contrast—true color definition.** Ordinary lighting dilutes color values and makes black ink look grey or shiny. Polaroid Lighting creates sharp contrasts making black stand out clearly against white and colors appear in their full value.

Glare hurts your eyes.
Polaroid ends glare.

POLAROID DESK LAMP

More than merely a lamp—it is actually a scientific instrument for better vision.

PRICE COMPLETE . . . $16.50

Other Polaroid* Items

Polarizing Microscope Attachment
Photoelastic Polariscope
Polarizing Projection Apparatus
Polaroid Film

Order direct from

POLARIZING INSTRUMENT CO.

632 Fifth Avenue **New York City**

** T. M. Reg. U. S. Pat. Off. by Polaroid Corp.*

EPPLEY STANDARD CELLS

for students' use

A CADMIUM STANDARD CELL FOR POTENTIOMETRIC DETERMINATIONS

The new style molded bakelite case presents definite advantages in both protection and appearance over the old style support.

For students' use, where protection from accidental current drains is desired, we offer this cell with a 10,000 ohm protective series resistance. This unit is of particular value when setting up experimental circuits.

Cat. No. 102R Standard Cell, Eppley, Students' Type. Voltage approximately 1.018 volt at average room temperatures. Guaranteed accurate to ± 0.1%. With 10,000 ohms protective series resistance $14.00

Cat. No. 102 Standard Cell, Eppley, Students' Type. Same as above but without protective series resistance $12.00

Write for descriptive folder.

EPLAB

THE EPPLEY LABORATORY, INC.

SCIENTIFIC INSTRUMENTS

NEWPORT, R.I.

U.S.A.

IRC

Initiative — Resolcefulness — Cooperation to advance the interests of the industry

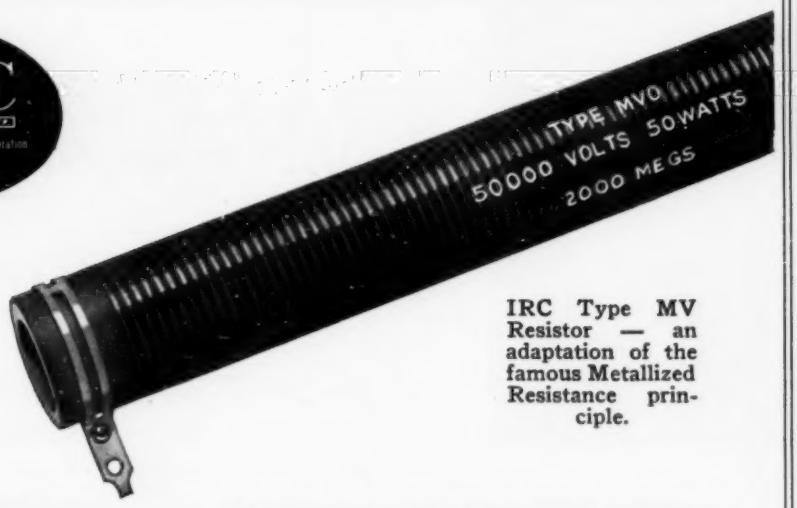

IRC Type MV Resistor — an adaptation of the famous Metallized Resistance principle.

RESISTORS FOR HIGH VOLTAGE

PROTECTIVE AND MEASURING DEVICES

IRC Type MV Resistors with the famous Metallized type resistance element in a unique spiral formation and incorporating the following characteristics are now available for high voltage uses:

Type	Power Rating	Max. D.C. Voltage Rating	Length	Diameter	Minimum Ohms	Maximum Ohms
MVG	4 W.	5,000	2″	9/16″	6,000 ohms	150 Meg.
MVP	10 W.	10,000	4 1/2″	3/4″	20,000 ohms	500 Meg.
MVA	25 W.	25,000	6 1/2″	1 1/8″	55,000 ohms	1,400 Meg.
MVO	50 W.	50,000	10 1/2″	1 1/8″	.1 Meg.	2,500 Meg.
MVR	150 W.	100,000	18 1/2″	2″	.35 Meg.	10,000 Meg.

TOLERANCE

±15% Standard ±5% and 10% available at extra cost.

TERMINALS

Lugs or ferrules are available as well as colloidal silver ends for the application of special terminals.

IRC Type MV High Voltage Resistors will stand as high as 50% voltage overload without breakdown. Resistance values maintained to ± 5% in general applications. If mounted in ceresin wax, this change may be decreased to as low as ± 2%.

Temperature Coefficient .02%/°C. to .05%/°C.

Complete descriptive catalog available upon request. IRC Resistance Engineers will gladly cooperate on problems requiring standard or special units for continuous or surge applications.

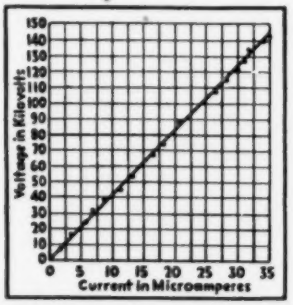

Calibration curve for two 2,000-megohm, 50-kv. resistors connected in series for measurement of voltages up to 150 kv. Type MVO

INTERNATIONAL RESISTANCE COMPANY

419 North Broad St., Philadelphia, Penna.

Contributions to the Mechanics of Solids

A VOLUME OF 29 ARTICLES BY MEN OUTSTANDING IN THE FIELD OF APPLIED MECHANICS, PUBLISHED IN HONOR OF THE SIXTIETH BIRTHDAY OF STEPHEN TIMOSHENKO

This volume, published primarily to do honor to a man whose work on the theory of elasticity, problems of stress analysis and vibration, and other aspects of applied mechanics is world famous, itself contains much interesting and valuable material on current problems in this field. Among the many distinguished *Contributions* are, for example: the article by Ludwig Prandtl dealing with a mechanical explanation of the phenomenon of hysteresis of plasticity in metals, von Karman's article on the application of the method of orthogonal functions to various problems in structural mechanics, G. I. Taylor's discussion of stresses and strains in certain crystals, and the article on certain characteristics of stress distribution in a plane field by von Mises. $5.00.

PROBLEMS IN MECHANICS

By G. B. Karelitz, J. Ormondroyd, and J. M. Garrelts

This new book contains nearly 800 problems on the application of the principles and theorems of mechanics to practical engineering. The famous collection of problems by I. V. Mestchersky is the basis of this book, but these original problems have been transposed to suit American practice and supplemented by a great many new problems. The problems are outstanding for their practical value and for the comprehensive range of topics they cover. They can be used with any textbook on mechanics. *To be published in the early spring.* $3.90 (probable).

MACMILLAN • NEW YORK

Please mention this journal when writing to advertisers

Journal of Applied Physics

Volume 10 January, 1939 Number 1

Pure Physics Begets Applied Physics

THE history of science is replete with examples of seemingly useless researches which after a few years have led directly to some of man's most useful tools. The simple experiments which Hittorf, Crookes, Hertz, J. J. Thomson and others performed with glass tubes, electrodes and magnets were scoffed at as "playthings" by the same type of man who today listens 'round the world with his radio, who has an x-ray photograph taken to locate broken bones or who clamors impatiently for better television. The discovery and separation of a heavy isotope of hydrogen is noted by an inch of type on the last page of our newspapers and yet within a decade the possibility of tracing the path of a food or a drug to any part of the body or the use of the nuclei of these newly isolated atoms to produce artificial radioactive compounds may help to save the life of the editor who whittled down the news item because of its small interest to the public. Even the neutron, the child of that so-called most useless field of research, *nuclear physics*, seems to be coming into its own as a possible cure for cancer.

These examples seem commonplace to a physicist. He knows that research in pure physics begets research in applied physics and yet he takes little part in efforts to stir up more public interest in this type of research. Is it not his duty to "shout from the house tops" the value of pure science? Perhaps by concerted effort on the part of those who really understand the benefits accruing to mankind from such research, a small part of those enormous sums which are spent for everything from tooth paste to battleships may be diverted toward pure science.

To make this suggestion a little more definite let us consider the usual auspices under which pure research is carried out. Outstanding are (1) private laboratories operating under some form of philanthropic endowment, (2) industrial research laboratories, (3) university laboratories and (4) governmental agencies. Little need be said about those laboratories included in the first category. Let us hope for more of them. Industrial laboratories are, of course, operated primarily for the profit of their parent companies and gradually the companies are learning that it is for their own good to establish pure research divisions in their laboratories. Much can be done to encourage more research in universities but the place above all others to expect research in pure science is in the governmental laboratories. How can society stand by and watch research on electrons, deuterons and neutrons become so important to everyone without lifting a single finger to see that its public servants include at least a small amount in the federal and state budgets for research in pure science? Probably all that is lacking is effective leadership. Surely, the physicist will try to help supply this need.

The U. S. Naval Research Laboratory

By Ross Gunn

Naval Research Laboratory, Washington, D. C.

THE Naval Research Laboratory, located on the Potomac River, in Washington, was established to meet the technical and scientific necessities of the Navy as emphasized by the lessons of the World War. As early as 1910 Thomas A. Edison recognized the necessity for a research organization within the Navy and, assisted by the active support of the Naval Consulting Board, he succeeded in interesting the Secretary of the Navy in the project. As a result of their recommendations, Congress appropriated money in 1916 to establish an experimental and research laboratory, "for laboratory and research work on the subject of gun erosion, torpedo motive power, the gyroscope, submarine guns, protection against submarine, torpedo and mine attack, improvement in submarine attachments, improvement and development in submarine engines, storage batteries and propulsion, airplanes and aircraft, improvement in radio installations and such other necessary work for the benefit of the Government service, including the construction, equipment and operation of a laboratory, the employment of scientific civilian assistants as may become necessary . . . ," *Naval Appropriation Bill 1916 H.R. 15947*. Although some of the above-enumerated functions are now prosecuted in specialized laboratories under the cognizance of various Naval bureaus, much of the purely scientific work is carried on at the Naval Research Laboratory. The formal opening of the Research Laboratory was delayed until July 2, 1923, because of the unusual situations arising from the World War.

The established mission of the Laboratory is, "To increase the safety, reliability, and efficiency of the Fleet by the application of scientific research and laboratory experimentation to naval problems." It is the policy of the Laboratory to undertake only those problems which have a direct value to the Navy and which are sponsored by some interested Naval bureau. Because the operation of a modern man-of-war draws on the experience of almost every branch of human endeavor, a variety of scientific problems is undertaken. Some of the problems are completely supported by an interested Naval bureau, others only partially supported and still others, often of the more forward-looking type, are supported by a direct Congressional appropriation for such purposes. This latter appropriation also covers the maintenance of the plant, provision of service

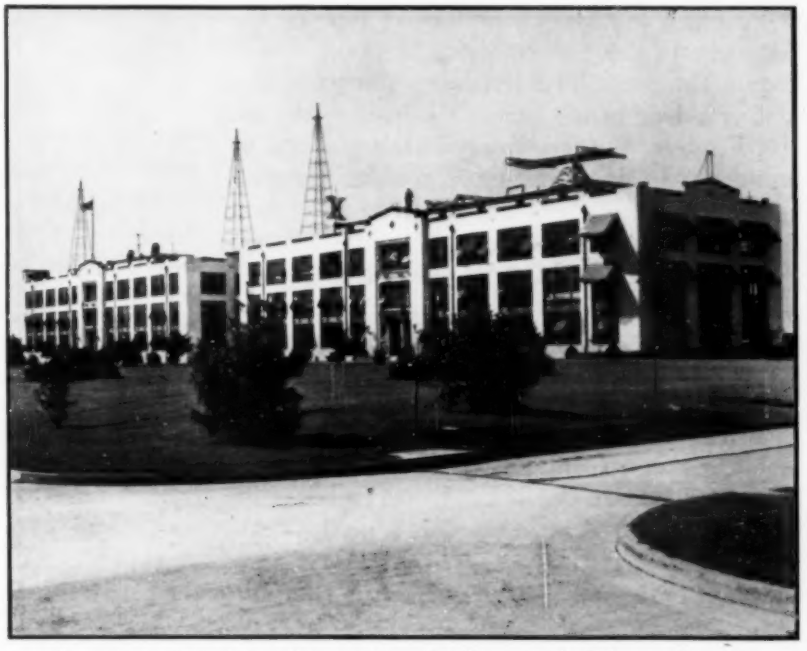

Fig. 1. The U. S. Naval Research main laboratory building and annex.

facilities, and part of the labor charges. The Laboratory undertakes problems for any Naval activity, but investigations for the Bureaus of Engineering, Aeronautics, Ordnance and Construction and Repair absorb most of its effort.

To maintain the close contact with the Navy necessary to carry out the mission, and to make the fruits of research immediately available for use in the Fleet, it has been found advisable to place administrative control of the Laboratory under the Chief of the Bureau of Engineering. A Naval officer of the rank of Captain and designated as the Director is directly attached to and in command of the Laboratory. The Director is the administrative head of the Laboratory and carries out the broad policies set by the Chief of the Bureau of Engineering, and is directly responsible to him in administrative and financial matters. The Director is assisted by an Assistant Director of the rank of Commander, by two administrative officer assistants of the rank of Lieutenant Commander, by a shop manager, and by a supply officer. From time to time officers with highly specialized training are assigned to the Laboratory for temporary duty. A civilian scientist with a wide experience in scientific and

FIG. 2. Vacuum tube test section.

engineering problems reports directly to the Director and serves as the Technical Adviser. The Naval Officer personnel changes every two to four years, and carries back to the Fleet a definite experience with the scientific method and its latest Naval developments. In a similar way the replacement officers coming direct from the Fleet bring to the Laboratory the immediate problems of the service afloat.

FIG. 3. A corner of the glassblower's room.

The scientific organization is permanent and founded on the policy that the research scientists shall have full authority and responsibility for the accomplishment of their work. Once a problem is considered by the administration and put in a concrete and specific form it is assigned to the research staff. Thereafter the administration avoids interference with the program for solution and in no case attempts to direct the research. In the interest of good administration, the scientific work of the Laboratory is assigned in accordance with the special talents of the scientists of each division.

Research divisions, each having a competent scientist as a superintendent, have been established in radio, sound, mechanics and electricity, metallurgy and thermodynamics, chemistry, and physical optics. An interior communication division carries on development tests of shipboard equipment. The divisions are subdivided into sections and each of these deals with some definite type of scientific problem. The scientific work is coordinated by the division superintendents and by the technical adviser.

The present staff of 96 scientists, engineers and research workers, including more than 20 with doctors degrees, is supported by an administrative, clerical and drafting force of 36, and by 93 men working in the shops. The principal officials

of the Laboratory as now constituted are:

Administrative Staff

Director	Captain H. M. Cooley, USN
Assistant Director	Commander L. K. Swenson, USN
Technical Adviser	Dr. Ross Gunn
Officer Assistant	Lt. Comdr. E. H. Pierce, USN
Officer Assistant	Lt. Comdr. A. F. Junker, USN
Shop Manager	Lieut. H. F. Miller, USN
Supply Officer	Lt. Comdr. G. W. Bauernschmidt, (SC) USN

Scientific Staff

Superintendent, Radio Division	Dr. A. Hoyt Taylor
Superintendent, Sound Division	Dr. Harvey C. Hayes
Superintendent, Mechanics and Electricity Division	Dr. Ross Gunn
Superintendent, Physical Optics Division	Dr. E. O. Hulburt
Superintendent, Chemistry Division	Dr. Parry Borgstrom
Superintendent, Metallurgy and Thermodynamics Division	Dr. R. H. Canfield
Interior Communication Division	Mr. W. B. Roberts

The superintendents are supported by a carefully selected body of scientists, engineers and technicians, well equipped by education and temperament to carry forward successfully difficult and involved physical and chemical investigations. As in the case of most active laboratories, there are more problems pressing for solution than there are men to solve them, so that many of the investigators are given more responsibility and opportunity for independent research than is called for by their rating and salary.

The plant of the Naval Research Laboratory is well adapted to carry on almost any type of scientific investigation. The Laboratory is located on tidewater of the Potomac River and is provided with a pier which can accommodate small vessels with a draft of 18 feet or less. There are now eight major and seven minor permanent buildings of harmonious external appearance specially designed to meet definite requirements. The total floor area available in these buildings exceeds $2\frac{1}{2}$ acres.

The main laboratory building and annex, having a total floor area of 72,000 square feet, house the administrative offices, drafting room, dispensary, and most of the purely scientific activities. The shop facilities for sheet and machine metal working are consolidated in another large building which also houses the high voltage power distribution system. One of the interesting major pieces of equipment located in the main shop building is a large temperature-controlled room about 14 ft. by 14 ft. by 9 ft., in which the temperature can be varied from $+50°C$ to $-30°C$, while almost any relative humidity is maintained and the pressure varied down to less than one-half an atmosphere, corresponding to an altitude of 25,000 feet. The refrigerating plant is adequate to care for a power dissipation within the room of five kilowatts under the above conditions. This room is used for the simulation of shipboard, submarine or aircraft conditions within the Laboratory and has been of value for the test of many types of apparatus.

A radio transmitter building is equipped with complete facilities for determining the performance under simulated service conditions of each new type of radio transmitter supplied to the Navy. Complete testing equipment for all sizes and types of vacuum tubes also is provided.

An experimental steel casting foundry is maintained by the Division of Metallurgy and is provided with a large electric arc furnace which will melt 2200 pounds of steel, with two large induction furnaces of capacity 300 and 125 pounds and with the usual auxiliary equipment necessary to handle the metal and automatically to record data. A separate small shop building is provided for wood working and for the elaborate testing equipment necessary to the conduct of the work in the Interior Communication Division. A special one-story laboratory building for the Chemistry Division is located in one corner of the grounds where chemical problems involving exceptional fire and explosion hazards may be undertaken. A powerhouse supplies heat and emergency electric power.

An enclosed rifle range, 100 yards long, and an explosion pit in which one may carry on dangerous experiments, complete the principal outside structures.

The scientific equipment in the Laboratory available to carry on Naval investigations is probably exceptional. In order to keep most of the investigations on a quantitative basis and

thus to orient the course of future development, adequate measuring equipment of all types is provided. In a great many cases, it has been necessary to supplement the measuring equipment available on the open market with specially developed devices or by entirely new methods. For example, the cathode-ray wattmeter method for the measurement of radiofrequency power was developed as the first step in a study of radiating antenna systems.[1] Similarly, a portable electrometer[2] operating on an entirely new principle was developed in 1929 to measure the electrostatic field around the *USS Los Angeles* as a part of a study of the electrical hazards of aircraft, and underwater sound standardization equipment using an absolute method[3] was devised in order that the performance specifications of naval sound equipment might be put on a quantitative basis.

Much of the work carried on by the Laboratory is, of necessity, secret or confidential and of definite importance to national defense. It is, therefore, quite impossible to give a complete description of the scientific work carried on, or even to indicate the trend of some of the more forward-looking investigations. However, certain technical papers have been released for publication, either because they are of little military value or because the resulting advancement of the art is considered more essential than the temporary advantage of secrecy. In considering the work of the Laboratory, it is convenient to discuss the activities in relation to the contributions of the several divisions, but one must not conclude that the value of a division to the Navy is measured by the achievements which can be recorded here. References to papers describing a few of the more basic contributions are included simply to illustrate the scope of the work undertaken.

The largest research unit is the Radio Division which was formed at the opening of the Laboratory from several research groups formerly attached to the Naval Air Station at Anacostia, D. C., the Bureau of Standards and the Washington Navy Yard. This division has been of inestimable value to the Navy in increasing the reliability and usefulness of radio communications in the Fleet. Much of the pioneer work in the development of high frequency radio equipment was carried on here.[4–6] Systematic studies were made of skip distances, propagation and directional radiation, including the direct measurement of transit times for round-the-world signals. The possibilities of the crystal controlled oscillator were early explored and applied to Naval transmitters[7] and to frequency standardization equipment.[8] This standardization equipment was immediately applied to the maintenance of assigned frequencies in the Fleet. Radio standardization work has been necessary because of the lack of other adequate sources of information on the performance of radio instruments at the highest frequencies.

The Sound Division carries on studies of the transmission of sound in water and the associated equipment necessary to generate and receive it. The Division developed the first successful acoustical device for measuring ocean depths from a ship underway by the use of echoes.[9] The standardization of the performance of underwater sound equipment by absolute measurement has been accomplished and has placed this type of investigation on a quantitative basis.[3] The Division undertakes to analyze the sounds or vibrations in a noisy compartment on a ship and to suggest methods for correcting the difficulty. A sonic method for locating imperfections in steel hull plating has been worked out[10] which may be of value in the inspection of metal objects of all kinds.

FIG. 4. High frequency wattmeter in use at the U. S. Naval Research Laboratory by J. D. Wallace.

The Mechanics and Electricity Division has

devoted attention to ordnance problems and to specialized electrical and electromechanical measuring devices and methods. As an example, the Division has recently completed the development of a simple but stable electrical micrometer for

FIG. 5. Dr. E. Klein using the apparatus for the measurement of absolute sound intensity in water in the U. S. Naval Research Laboratory.

the measurement of mechanical displacements of the order of a wave-length of blue light and larger.[11] This micrometer is being used in a strain gauge, torsion meter, vibration meter, and several other Naval devices. A fundamental study of the general problem of electric power production, storage and utilization has been carried on for some time.

The Physical Optics Division has carried on a program of investigation of the transmission and absorption of ultraviolet, visible and infra-red radiations by the atmosphere, haze and fog.[12] A similar program was completed for pure water and for sea water.[13] Fundamental research on the polarization of light at sea led to improved optical filters on sextants, binoculars and other optical instruments. The photoelastic section is occupied in studying the stresses in ship structures, with results which have influenced the improvement of ship construction. In cooperation with the Radio Division a theoretical analysis has been accomplished of the facts of radio wave propagation which is yielding considerable insight into the phenomena and the complex variations with latitude, magnetic disturbance and the sunspot cycle.[14] The spectroscopic section cooperates with the Chemistry Division in chemical analysis by means of ultraviolet, infra-red, and Raman spectroscopy.

The Division of Physical Metallurgy and Thermodynamics has carried on investigations on the properties of metals and methods for testing them nondestructively. The radiographic method of testing exceptionally thick sections of steel by the use of gamma-rays was developed by this Division and first applied to the inspection of Naval castings.[15] A new magnetic method of locating certain common types of imperfections in ships' hull plating has been devised,[16] and applied to full size plates for inspection purposes. A general investigation of the foundry practices employed in the production of steel castings has been underway for some years and has led to methods which insure a better grade of casting at reduced cost. This investigation included exhaustive studies of the strength and other mechanical properties of hot and cooling steel, the proper design of patterns, studies of molding sands, and several related problems.[17] Because the Navy is a large consumer of steel castings and operates several foundries, these investigations yield large returns.

The Chemistry Division carries on a large number of chemical investigations. Considerable work has been undertaken on the chemical and physical properties of fuel oils and gasolines.[18] Attention has been devoted to the study of the stability of gasoline in storage with the object of avoiding excessive corrosion of the storage tanks and the formation of gummy residues. The Division has cooperated in fundamental studies of submarine storage batteries, improved their operation, and developed auxiliary devices for use with them. The conditioning of air in a submarine is an important problem which has been extensively studied. A simple method for measuring the oxygen content of feed water in Naval boilers has been developed.

In addition to the scientific work actively

prosecuted in the various divisions, the Laboratory maintains a few Naval Research Fellowships at some of the leading universities. These fellowships are usually held by young men who have nearly competed the work for an advanced degree. They work directly under the supervision of competent professors on specific problems of Naval interest.

Perhaps the most valuable feature of the Naval Research Laboratory is that it serves as a reservoir of accumulated scientific and technical experience so coordinated with the known Naval requirements that this experience may immediately be applied to the problems of the Fleet. This function is widely employed within the Navy and the scientists and engineers devote considerable time to consultation.

It is considered to be the province and duty of the Research Laboratory to carry each development to the point where its reliability, simplicity and applicability to service requirements have been fully demonstrated. The Laboratory further attempts to adapt new equipment to the standard practices of the operating organization or, by actual service demonstration, convince them that the use of the new equipment will materially reduce their operating difficulties. With the object of carrying out these principles, the Laboratory cooperates closely with the Fleet and it is not uncommon for a small group of scientists from the Laboratory to spend a month at sea, collecting data, running final tests, or instructing the operating personnel of the Fleet in the use of new equipment. Occasionally a ship is assigned to the Laboratory for a period of weeks to collect scientific information necessary for the prosecution of the work. As a result of these frequent contacts, the naval scientist has some understanding of the difficulties of the operating force and they, in turn, learn something of the possibilities of scientific research and seem more inclined to accept new devices and methods.

A problem presented to the Naval Laboratory for solution or one suggested by a Laboratory scientist is carefully considered by the administration and with the cooperation and advice of the scientific staff, the problem is reduced to a concrete and specific form. The objectives are clearly indicated and the problem is examined with a view to determining if it is worth doing, if it is likely to be solved in a sufficiently simple form to be of value, and if adequate support in personnel and equipment is available. In the event that the answers to these questions are satisfactory, the problem is assigned to the scientific staff which assumes complete responsibility thereafter, unless for some reason satisfactory progress is not being made or support is withdrawn. In such cases the administration may reassign the problem to a new group or cancel it.

The scientist or group assigned to a project studies the background and application of the problem and attempts to reduce it to its simplest elements. The important thing in scientific research is to have an instinct for the essential. This is discovered, a proper perspective established and active work undertaken. The further processes by which the solutions to problems are achieved needs no rehearsal in these columns. However, in the final decision as to the solution best adapted to the Naval Service, the item of simplicity in operation and performance is con-

FIG. 6. Air view of the Naval Research Laboratory.

sidered to be of great importance. A library of over five thousand reference volumes subscribes to all the important periodicals of the world. These are reviewed and index cards made out for articles which have a possible bearing on naval problems. If the solution of a problem results in new apparatus, the Laboratory carries its development and test only to a point where guiding specifications can be accurately drawn up for its manufacture by private industry. Therefore, there is no competition with manufacturers and the Laboratory terminates its activity as soon as a satisfactory working model is developed which passes the service tests.

It is recognized in many quarters that a carefully considered program of scientific research, actively prosecuted in time of peace, is essential to national security. Moreover, since it is necessary to maintain secrecy in certain studies, and since the military importance of obtaining a solution in many cases far outweighs economic factors, it seems necessary to carry out such work in a laboratory controlled and supported by the Navy. The Naval Research Laboratory is organized to meet the scientific demands of the Service afloat.

Bibliography

1. A. Hoyt Taylor, "The Measurement of Radio Frequency Power," Proc. I.R.E. **24**, 1342 (1936).
2. R. Gunn, "Principles of a New Portable Electrometer," Phys. Rev. **40**, 307 (1932).
3. E. Klein, "Absolute Sound Intensity in Liquids by Spherical Torsion Pendula," J. Acous. Soc. Am. **9**, 312 (1938); **10**, 105 (1938).
4. A. Hoyt Taylor, Proc. I.R.E. **3**, 677 (1925); **14**, 521 (1926); **19**, 103 (1931).
5. A. Hoyt Taylor and E. O. Hulburt, Phys. Rev. **27**, 189 (1926).
6. A. Hoyt Taylor and L. C. Young, Proc. I.R.E. **16**, 561 (1928); **19**, 1491 (1929).
7. A. Crossley, Proc. I.R.E. **15**, 9 (1927).
8. R. B. Owens and R. H. Worrall, Proc. I.R.E. **16**, 778 (1928).
9. H. C. Hayes, J. Frank. Inst. **197**, 323 (1924).
10. H. C. Hayes, J. Opt. Soc. Am. **8**, 220 (1937).
11. W. C. Hall and R. Gunn, Phys. Rev. **51**, 1027 (A) (1937).
12. E. O. Hulburt, J. Opt. Soc. Am. **25**, 125 (1935).
13. E. O. Hulburt, J. Opt. Soc. Am. **22**, 408 (1932).
14. E. O. Hulburt, Rev. Mod. Phys. **9**, 44 (1937).
15. C. S. Barrett, R. F. Mehl and G. E. Doan, Am. Soc. Test. Mat. **18**, 1192 (1930).
16. R. H. Canfield, paper before Soc. Naval Arch. and Engr., May 17, 1938.
17. C. W. Briggs, Trans. Am. Found. Assoc. **45**, 385 (1937).
18. P. Borgstrom, R. D. Norton and O. I. Lewis, J. Am. Soc. Naval Eng. **46**, 173 (1934).

Resumés of Recent Research

Recent advances in experimental and theoretical physics are described in these columns in nontechnical language. It is intended that sufficient background be given to introduce the reader to the subject.

The Question of Superstructure in $FeNi_3$

In general, x-ray diffraction may be used to tell us both how atom sites in a crystal are arranged, and, if the crystal has more than one kind of atom, how the atoms are arranged on the sites. In a metallic alloy this is usually at random, but occasionally a more orderly arrangement is found, which gives rise to new lines in the x-ray diffraction pattern, and the alloy is then said to have a superstructure.

Resistivity and specific heat data on permalloy of compositions near $FeNi_3$ have indicated that this alloy might have such an ordered structure, but since iron and nickel are close neighbors in the periodic table, they reflect x-rays with nearly equal intensities, and the extra lines would ordinarily be too weak to detect. They may be strengthened by choosing a wave-length near the K critical absorption limit of iron, since the reflecting power of an element is less near its absorption limit. Combining this with the use of a curved rocksalt crystal to select and focus the proper wave-length, and with a focusing camera covering the range which includes the strongest superstructure lines to be expected, F. E. Haworth[1] has made an extended search for the lines in $FeNi_3$ and has failed to find any, although by the same technique he was able to detect superstructure in CuZn under conditions such that the intensity of the extra lines was only one-twenty-eighth that expected of the $FeNi_3$ lines. He thus concludes that no ordering exists in $FeNi_3$ unless it is of such short range that no x-ray effect is observable.

In a discussion of the other evidence available on this question he suggests that a comparison of the slopes of the resistivity *vs.* temperature curves for the annealed and cold worked or quenched materials may be used as an additional criterion for the presence or absence of superstructure, and shows that in the case of $FeNi_3$ it supports the conclusion drawn from the x-ray evidence, as does also the fact that the change in magnetic saturation at room temperature is negligible.

[1] F. E. Haworth, Phys. Rev. **54**, 693 (1938).

Forces between Ions in Solution

We are familiar with the fact that, because of the high temperature in the sun and stars most molecules are broken up into atoms, and most atoms are broken up into ions and electrons. Starting from room temperature, in a molecular gas or vapor any rise of temperature causes a progressively greater dissociation of the molecules. For molecules dissolved in a liquid, on the other hand, this is no longer true. For several substances which in aqueous solution are partially dissociated into ions, the dissociation is known to pass through a maximum value, and to decrease again; for each of these substances there is a characteristic temperature θ at which this maximum occurs. What properties of the molecule determine the value of θ for each species? This question, among others, is discussed in a paper by R. W. Gurney in the *Journal of Chemical Physics*[1] where it is shown that the determining factor is the relative magnitudes of the electrostatic and the non-electrostatic forces between the ions. When a molecule is split up into a positive ion and a negative ion, there is, of course, the ordinary electrostatic attraction between these charges of opposite sign. But in addition there are also chemical or exchange forces; when these are relatively large the temperature θ will be high, and when they are relatively small, the temperature θ will be low. It is shown that all the available data are consistent with this prediction.

[1] R. W. Gurney, J. Chem. Phys. **6**, 499 (1938).

Electron Microscope Studies of Thoriated Tungsten

The literature contains many cases where the electron microscope has been profitably applied to the study of surface phenomena that influence the electron emission. Recently[1] A. J. Ahearn and J. A. Becker at the Bell Telephone Laboratories used an electron microscope to study thoriated tungsten.

The electron image of thoriated tungsten shows considerable variation in emission between adjacent regions, i.e., the image is patchy. These patches have sizes and shapes which agree with those of the grains appearing on photomicrographs of the metal surface.

The process of activating these filaments consists essentially in accumulating thorium on the surface by diffusion from the interior. The electron microscope shows how the thorium comes to the surface and how it migrates over the surface. "Eruptions" occur at a relatively small number of points from which the thorium rushes to the surface. The electron images in Fig. 1 show the life history of typical thorium eruptions. These bright spots grow in size and brightness. Eventually as shown by picture *h* the entire filament becomes covered with thorium, i.e., it becomes activated. A careful analysis of the size and distribution of these eruptions together with an analysis of the size and distribution of thorium oxide globules in the tungsten shows that when an eruption occurs all of the thorium in the globule escapes to the surface.

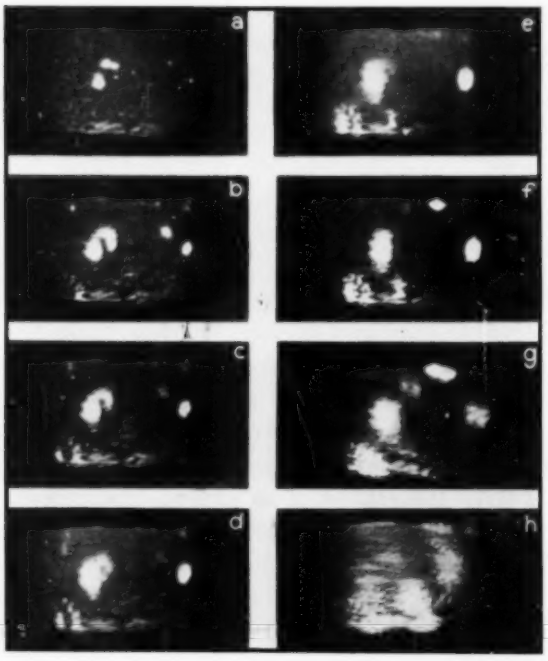

FIG. 1. Thorium eruptions on polycrystalline thoriated tungsten ribbon.

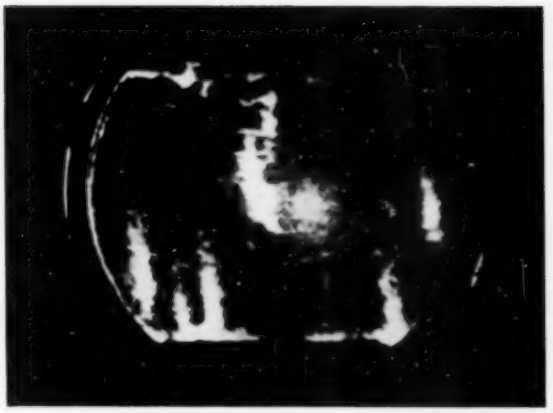

FIG. 2. Thorium eruptions and the migration of thorium in a preferred direction over the surface of a single crystal of thoriated tungsten.

The ribbon filament in Fig. 1 is polycrystalline. Here the growing eruption spots are circular in shape. This shows that the migration of thorium over the surface is isotropic. Fig. 2 shows some eruptions on a ribbon filament which consists of a single crystal. Here instead of circular spots we have a group of parallel bands. This shows that there is a strongly preferred direction of migration on the single crystal. X-ray analysis shows that this preferred direction of migration is along the (111) direction on a (211) surface. This is the direction in which the rows of surface atoms are spaced farthest apart.

Electronic Conduction in Insulating Crystals Under Very High Field Strength

The flow of electrons in metals follows Ohm's law, because their number is abundant and because they suffer friction proportional to their velocity. In insulators in general neither of these conditions is fulfilled. Conducting electrons are a foreign substance in these materials, which will be trapped if they move too slowly, and which can be accelerated to ionizing velocities, if the field strength applied is sufficiently high.[1] The latter situation can be

[1] A. J. Ahearn and J. A. Becker, Phys. Rev. **54**, 448 (1938).

studied by testing the breakdown strength of the material and observing the accompanying optical phenomena,[1] but additional information might be expected if the whole current-voltage characteristic up to the breakdown point could be measured. In a new paper[2] A. von Hippel has succeeded in doing this and by measuring the photoelectric response of his crystals also a consistent picture of the phenomena preceding breakdown has been gained.

The current rises steeply with voltage but remains surprisingly small (10^{-9} to 10^{-8}A). The breakdown comes as a sudden discontinuity not so much announced by the value of the preceding current as by its fluctuation. The current decreases in time and the photoelectric observation reveals that this is due to building up of space charges by electron trapping. The magnitude of the polarization can be measured by photoelectric observation. With the aid of an amplifier a statistical counting effect as in a Geiger counter is heard under illumination. In mica the amazing field strength of 10 million volts/cm has been reached!

The results indicate that the steep rise of the current-voltage characteristic is mainly due to field emission, and not to ionization processes. A more detailed discussion, making use of the lattice structure of the alkali-halides, is given. The probability of speeding up surplus electrons to ionizing velocities does not become appreciable before the breakdown point. Breakdown then starts immediately, because the large number of impacts across the crystal creates very large avalanches and a field distortion accelerating the process. At local inhomogeneities of the lattice short avalanches may be produced at lower voltages thus accounting for a part of the noise observed.

X-Ray Analysis of the Structure of Water From a Fourier analysis of the x-ray scattering curve of water, one obtains directly a radial distribution function giving the number of neighboring molecules to be found at any distance from a given water molecule. In terms of such a distribution function, with the origin always at the center of a molecule, a liquid shows a definite structure; the density of neighboring molecules being greater at certain distances and less at others. In the present study* distribution curves are obtained for five temperatures ranging from 1.5 to 83°C.

The distance from the center of any water molecule to the nearest neighboring molecules is found to be about 2.9A, increasing slightly with temperature. The number of nearest neighboring molecules is roughly 4. Thus water has a very open type structure, and differs markedly from simple liquids such as mercury and sodium, which have about 10 nearest neighbors and resemble a close packing of spheres. Because of its electronic configuration, the water molecule tends to bond itself tetrahedrally to 4 neighboring molecules. In the crystalline structure of ice, each water molecule is tetrahedrally bonded to 4 neighboring molecules and the x-ray results show that the same tendency persists to some extent in the liquid.

The intermolecular distance in water is 2.9A, slightly greater than 2.76A, the distance in ice. Since the volume of water is less than that of ice, it might at first sight seem anomalous that the intermolecular distance increases on melting. However, the density of a substance depends on both the intermolecular distances and the number of neighbors. The distribution curves show that in water there are neighbors at distances between the nearest and next nearest neighbors in the ice structure. This "filling in" gives an effectively greater number of neighbors, and produces an increase in density which more than compensates for the decrease due to larger intermolecular distances.

The x-ray results seem to indicate that in water the desire for tetrahedral bonding is only partially attained, and that at any instant a molecule will be bonded to less than 4 neighboring molecules. Water can be described as a broken-down ice structure. With rising temperature there is a progressive breaking down of the tetrahedral structure, and the resulting "filling in" effect produces an increase in density. At the same time the increase in intermolecular distance produces a decrease in density. The minimum volume of water at 4°C results from these two opposing effects.

[1] A. von Hippel, J. App. Phys. **8**, 815 (1937).
[2] A. von Hippel, Phys. Rev. **54**, 1098 (1938).

* J. Morgan and B. E. Warren, J. Chem. Phys. **6**, 666 (1938).

Nobel Prize Goes To Enrico Fermi

THE Nobel prize for physics has been awarded this year (1938) to Enrico Fermi. This fact did not surprise his colleagues. It was given to him primarily for the discoveries which he and his co-workers have made in their investigations with neutrons. Fermi has, however, made many other outstanding contributions to various fields of modern theoretical and experimental physics.

Fermi is 37 years old and received most of his education in Italy. There he obtained a solid foundation of classical physics and mathematics. He began his studies at Pisa, lectured at Florence for a few years and since 1926 has been Professor of Physics at the University of Rome, where, for the past few years, he has been working in an excellent new laboratory. He studied for some time at Göttingen and later visited Leyden. At that time Fermi had already completely mastered classical and modern physics, and while at Leyden impressed everyone with the clarity and simplicity of his discussions. At a student group meeting there, it was Fermi's turn to give a nonsense talk. Starting with the most general equation consisting of an equality sign with nothing written on either side of it, Fermi derived interesting formulae in such a convincing manner that Ehrenfest jokingly remarked that he would from then on refuse to believe any of Fermi's physics.

Extreme clarity and simplicity is characteristic of all of Fermi's work as well as his personal life. At Rome, he starts his work very early in the morning which, in itself, is sufficient proof that he is not merely a theoretician. Every afternoon he conducts a seminar with his colleagues and students during which everyone seems to take an active part in the lively discussions. A friendly spirit of cooperation is always present among those who have worked with him.

Fermi is interested in fields of science other than physics but he has no typical hobbies. His recreation consists of sports: he is an expert at tennis, swimming and skiing.

We cannot discuss Fermi's contributions to physics in every detail. His theoretical papers have one characteristic: he takes the laws known from one field of physics and applies them to another part in such a clear and logical manner that the result becomes almost obvious. An example of this type of reasoning is the so-called Fermi-Dirac statistics. When it was found that in an atom no two electrons can exist in the same quantum state, Fermi pointed out that the same rule might govern the motions of the molecules in a gas. This clarified to a great extent the application of quantum theory to statistical mechanics and it became of first rate importance in the treatment as a gas of the free electrons in a metal. Some time later, Fermi pointed out further that the electrons in a single atom, in turn, can also be treated as a gas. He and his co-workers succeeded in deriving many atomic properties by means of this statistical method. Another outstanding contribution is Fermi's theory of the beta-radioactivity. Here again, his program consisted of adapting the theory of radiation to the problem of emission of a beta-particle. According to Fermi's hypothesis, inside a nucleus a neutron can change itself into a proton and the energy gained in this process is emitted in the

form of an electron and a neutrino. It was his beautiful theoretical treatment of this process which quickly revived confidence in the existence of the mysterious neutrino that had been invented earlier by Pauli to explain discrepancies in the conservation of energy in beta-radioactivity. Although his beta-theory is as yet incomplete, it is nevertheless the most important advance in recent nuclear theory.

Fermi's experimental work also excels in its clarity and directness. One of his first experiments was that done with Rasetti dealing with the behavior of atoms in an alternating magnetic field. His recent experimental work, for which he obtained the Nobel prize, deals with neutrons. After the discovery of the neutron by Chadwick, Fermi understood at once that this new particle was the ideal projectile for producing nuclear reactions. Since it has no charge, it is not repelled by nuclei and even very slowly moving neutrons can come near enough to an atomic nucleus to produce an interaction. In fact, it was soon discovered by Fermi and his collaborators that, in many cases, the slower the neutrons the more effective was the reaction. By means of the bombardment of various elements with fast and slow neutrons they produced a large number of new isotopes, most of which are radioactive. An outstanding achievement was the discovery of two new elements which extended beyond the original limit of the periodic system.

In Italy, Fermi is recognized as the outstanding physicist of his country. He has been a member of the Academia d'Italia since its creation by Mussolini in March, 1929. He received honorary degrees from the Universities of Heidelberg and Utrecht. He has been a regular visitor to the United States, his first visit being on the invitation of the University of Michigan to lecture in the Symposium of Theoretical Physics in the summer of 1930. These symposium lectures have been repeated in several subsequent summers. He has also lectured at Stanford University and Columbia University. He enjoys his visits here very much. It was interesting to observe the rapidity with which he learned to lecture in English at the occasion of his first visit to the University of Michigan. In his lectures, he succeeds in making the most complicated problems appear exceedingly simple and students gain the impression that they can easily reproduce the mathematical derivations. The same is true when he describes complicated experimental apparatus.

We cannot conclude this description of Fermi's investigations without mentioning the interest with which Mrs. Fermi follows her husband's work. In addition to educating their two children, Nella and Giuglio, Laura Fermi found the time to cooperate with Ginestra Amaldi, the wife of one of Fermi's collaborators, in writing a delightful little popular book, *Alchimia Del Tempo Nostro* on the modern aspects of radioactivity, which should certainly be published in English.

S. A. Goudsmit
University of Michigan, Ann Arbor, Michigan

Here and There

Westinghouse Research Fellowships for 1939

The Westinghouse Electric and Manufacturing Company last year announced the establishment of ten post-doctorate fellowships for research in physics, including chemical physics, physical metallurgy, and applied mechanics. Five Fellows were appointed in 1938 and five additional appointments will be made in 1939. Fellows will devote their entire time and energies to work on their research project at the Westinghouse Research Laboratories in East Pittsburgh. It is expected that they will also participate actively in the seminars and colloquia held at the Laboratories and in the neighboring institutions of higher education. Appointments are made for a period of one year and Fellows are eligible for one reappointment for a like period. The salary will be paid semi-monthly at the rate of $2400 a year. The work of the Fellows will be carried on under the general supervision of Dr. E. U. Condon.

Application should be made on available forms and should be addressed to the office of the Manager, Technical Employment and Training Department, Union Bank Building, Pittsburgh, Pennsylvania. Applicants must be American citizens under the age of thirty-five, who have had scientific training equivalent to that represented by a Doctor's degree from a recognized university. Applications will be received at any time up to March 1, 1939, and formal announcement of awards will be made early in April, 1939. Tenure of the Fellowship may begin at any time thereafter except that all Fellows are expected to begin their work not later than October 1, 1939.

★

Recent Awards

The John Fritz Medal for 1939 has been awarded to Dr. Jewett for "vision and leadership in science and for notable achievement in the furtherance of industrial research and development in communication." This medal is awarded annually by a board composed of four representatives of each of four national engineering societies. Among previous recipients of the medal were Alexander Graham Bell, Thomas A. Edison, Guglielmo Marconi, John J. Carty and Michael I. Pupin.

Science reports that in accordance with the recommendations made to the King of England by the Council of the Royal Society, London, Royal Medals have been awarded to Dr. Francis William Aston, F.R.S., in recognition of his discovery of the isotopes of non-radioactive elements, and to Professor Ronald Aylmer Fisher, F.R.S., in recognition of his contributions to the theory and practice of statistical methods.

The following awards of medals have been made by the President and Council of the Royal Society, London: The Copley Medal to Professor Niels Bohr, For. Mem. R. S., in recognition of his distinguished work in theoretical physics and particularly in the development of the quantum theory of atomic structure. The Davy Medal to Professor G. Barger, F.R.S., in recognition of his distinguished researches on alkaloids and other natural products. The Darwin Medal to Professor F. O. Bower, F.R.S., in recognition of his work of acknowledged distinction in the field in which Darwin himself labored. The Hughes Medal, awarded jointly to Dr. J. D. Cockcroft and Dr. E. T. S Walton, in recognition of their discovery that nuclei could be disintegrated by artificially produced bombarding particles.

Dr. Robert W. Wood, who retired this year from the professorship of experimental physics at the Johns Hopkins University, has been awarded the Rumford Medal of the Royal Society in recognition of his work in physics and optics. Dr. Wood is a foreign member of the society. The Rumford Medal was founded by Benjamin Thompson Rumford, who died in 1814.

On November 4 at a joint meeting of the American Section of the Society of Chemical Industry and of the American Chemical Society, at the Chemists' Club, New York City, Dr. John Van Nostrand Dorr, president of the Dorr Company, Incorporated, was presented with the Medal of the Society of Chemical Industry. The medal is given for "valuable application of chemical research to industry," and was awarded to Dr. Dorr for his inventions that have permitted large-scale, low-cost operations in many chemical, metallurgical and sanitational operations.

A grant of $600 has been awarded to Dr. Frank J. Studer, of the department of physics at Union College, by the American Institute of Electrical Engineers for fundamental research on the physics of resistance welding.

World's Fair Plans

Professor Albert Einstein will be chairman of the Advisory Committee on Science of the New York World's Fair, which will cooperate in preparing a central exhibit of science. Other members of the committee are: Dr. Robert Chambers, of New York University, zoology; Dr. Karl T. Compton, president of Massachusetts Institute of Technology, physics; Gano Dunn, of J. G. White Engineering Corporation and president of Cooper Union, industrial research; Dr. Frank B. Jewett, vice president of the American Telephone and Telegraph Company, industry; Waldemar Kaempffert, *The New York Times*, the public; Paul B. Mann, Evander Childs High School, New York City, children's interests; Professor R. H. McKee, Columbia University, chemistry; Charles F. Roth, manager of the Grand Central Palace, New York City, industrial exposition technique; Professor Edmund W. Sinnott, Columbia University, botany, and Dr. Gerald Wendt, director of science at the fair, who will act as secretary to the committee.

Science, November 18, 1938

New Appointments and Promotions

Dr. H. S. W. Massey has been appointed from January 1, 1939, to the Goldsmid chair of mathematics tenable at University College, London. Since 1933 he has been lecturer in mathematical physics at Queen's University, Belfast.

Dr. John J. Livingood, who has been working in cooperation with Professor E. O. Lawrence, of the University of California, with the cyclotron, has been appointed instructor and tutor in physics at Harvard University.

Associate Professor P. Gerald Kruger has been made acting Head of the Department of Physics of the University of Illinois for the first semester. He takes the place of Professor F. W. Loomis who has leave of absence which he is spending in Europe.

★

Necrology

Dr. Edwin Herbert Hall, professor emeritus of physics at Harvard University, died on November 20 at the age of eighty-three years.

Among Our Authors

Sanford F. Essig, a native of Ohio and a graduate of Ashland College, received his M.S. degree in Physics at Ohio State University in 1929. The following year was spent there in graduate work and in 1930 he joined the RCA Victor Company where the next four years were spent under Zworykin in electronic research and development work. Since 1934 this same type of work has been continued while he has been associated with Philco Radio and Television Corporation.

George C. Higgins, who is now Professor of Physics at the Intermountain College of Billings Polytechnic Institute at Billings, Montana, received his B.S. from Iowa State College in 1934; was a Graduate Assistant there from 1934 to 1938 when he received his Ph.D. in Applied Physics.

Ross Gunn was born at Cleveland, Ohio, in 1897. He graduated in Electrical Engineering from the University of Michigan; was an instructor there and received an advanced degree in physics. He carried on pioneer work in aircraft radio at McCook Field in 1922–3. Becoming an instructor in physics at Yale University, he earned a Ph.D. in Physics in 1926. In 1927 he joined the Naval Research Laboratory as a research physicist. He is now Superintendent of the Mechanics and Electricity Division and Technical Adviser for the entire Laboratory.

George C. Higgins

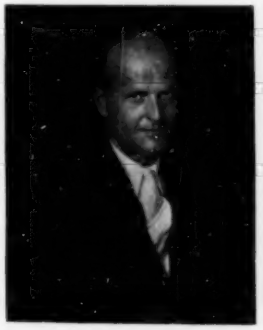

Ross Gunn

Sanford F. Essig

Contributed Original Research

Fine Grain Photographic Development

GEORGE HIGGINS
Department of Physics, Iowa State College, Ames, Iowa
(Received July 27, 1938)

The effect of different fine grain photographic developers upon the effective emulsion speed and graininess of photographic materials was studied quantitatively. Fine grain developers were found to be more effective in reducing the graininess of fast, coarse grain emulsions than of slow, fine grain emulsions. The effective emulsion speed of slow, fine grain emulsions when developed in an MQ borax developer was found to be at least equal to that of a fast, coarse grain emulsion when developed in an ultra-fine grain developer which gave negatives of as low graininess on the fast emulsion as the MQ borax gave on the slow emulsion. Slight improvement in graininess can be obtained by using ultra-fine grain developers on fine grain emulsions, but only at some sacrifice of effective emulsion speed.

I. INTRODUCTION

THE growing popularity of the miniature camera has brought the subject of fine grain development to the attention of many amateur and professional photographers with the result that numerous fine grain photographic developers have been produced. The claims made for these developers by the photographers who have devised them and by those who have used them have been very conflicting.

Fine grain photographic developers are used by photographers for the purpose of securing negatives which can be enlarged without the resulting positive print exhibiting an objectionable nonhomogeneity. This type of nonhomogeneity is called graininess in order to clearly distinguish it from the effect produced by the resolution of the individual silver grains. The graininess of the print is determined not only by the size of the individual silver grains in the negative but also by the distribution of these grains. Even with a coarse grain negative the individual grains are not visible at a magnification of ten diameters while an enlargement of ten diameters appears very mottled due to the grouping of several individual grains into clumps.

It is well known that the effective emulsion speed of a photographic film depends upon the developer used. Many of the fine grain developers in use at the present time require as much as two times the normal exposure to yield negatives of proper printing density, while some photographers report that other fine grain developers will give satisfactory negatives when the exposure given is one-half of that normally used.

A review of the literature indicates that:

1. There has been no uniformity in the methods of measuring graininess, and in some cases the investigators have failed to recognize the difference between grain size and graininess.
2. Investigations have been reported in which there has been insufficient control of density and gamma of the developed photographic material.
3. Graininess varies with the density and gamma of the developed photographic material.
4. Developers containing *p* phenylenediamine give less graininess than pyro and MQ developers but require that the negatives be given about double the normal exposure.
5. There is disagreement as to the results obtained when films are developed by Odell's system of physical development.
6. There is disagreement as to whether the type of developer is of greater importance on coarse or fine grain emulsions.
7. There is disagreement in regard to the effect of developers on emulsion speed.

The present investigation was undertaken to determine the effect of different fine grain photographic developers upon the graininess and effective emulsion speed of photographic material.

II. Apparatus and Method of Procedure

The film to be developed was placed in a specially designed camera and given a graded series of exposures. This camera was designed to expose 4 sq. cm of film directly to the light source at each exposure. The exposures formed a geometric progression having a ratio of two. A 40-watt 115-volt Mazda light bulb was used in conjunction with a 2-in. sq. No. 78 Wratten filter to furnish artificial daylight for the exposures. The voltage across this bulb was maintained at 110 volts by means of a resistance in series with a bank of storage batteries. The exposures were made by a rotating sector disk with a 36° opening. This sector disk was driven by a Telechron synchronous motor which made one revolution per sec.

The exposed film was then placed in a standard 35-mm Corex developing tank and developed in the solution to be tested. The film was agitated continuously during development by an electric motor driven agitator which made twelve complete oscillations of the developing reel per minute. The temperature of the developing solution was held constant to within ± 0.5°C. After development, all films were fixed in an acid-hardening fixing bath (Eastman F-5) and then washed in running water for one hour. A chrome alum-hardening stop bath was used in all cases where it was recommended by the manufacturer of the developer. All special instructions of the manufacturer as to temperature of development and method of washing were adhered to rigorously.

Next the optical density of each step on the developed and dried sensitometric strip was measured with a densitometer. The film was placed in direct contact with the ground surface of a photronic cell and then covered by a thin Bakelite plate in which a 5-mm hole had been drilled. A low resistance galvanometer was connected directly across this photronic cell to measure its output when the light from an automobile spot light illuminated it. The optical density ($\log_{10}$ (incident light/transmitted light) of each step was computed from the galvanometer deflections observed when light passed through the clear film and when the light passed through the silver deposit. Characteristic curves were then drawn for each developer by plotting optical density *versus* log of time of exposure (illumination was constant). The gamma and effective emulsion speed for each sensitometric strip was computed from the characteristic curve. Since the gamma to which a film has been developed is the tangent of the angle between the straight portion of the characteristic curve and the exposure axis, it could be measured directly from the curve. The effective speed of an emulsion when used with any developer was taken to be that exposure which is necessary to produce a given density at a given gamma. It is well known that the straight line portions of the characteristic curves for a given emulsion and developer all intersect at the same point regardless of the gamma to which the sensitometric strips have been developed. For most developers except those containing a bromide, this point of intersection is on the exposure axis. This means that the ratio between the effective emulsion speeds of a film, when developed in two different developers, is the ratio of the antilogs of the intercepts on the exposure axis of the straight line portions of their families of characteristic curves. The exposure necessary to produce a given density at a given gamma when the film was developed in Eastman DK 76 was arbitrarily taken as unity and the effective speed of any developer when used with a given film was computed by dividing the antilog of the intercept of the straight line portion of its family of curves for DK 76. Thus a developer with an effective

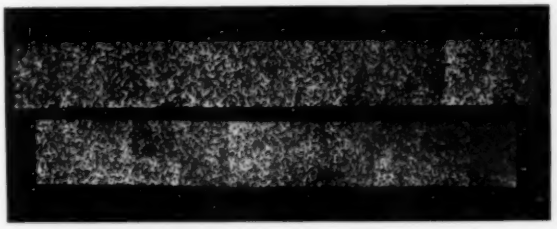

Fig. 1. Photomicrographs of developed supersensitive panchromatic film are arranged in order of graininess in the top row. Photomicrographs of developed Finopan film are arranged in order of graininess in the bottom row.

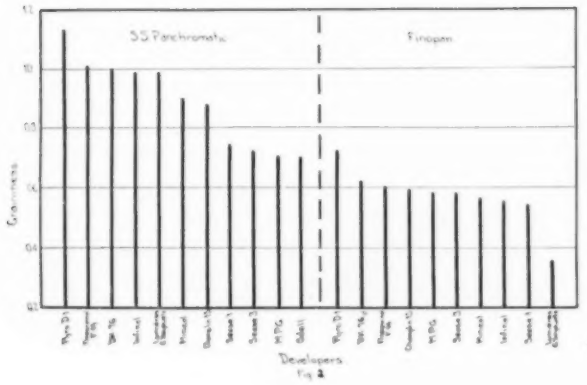

Fig 2

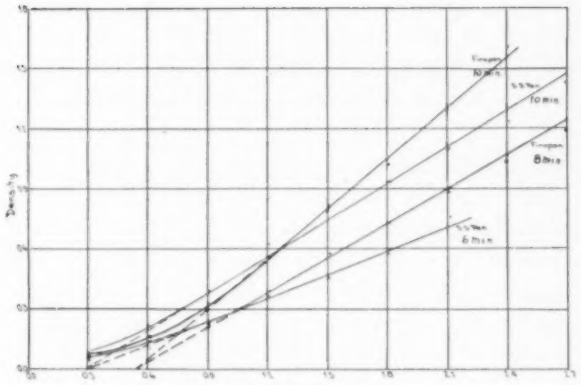

Fig 3 DK 76

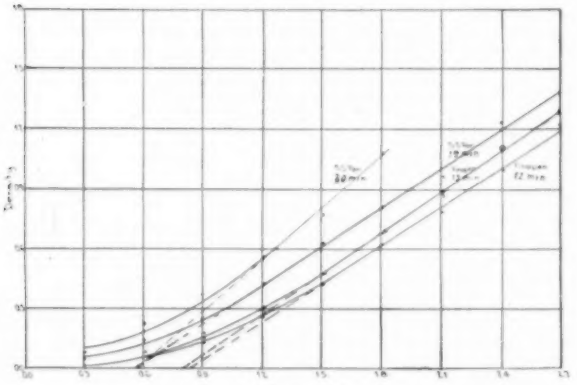

Fig 4 Champlin 15

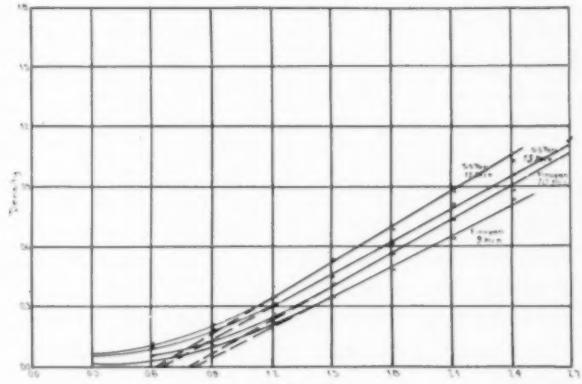

Fig 5 MPG

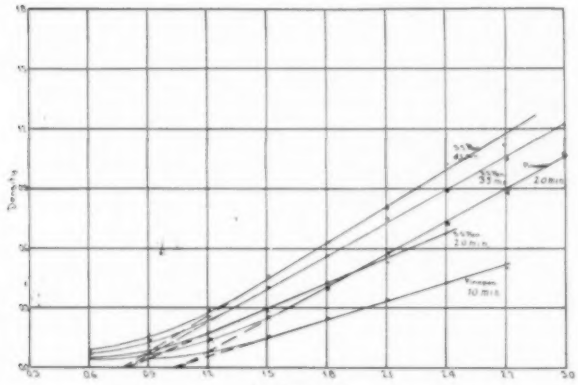

Fig 6 Seane 1

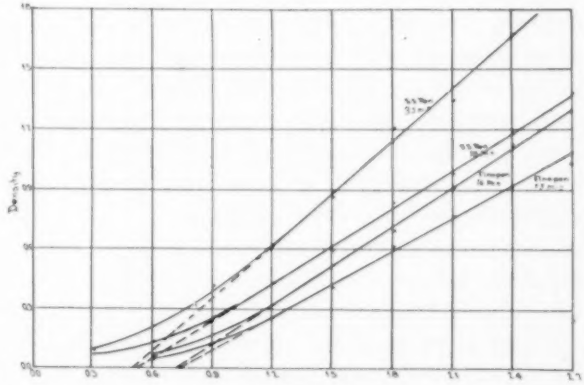

Fig 7 Seane 3

speed of two would require that a film developed in it be given twice the exposure given to a film developed in DK 76 if both developers were to produce the same density at the same gamma.

The graininess of the developed photographic materials was measured by observing the distance at which photomicrographs (Fig. 1) of the silver deposits appeared homogeneous. All photomicrographs used in a given study were mounted on the same support and viewed simultaneously. Each photomicrograph was taken at 600 diameters magnification and printed by projection on $8\times10''$ glossy paper so that there was a total magnification on the positive of 2400 diameters.

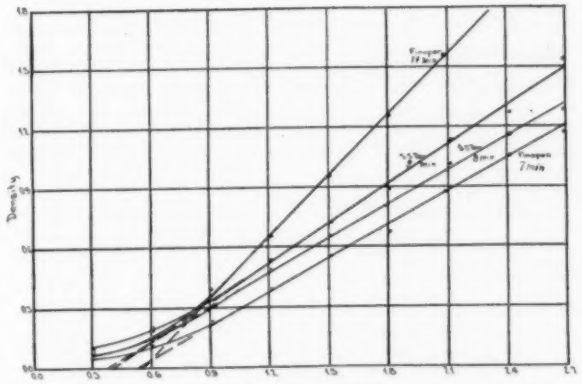

Fig 8 Fineprimol F14

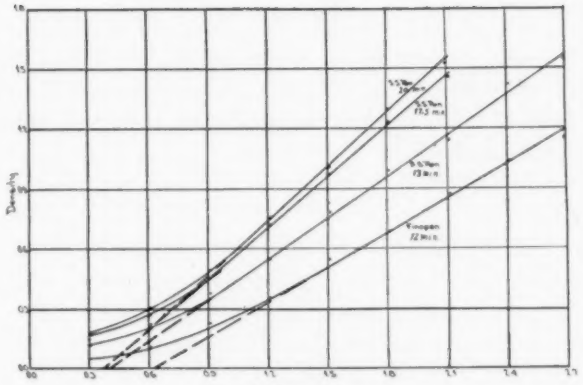

Fig 9. Mimicol

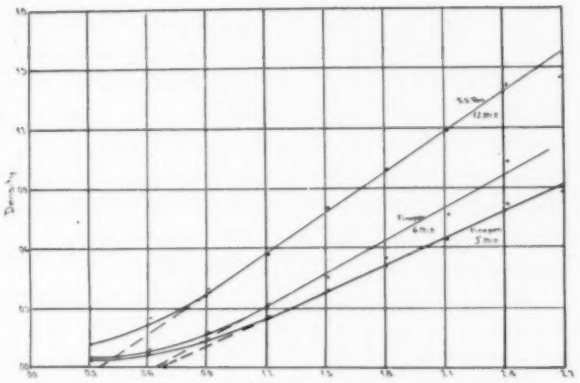

Fig 10. Infinol

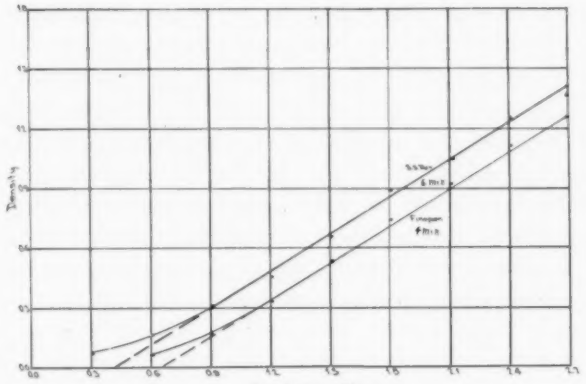

Fig 11. Pyro D1

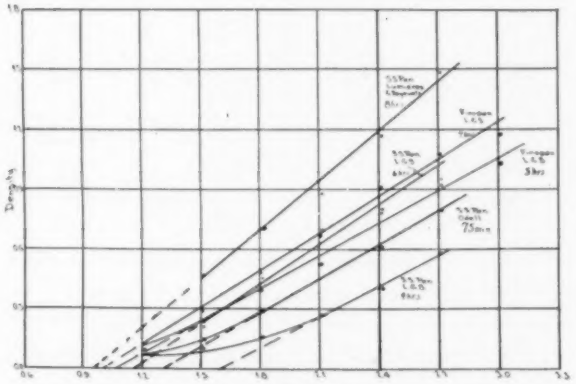

Fig 12 Physical

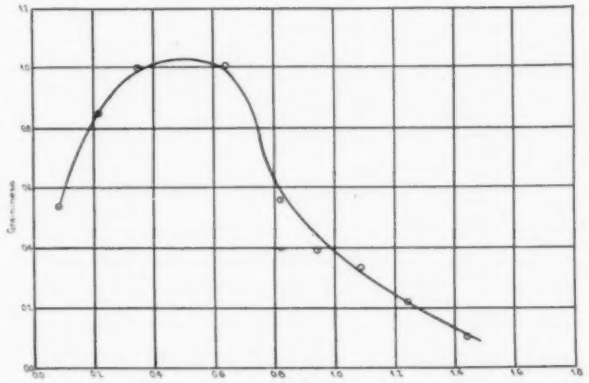

Fig 13 SS Panchromatic Developed In DK 76 To A Gamma Of 0.60

Care was taken to print all photomicrographs of samples of equal density so they appeared of the same density when viewed from beyond their merging distances. To eliminate the effect of the differences in visual acuity of observers, the graininess of Eastman supersensitive panchromatic film when developed in Eastman DK 76 to a gamma of 0.6 and a density of 0.4 was taken as a standard and the graininess of any photographic deposit was defined as the merging distance for the photomicrograph of this deposit divided by the merging distance for the photomicrograph of the standard. All measurements on graininess reported in this study are the mean

values of the results of twenty observations. Twelve observations were made by different observers and eight observations were made by four observers who repeated their observations on different days.

III. Results

One ordinary, one fine grain, and nine ultra-fine grain developing solutions were tested. The ultra-fine grain developers selected were Finegrainol F-14, Infinol, Minicol, Champlin No. 15, M.P.G., Sease's *p* phenylenediamene No. 1[14] Sease's *p* phenylenediamene-glycin No. 3[14] Odell's system of physical development,[15, 16] and the Lumieres and Seyewetz[17] system of physical development. The fine grain developer used was Eastman DK 76[4] and the ordinary developer used was Eastman D-1, pyro.[4] Infinol, Minicol, Champlin 15, and M.P.G. were purchased in liquid form ready to use, while DK 76 and Finegrainol F 14 were made up with distilled water from commercially prepared photographic powders. All other developers were prepared according to the instructions in the literature cited. These developers were used with Eastman supersensitive panchromatic 35-mm film which was taken as a representative high speed, coarse grain emulsion and with 35-mm Agfa Finopan which was taken as a representative slow speed, fine grain emulsion.

Since it has been shown that the graininess of a negative varies with density and gamma, the effect of the various developers upon graininess was studied by comparing the graininess of negatives of the same density and the same gamma. The effect of the various developers upon the graininess of Eastman Super-Sensitive panchromatic and Agfa Finopan film is shown in Tables I and II. The same data are represented graphically in Fig. 2. The speed of the developer, as recorded in these tables, was computed from the data shown in Figs. 3–12.

The results of a study on the variation of graininess with density are shown in Fig. 13. The graininess of each density was determined from the photomicrographs of each step on the sensitometric strip. (Fig. 14.) Each photomicrograph was made under identical conditions of

Table I. *Supersensitive panchromatic.**

Developer	Dev. Time	Gamma	Density	Speed	Graininess
Pyro D1	6 min.	0.63	0.483	1.32	1.13
Finegrainol F-14	9 min.	.64	.383	1.18	1.01
DK 76	10 min.	.61	.395	1.00	1.00
Infinol	12 min.	.66	.394	1.07	0.99
Lumieres and Seyewetz	6 hr.	.66	.434	7.59	0.99
Minicol	13 min.	.67	.376	1.23	0.90
Champlin No. 15	19 min.	.65	.423	1.78	0.88
Sease No. 1	45 min.	.60	.454	3.09	0.75
Sease No. 3	18 min.	.64	.424	1.62	0.73
M.P.G.	15 min.	.60	.348	2.24	0.71
Odell	75 min.	.58	.514	10.45	0.71

* All solutions were used at 18°C except Champlin No. 15 which was used at 20°C.

Table II. *Finopan.**

Developer	Dev. Time	Gamma	Density	Speed	Graininess
Pyro D1	4 min.	0.60	0.334	1.26	0.73
DK 76	8 min.	.58	.364	1.00	.63
Finegrainol F-14	7 min.	.56	.392	1.03	.61
Champlin No. 15	12 min.	.60	.417	1.86	.60
M.P.G.	10 min.	.58	.429	1.88	.59
Sease No. 3	13 min.	.56	.411	1.57	.59
Minicol	12 min.	.57	.362	1.26	.57
Infinol	6 min.	.57	.450	1.32	.56
Sease No. 1	20 min.	.56	.400	3.24	.55
Lumieres and Seyewetz	7 hr.	.60	.472	3.02	.36

* All solutions were used at 18°C except Champlin No. 15 which was used at 20°C.

exposure and development, both as regards to negatives and prints. These curves are in complete accord with those reported by Hardy and Jones.[6]

The graininess of negatives developed by the same developer to equal densities but different gammas is shown in Table III. These data indicate that graininess does increase with gamma as reported by Kreveld and Scheffer.[12]

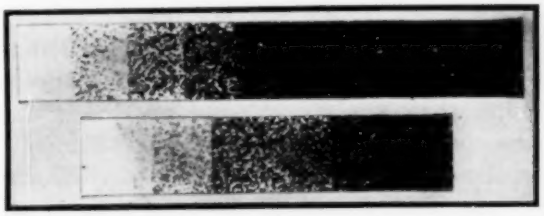

FIG. 14. Density *versus* graininess. Developer DK 76 used on the upper strip and Lumieres and Seyewetz on the lower.

A special study was made of Odell's method of physical development since the claims made for this developer have not been verified by other investigators. Odell[16] suggests that the variation in the results obtained with his system of development may be due to the condition of the hypo and sodium sulphite used in making the solutions and recommends that the *p*H be held between 9.20 and 9.30. The results of sensitometric strips developed under identical conditions of time and temperature but in solutions of different *p*H are shown in Fig. 15. Upon examination of the grains of negatives developed in the solution with a *p*H of 9.20, it was apparent that the silver grains were not deposited entirely by physical development since they were not spherical in shape. Physical development differs from chemical development in that the silver deposited by physical development is furnished by the developing solution while the silver deposited by chemical development comes from the silver halide of the emulsion. It is possible to develop a negative with

TABLE III. *Supersensitive panchromatic.*

DEVELOPER	DEV. TIME	DENSITY	GAMMA	GRAININESS
Lumieres and Seyewetz	4 hr.	0.411	0.52	0.71
Lumieres and Seyewetz	6 hr.	.454	.66	0.99
Lumieres and Seyewetz	8 hr.	.462	.83	1.08
DK 76	6 min.	.366	.40	0.77
DK 76	10 min.	.393	.61	1.00

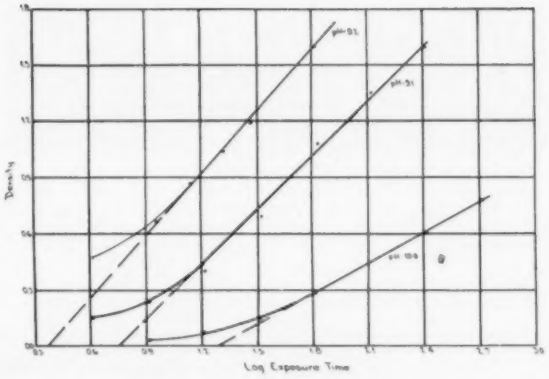

FIG. 15. Odell's solutions.

physical developing solutions after it has first been fixed in hypo to remove the possibility of any chemical development. Investigations of films developed after fixing indicate that the grains deposited by pure physical development are spherical in shape. Photomicrographs of negatives developed according to Odell's system of physical development, the Lumieres and Seyewetz system of true physical development in which the negatives are fixed before developing, and in Eastman DK 76, a chemical developer, are shown in Fig. 16. Odell's solutions were then made up without hypo or silver nitrate to prevent the possibility of any physical development. The results of sensitometric strips developed in these solutions under standard conditions in regard to time and temperature are shown in Fig. 17 together with the curves for Odell's solutions of *p*H 9.2 complete with forebath.

Odell reports[15] that, if films to be developed by his system of physical development are given a treatment in a KI forebath before developing, the time of development is shortened from two hours to one hour and the necessary exposure is reduced from five times normal to normal. The curves shown in Fig. 18 were obtained by developing identical sensitometric strips under the same conditions as regards temperature and time after first treating one strip with the KI forebath. These curves indicate that the forebath does shorten the developing time but does not increase the effective speed of the developer appreciably since the exposure necessary to produce the same density at the same gamma would be practically the same.

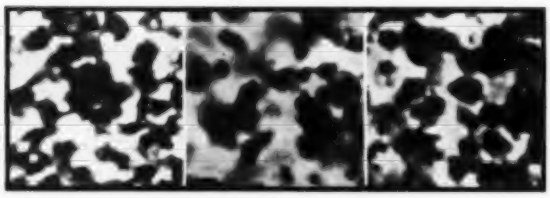

a b c

FIG. 16. Photomicrographs of developed negatives. (a) DK 76, (b) Odell, and (c) Lumieres and Seyewetz.

IV. DISCUSSION

The curves shown in Fig. 17 indicate that Odell's system of physical development is chiefly chemical development since the densities obtained in the regular development time when the silver nitrate and hypo were removed are equal to the densities obtained when they were present. However, it must be kept in mind that the amount of chemical development shown in these curves is reduced to some extent by the fact that the hypo removes some silver bromide before it can be developed chemically. The hypo was removed from the test solutions since some of the silver halide dissolved by it would be deposited as silver by the developing agent. Tests were made with solutions from which the silver nitrate alone had been removed and they indicated that, if the film was given the KI forebath before developing as recommended, very little silver halide was removed by the hypo in the developer. To check the amount of physical development, several films were fixed first and then developed in Odell's solutions, but with the exposures used on the other sensitometric strips the densities produced in the regular development time of one hour were too low to be determined accurately.

Odell's solutions used in the graininess measurements had a *p*H of 10.4 and, while these solutions produced a very low graininess, they were of no practical value since it was necessary that films developed in them be given eleven times normal exposure. The photomicrographs of a negative developed in the solution of *p*H 9.2 which is shown in Fig. 16 indicates that, while the proper *p*H does decrease the exposure required, it increases the graininess to the point where it is about equal to that produced by pyro. This is in agreement with the graininess reported by English.[5]

It is evident from Fig. 2 that even the best ultra-fine grain developers produce negatives on a fast, coarse grain emulsion which exhibit about the same graininess as negatives on a slower fine grain emulsion which have been developed in an ordinary developer such as pyro. A fine grain emulsion developed in a MQ-borax developer such as DK 76 will produce negatives with about the same graininess as a coarse grain emulsion developed in a *p* phenlyenediamine formulae and requires about the same exposure. This is in agreement with the work of Vittum and Crabtree.[24]

While the ultra-fine and fine grain developers all yield negatives with about the same graininess on fine grain emulsions, they fall into several groups when the graininess of negatives made from coarse grain emulsions is considered. A statistical examination of these data indicated that the differences between groups were very significant but the differences within groups were not significant. This result agrees with that of Kreveld and Scheffer[12] who found that fine grain developers were more effective in reducing the graininess in fast, coarse grain emulsions than in slow, fine grain emulsions.

The results of tests on the Lumieres and Seyewetz system of physical development are unusual in that, while the graininess of a fine grain emulsion developed by this method is very low, the exposure required is less than that for a fast, coarse grain emulsion treated similarly. The graininess of the fast coarse grain emulsion when developed by this system was equal to that produced by DK 76. This inconsistency may be due to the fact that the film is fixed first and developed afterwards with the result that the fast and slow film could not be treated alike due to different fixing times.

Since the negatives used to compare graininess

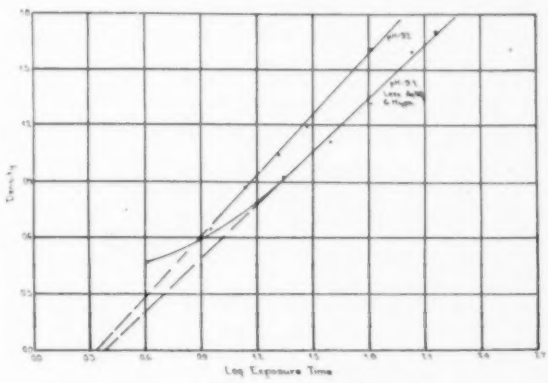

FIG. 17. Odell's solutions.

were not developed to exactly the same density and gamma, the effect of correcting these variations by means of the data in Fig. 13 and Tables I–III was examined but the only change was a slight but insignificant increase in the graininess of all developers when used on Agfa Finopan.

All density measurements were made with the emulsion in direct contact with the finely ground glass surface protecting photo-cell. B. C. Hiatt and C. Tuttle[7] have shown that densities measured in this manner correspond to diffuse density as defined by a visual densitometer. Diffuse density is the density of importance in contact printing, but the illumination used in making enlargements by projection is controlled principally by the specular density of the negative. Diffuse density is always less than specular density and the difference increases as the grain size decreases. Since, for low graininess, small grain size and even distribution are necessary, the gamma computed from the densities measured by the photo-cell is actually lower than the effective gamma of the developed negative of low graininess when used for projection printing. To check the practical magnitude of this difference between the measured density and gamma and the density and gamma as actually used in projection printing the sensitometric strips were magnified ten diameters in a Leica projecting printer, which has a modified condenser system of illumination, and the density measurements were repeated with the photo-cell in the position normally occupied by the printing paper. The measurements on the density of sensitometric strips developed in DK 76 agreed with the previous measurements to within one percent while the measurements on the density of sensitometric strips developed in Sease No. III were less than five percent higher. This agreement indicates that these data are valid for negatives which are to be used for either projection or contact printing.

V. Conclusions

1. Fine grain developers are more effective in reducing the graininess of fast, coarse grain emulsions than slow, fine grain emulsions.

2. The graininess of a fast, coarse grain emulsion when developed in an ultra-fine grain developer is at least equal to that of a slow, fine grain emulsion when developed in an MQ borax developer.

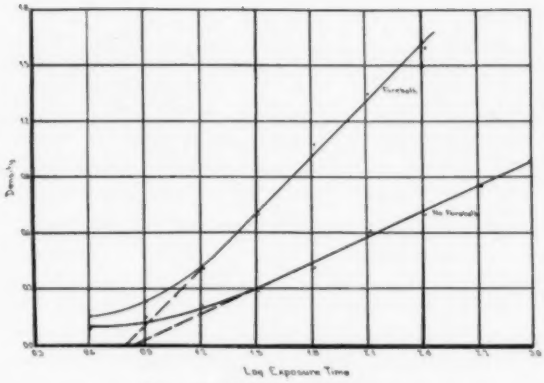

Fig. 18. Odell's solutions.

3. The effective emulsion speed of a slow, fine grain emulsion when developed in a MQ borax developer is at least equal to that of a fast, coarse grain emulsion when developed in an ultra-fine grain developer which will give negatives of as low graininess on the fast emulsion as the MQ borax gives on the slow emulsion.

4. Manufacture is more important than method of development in the control of graininess.

5. Odell's system of physical development is actually a combination of chemical and physical development.

6. Developers known to contain *p* phenylenediamine yield negatives of less graininess than ordinary developers but reduce the effective speed of the emulsion.

7. The graininess of a given emulsion when developed in a given developer depends upon the gamma to which it is developed and the density of the deposit.

8. To obtain negatives of low graininess, one should use a fine grain emulsion, expose fully, and develop in an MQ borax developer to as low a gamma as practical. Slight improvement in graininess can be obtained by using ultra-fine grain developers with fine grain emulsions, but only at some sacrifice of effective emulsion speed.

Acknowledgment

The author wishes to express his indebtedness to Dr. P. H. Carr for the valuable suggestions and criticisms which he made while supervising this investigation, and to the many members of the physics staff who helped take observations on graininess.

Bibliography

1. Harry Champlin, *Champlin on Fine Grain* (Camera Craft Pub. Co., San Francisco, 1937).
2. Harry Champlin, *Concerning Champlin 15* (Camera Craft Pub. Co., 1937), **44**, pp. 426–428.
3. O. E. Conklin, "Some Applications of the Comparison Microscope in the Film Industry." Trans. Soc. Mot. Pict. Eng. **16**, 162 (1931).
4. Eastman Kodak Co., *Elementary Photographic Chemistry* (Eastman Kodak Co., Rochester, New York).
5. F. L. English, "Some Factors Affecting Grain Size." Am. Phot. **31**, 305–315 (1937).
6. A. C. Hardy and L. A. Jones, "Graininess of Photographic Materials Used in the Motion Picture Industry." Trans. Soc. Mot. Pict. Eng. **14**, 107 (1922).
7. B. C. Hiatt and C. Tuttle, "Notes on the Measurement of Photographic Densities with a Barrier Type of Photocell." J. Soc. Mot. Pict. Eng. **26**, 195–203 (1936).
8. E. T. Howell, "Modern Developers and Development." American Annual of Photography **50**, 211–220 (1936).
9. L. A. Jones and N. Deisch, "The Measurement of Graininess in Photographic Deposits." J. Frank. Inst. **190**, 657–683 (1920).
10. L. A. Jones, *Photographic Sensitometry* (Eastman Kodak Co., Rochester, New York).
11. A. van Kreveld, "Objective Measurements of Graininess of Photographic Materials." J. Opt. Soc. Am. **26**, 170–176 (1936).
12. A. van Kreveld and J. C. Scheffer. "Graininess of Photographic Materials in Objective Absolute Measure." J. Opt. Soc. Am. **27**, 100–109 (1937).
13. J. Lanctot, "The Control of Graininess." American Annual of Photography **49**, 53–55 (1935).
14. Morgan and Lester, *Leica Manual* (Morgan and Lester Publishing Co., New York, 1937), p. 19.
15. A. F. Odell, "Physical Development of Plates and Films." New Photo-Miniature **2**, 57–88 (1935).
16. A. F. Odell, "After Four Years of Physical Development." Camera **54**, 145–154 (1937).
17. R. E. Owen, "Physical Development and the Nature of the Latent Image." Phot. J. **69**, 278–280 (1929).
18. F. E. Ross, *The Physics of the Developed Photographic Image* (Eastman Kodak Co., Rochester, New York), p. 21–34.
19. H. Sanders and M. Germain, "What We Think of Champlin 15 Fine Grain Developer." Camera Craft **45**, 9–13 (1938).
20. G. Schwarz, "Fine Grain Emulsions, Fine Grain Developers and Sensitivity." Kinotech. **19**, 51–53 (1937).
21. E. W. H. Selwyn, "A Theory of Graininess." Phot. J. **75**, 571–580 (1935).
22. S. D. Threadgold, "Measurement of Graininess." Phot. J. **72**, 348 (1932).
23. C. Tuttle, "The Relation Between Diffuse and Specular Density." J. Opt. Soc. Am. **12**, 559–565 (1926).
24. P. W. Vittum and J. I. Crabtree, "A New Fine Grain Developer." Am. Phot. **30**, 188–192 (1936).
25. J. H. Webb, "Relation between Reciprocity Law Failure and the Intermittency Effect in Photographic Exposure." J. Opt. Soc. Am. **23**, 157–169 (1933).

Letter to the Editor

I am very thankful to Doctors Withrow and Rassweiler[1] for drawing attention to Dr. Kondratjew's[2] wrong interpretation of my statement[3] that the HCO bands occur "feebly in a Bunsen flame as noted by Rassweiler and Withrow, and with greater intensity in the flame of ether as shown by a photograph by Emeléus." My reference here was only to the spectrum of the ordinary ether flame, (spectrum *d*, Fig. 1, of Emeléus' paper,[4] as correctly stated by Doctors Withrow and Rassweiler) and not to that of the cool flame (spectrum *c*, Fig. 1, of the same paper by Emeléus). The ordinary ether flame, however, gives both the *A* and *B* groups of the HCO bands, whereas the ethylene flame burning ordinarily yields only the *A* bands.

I am sorry I could not point out Dr. Kondratjew's mistake first for it was only in last May that I had the opportunity of reading the relevant journal. In the meanwhile, Doctors Withrow and Rassweiler had already published the correction.

Wm. Vaidya

Physics Department,
University College,
Rangoon, Burma.
November 5, 1938.

[1] J. App. Phys. **9**, 366 (1938).
[2] Acta Phys. chim. **4**, 556 (1936).
[3] Proc. Roy. Soc. **A147**, 513 (1934).
[4] J. Chem. Soc. 2948 (1926).

A Resonance Curve Method for the Absolute Measurement of Impedance at Frequencies of the Order 300 mc/Second

R. A. CHIPMAN
Cruft Laboratory, Harvard University, Cambridge, Massachusetts
(Received July 27, 1938)

A general theory is developed, together with a simplified experimental procedure, which permits the absolute measurement of the magnitude and phase angle of any value of complex impedance, in terms of the characteristic impedance of a parallel-wire line to which the impedance to be measured is connected as one termination. The observed quantities are the shape of the resonance curve of the current in one of the line's terminations obtained by varying the line length, and the length of line for maximum current. The effects of distributed line resistance and of radiation resistance on the impedance measurements are discussed in detail. Examples are given of the measurement of the impedance of straight resistance wires, and of the resistance of "metallized" resistors, at a frequency of 377 mc/sec.

The accuracy of the method varies considerably throughout the total range of resistance and reactance, but is high for any combination of the two from a few ohms to a few thousand ohms. The possible accuracy varies approximately inversely as the frequency. At a frequency of 300 mc/sec. an optimum accuracy of about one percent may be expected.

In an appendix some experimental data on the radiation resistance of a parallel-wire line are described.

I. INTRODUCTION

THE distributed inductance and capacitance and the resonant properties of a parallel-wire line seem to have been first adapted to the measurement of reactance at very high radio-frequencies by Drude,[1] who used them as a basis for measurement of dielectric constants. Wuckel[2] has measured absolutely the resistance of the conductors composing a resonant line by observing the relative amplitudes of successive current maxima along the line. More recently Schmidt,[3] Hempel,[4] and Bruckmann[5] have described methods for measuring any unknown impedance in terms of the characteristic impedance of a parallel-wire line to which the unknown is connected as a termination. Their methods require, variously, measurement of maximum and minimum currents or voltages, resonant line lengths, and currents or voltages at certain spots along the line. Such methods have the disadvantage of being useful only when the minimum current is not too small for accurate observation, and will not satisfactorily measure impedances whose resistance components are very high or low compared with the characteristic impedance of the line.

Other procedures which have been worked out for measuring impedances at very high frequencies are not absolute, but allow comparison of two impedances, one of which may be assumed known. The methods of King[6] and Krause[7] are notable examples. These methods also are suitable only for limited ranges of resistance and reactance.

The method described in the present paper is capable of measuring a much wider range of impedance magnitudes and phase angles than any of the methods mentioned above. It also has advantages over some or all of these methods with respect to experimental simplicity, adaptability to higher frequencies, and the accuracy of measurement in all ranges of impedance.

II. THEORY OF DETERMINATION OF REFLECTION COEFFICIENTS

The general formula for the complex current amplitude at any point x of a transmission line of length l terminated in arbitrary impedances Z_i and Z_t, produced by an e.m.f. in series with Z_i, has been derived by Pierce[8] and by Carson[9] using different approaches.

Using Pierce's form of notation, the current at

[1] P. Drude, Wied. Ann. **61**, 466 (1897).
[2] R. Wuckel, Ann. d. Physik **73**, 427 (1924).
[3] O. Schmidt, Hoch: tech. u. Elek:akus. **41**, 2 (1933).
[4] W. Hempel, E. N. T., **14**, 33 (1937).
[5] H. Bruckmann, Hoch: tech. u. Elek:akus. **51**, 128 (1938).
[6] R. King, Proc. I.R.E. **23**, 885 (1935).
[7] W. Krause, Hoch: tech. u. Elek:akus. **45**, 128 (1935).
[8] G. W. Pierce, *Electric Oscillations and Electric Waves* (New York, 1920), Eq. (30), p. 330.
[9] J. R. Carson, *Electric Circuit Theory and Operational Calculus* (New York, 1926), Eq. (243), p. 133.

the end $x=l$ of such a line is given by

$$I_l=\frac{E}{Z_0+Z_i}\times\left\{\begin{matrix}e^{-(\alpha+j\beta)l}+\mathrm{Y}e^{-(\alpha+j\beta)l}+\mathrm{XY}e^{-3(\alpha+j\beta)l}\\+\mathrm{XY}^2e^{-3(\alpha+j\beta)l}++\end{matrix}\right\}. \quad (1)$$

where

Z_0 = characteristic impedance of the line,
Z_i = terminal impedance at the end $x=0$,
Z_t = terminal impedance at the end $x=l$,
E = e.m.f. in series with Z_i,
$(\alpha+j\beta)$ = propagation constant of the line,
X, Y = reflection coefficients at the ends of the line.

$$\mathrm{X}=(Z_0-Z_i)/(Z_0+Z_i), \quad (2)$$

$$\mathrm{Y}=(Z_0-Z_t)/(Z_0+Z_t). \quad (3)$$

Taking out a factor $(1+\mathrm{Y})e^{-(\alpha+j\beta)l}$ the right-hand side of Eq. (1) becomes a series. Summing this series, and introducing from (2) $Z_i+Z_0=2Z_0/(1+\mathrm{X})$ gives, symmetrically,

$$I_l=\frac{E(1+\mathrm{X})(1+\mathrm{Y})}{2Z_0}\left\{\frac{e^{-(\alpha+j\beta)l}}{1-\mathrm{XY}e^{-2(\alpha+j\beta)l}}\right\} \quad (4)$$

or

$$I_l=I_0\cdot f(l), \quad (5)$$

where I_0 is independent of the length of the line, and

$$f(l)=e^{-(\alpha+j\beta)l}/(1-\mathrm{XY}e^{-2(\alpha+j\beta)l}). \quad (6)$$

Experimentally, observing I_l on varying l gives the shape of a current resonance curve, and the length of the line for maximum current. The theoretical problem is to transform Eq. (6) to obtain an expression for the complex product XY of the reflection coefficients in terms of these two observable quantities.

Substituting in Eq. (6)

$$\mathrm{XY}=e^{-2(p+jq)} \quad (7)$$

leads to

$$f(l)=\frac{1}{2(\mathrm{XY})^{\frac{1}{2}}\sinh\{(\alpha l+p)+j(\beta l+q)\}}. \quad (8)$$

When the current indicating device is a thermocouple, only the absolute magnitude of $f(l)$ is important. This is

$$|f(l)|=\frac{1}{2\{|\mathrm{XY}|\sinh^2(\alpha l+p)+|\mathrm{XY}|\sin^2(\beta l+q)\}^{\frac{1}{2}}}. \quad (9)$$

The maximum value of $f(l)$ will occur at a line length l_0 given by

$$\beta l_0+q=n\pi, \quad (10)$$

where n is any integer.

To a very high degree of accuracy for typical lines at very high frequencies $\beta=2\pi/\lambda$. Hence Eq. (10) leads to

$$q=2\pi\{(n\lambda/2)-l_0\}/\lambda. \quad (11)$$

From Eq. (7) the phase angle ϕ of the product XY is $-2q$, which from Eq. (11) is

$$\phi=4\pi\{l_0-(n\lambda/2)\}/\lambda. \quad (12)$$

From Eq. (9), the maximum value of the current occurs at $l=l_0$ and is proportional to

$$\frac{1}{|\mathrm{XY}|^{\frac{1}{2}}\sinh(\alpha l_0+p)}. \quad (13)$$

The *increase* in line length δl_1 which will reduce the current in the termination to g times this maximum value $(0<g<1)$ is given by

$$\sinh^2[\alpha(l_0+\delta l_1)+p]+\sin^2(2\pi\delta l_1/\lambda)=\{\sinh^2(\alpha l_0+p)\}/g^2, \quad (14)$$

which follows from Eqs. (9) and (11).

Similarly the *decrease* in line length δl_2 which will reduce the current to the same value is given by

$$\sinh^2[\alpha(l_0-\delta l_1)+p]+\sin^2(2\pi\delta l_2/\lambda)=\{\sinh^2(\alpha l_0+p)\}/g^2. \quad (15)$$

Equations (14) and (15) can be solved for any values of α and l_0, to give a relation between the width $(\delta l_1+\delta l_2)$ of a current resonance curve at any height g-times its maximum height and the magnitude of the corresponding reflection coefficient XY, (since $p=\log_e 1/|\mathrm{XY}|^{\frac{1}{2}}$). If α is small enough to be neglected, Eqs. (14) and (15) reduced to a single equation which is solved very easily.

In Fig. 1 the full curve is the solution of these equations for $\alpha=0$, $g=1/\sqrt{2}$. This curve is inde-

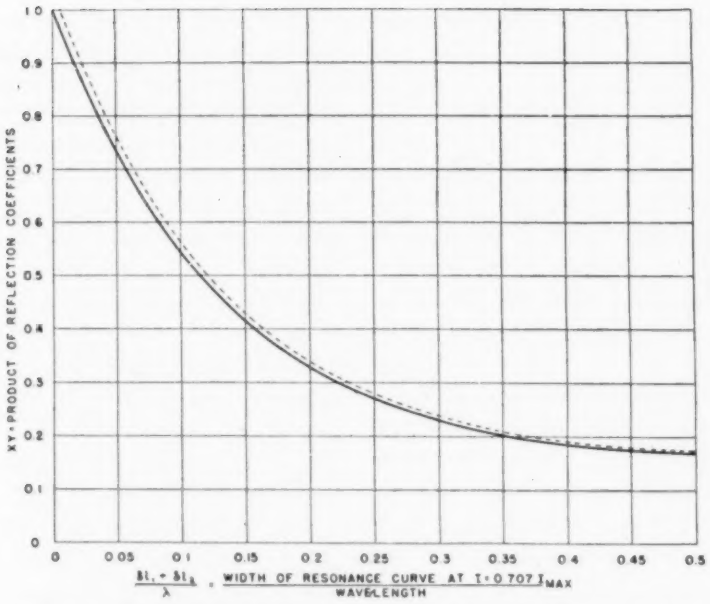

FIG. 1. The product of the reflection coefficients at the two ends of a parallel-wire transmission line as a function of the width of the resonance curve of the current in one of the line's terminations. The full curve is for zero attenuation along the line. The dotted curve is for attenuation constant $\alpha = 5 \times 10^{-4}$/cm, resonant line length $l_0 = 40$ cm. A resonance-curve width at any height can never exceed one-half wavelength.

pendent of line length. The dotted curve shows the sum of the solutions of the two equations in the form $|XY|$ plotted against $(\delta l_1 + \delta l_2)/\lambda$ for $\alpha = 5 \times 10^{-4}$/cm, $l_0 = 40$ cm, and the same value of g. (This value of g is chosen because the output of the thermocouple current indicator at $x = l$ varies as $(I_l)^2$, and it is convenient to measure the width of the resonance curve of thermocouple output at one-half its peak height.) The full significance of the relationship of these two curves to impedance measurements is discussed in Section V.

Figure 1 and Eq. (12) allow the determination of the magnitude and phase angle of the product XY *of the complex reflection coefficients at the ends of a transmission line of any length terminated in arbitrary impedances, when the resonant length of line and the shape of the resonance curve of the current in one of the line's terminations, obtained by varying the line length about resonance, have been determined experimentally.*

When α is negligible, the magnitude of XY can also be found in the following way. From Eqs. (5) and (9), substituting for p from Eq. (7), the maximum value of the current at the end $x = l$ of the line is then

$$I_{\max} = I_0 \cdot \frac{1}{1 - |XY|} \quad \text{when} \quad \beta l + q = n\pi.$$

The minimum current is

$$I_{\min} = I_0 \cdot \frac{1}{1 + |XY|} \quad \text{when} \quad \beta l + q = \frac{(2n-1)\pi}{2}.$$

Hence

$$\frac{I_{\max}}{I_{\min}} = \frac{1 + |XY|}{1 - |XY|}, \tag{16}$$

from which $|XY|$ is easily determined when $I_{\max}$ and $I_{\min}$ have been measured experimentally.

As mentioned in Section I, this procedure has poor accuracy if $I_{\min}$ is very small, but is useful when the two currents are of the same order of magnitude. Its accuracy is not appreciably affected by values of α up to 10^{-4}/cm for a one-half-wave-length line.

If $|XY| = |X|$ and is real, Eq. (16) reduces to

$$\frac{I_{max}}{I_{min}} = \frac{Z_0}{R} \quad \text{or} \quad \frac{R}{Z_0}, \tag{17}$$

where R is any unknown terminal resistance whose reflection coefficient is X. The factor to be used on the right of the equation depends on whether R is greater or less than Z_0. This equation is useful for rapid approximate resistance measurements when the value of Y is sufficiently close to unity.

To measure an unknown impedance connected as the input impedance Z_i of a line, its reflection coefficient X must be extracted from the measured product XY, which requires that the reflection coefficient Y for the thermocouple and associated equipment at the other end of the line be known.

This coefficient Y can be determined by measuring the product XY under conditions where $X = \pm 1 + j0$, i.e. with the line perfectly short-circuited or completely open-circuited at its input end.

Taking the case $X = +1 + j0$, for example, the resulting measurement has the form $|Y| \cdot \exp(j\phi_Y)$. A measurement of the product XY with any unknown impedance as Z_i and the same thermocouple equipment mentioned above as Z_t has the form $|XY| \cdot \exp(j\phi_{XY})$. The reflection coefficient X for the unknown Z_i is then given by

$$\frac{|XY|}{|Y|} \cdot \exp\{j(\phi_{XY} - \phi_Y)\}.$$

The quantity $(\phi_{XY} - \phi_Y)$ is by Eq. (12) at constant wave-length a function only of the difference between the two resonance line lengths measured respectively in the determinations of XY and Y. The latter line length therefore becomes a reference constant for any one apparatus, and for the determination of the phase angle ϕ' of the coefficient X replaces the quantity $n\lambda/2$ in Eq. (12). Denoting this length by l_r,

$$\phi' = 4\pi(l_0 - l_r)/\lambda. \tag{12a}$$

From Eqs. (2) and (12a) it can be seen that an *inductively reactive* Z_i will make the resonant line length always *less than* l_r, by a maximum of one-quarter wave-length in the case of an infinite purely inductive reactance. A capacitively reactive Z_i similarly will make the resonant line length *greater than* l_r, likewise by a maximum of one-quarter wave-length for an infinite purely capacitive reactance.

Because a thermocouple is invariably inductively reactive, the line length l_r is always somewhat shorter than a length $n_0\lambda/2$, the *nearest* integral number of half-wave-lengths. If α is large, the value of Y varies slightly in magnitude, though not appreciably in phase angle, with the value of n_0. Experimentally it will usually be most convenient to have $n_0 = 1$ or 2.

III. Calculation of a Terminal Impedance from Its Reflection Coefficient and the Characteristic Impedance of the Line

From Eq. (2),

$$Z_i = Z_0 \cdot \{(1-X)/(1+X)\}$$

or, since Z_i, X and Z_0 are all complex,

$$R_i + jX_i = (R_0 + jX_0) \cdot \{(1 - A - jB)/(1 + A + jB)\}, \tag{18}$$

where $X = |X|e^{j\phi'}$ has been replaced by $A + jB$, so that

$$A = |X| \cos \phi' \quad B = |X| \sin \phi'.$$

While (17) can be solved for all values of X and Z_0, it is true in general at very high frequencies that X_0/R_0 can be kept considerably below 10^{-3} and that Z_0 can therefore be regarded as a pure resistance. In this case (17) leads to

$$R_i = Z_0 \cdot \{(1 - A^2 - B^2)/(1 + A^2 + B^2 + 2A)\}, \tag{19a}$$

$$X_i = \pm Z_0 \cdot \{2B/(1 + A^2 + B^2 + 2A)\}. \tag{19b}$$

These are the equations from which the components of any unknown impedance must be calculated when its reflection coefficient has been measured experimentally.

To visualize the inter-relations of the variables R_i, X_i, $|X|$ and ϕ' over their entire range, it is convenient to plot on coordinates of $|X|$ and ϕ' lines of constant R_i/Z_0, X_i/Z_0, Z_i/Z_0 and $\theta = \tan^{-1} X_i/R_i$. This has been done in Fig. 2. The coordinate system consists of concentric circles of constant $|X|$, from 0 at the center in

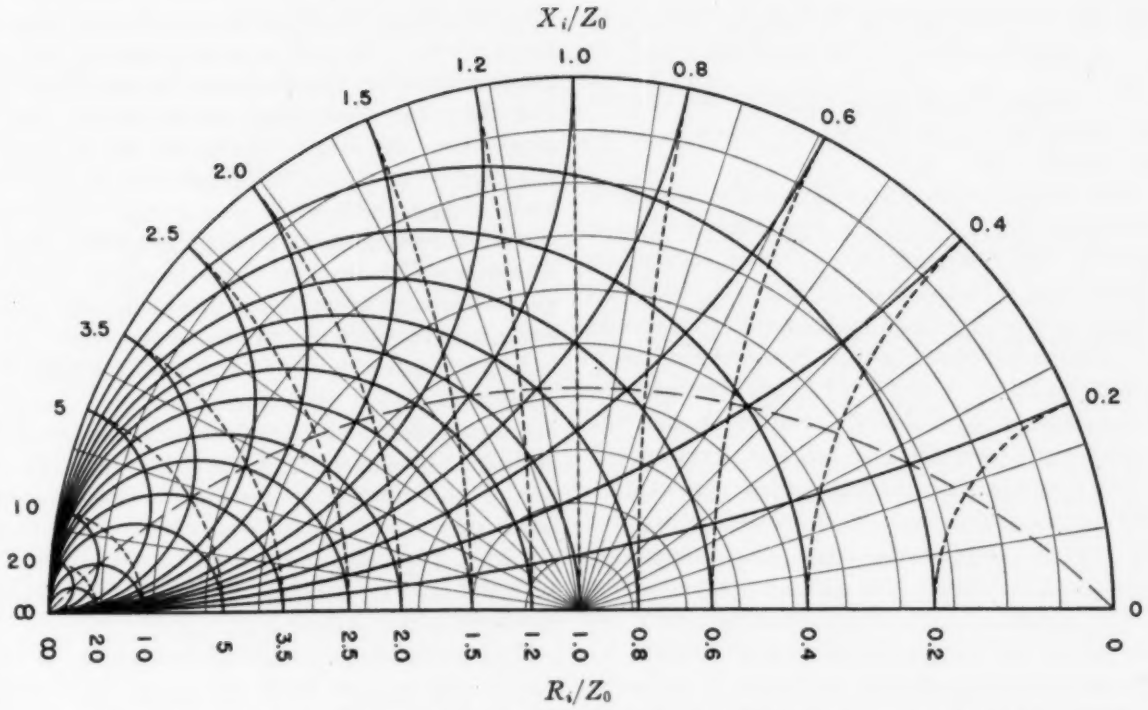

FIG. 2. The components of an impedance in terms of its reflection coefficient $Xe^{j\phi'}$ when connected as a termination of a parallel-wire transmission line whose characteristic impedance is Z_0. The coordinates are concentric circles of constant $|X|$ from 0 at the center in units of 0.1 to 1.0 at the outside, and radial lines of constant ϕ', from 0 at the right in units of 0.05π counterclockwise to π.

units of 0.1 to 1.0 at the outside, and radial lines of constant ϕ' from 0 at the right in units of 0.05π counterclockwise to π. The line $\phi'=0$ corresponds to the line length l_r defined in Section II.

This diagram is symmetrical about the base-line for change in sign of ϕ', X_i and θ. It indicates inductively or capacitively reactive impedances, respectively, according as the sign of ϕ' from Eq. (12a) is negative or positive. From the diagram the resonance-curve width and the resonant line length to be expected in the measurement of any size of impedance can be found, and the possible accuracy of the measurement estimated. In particular the following indications are important:

1. The measurement of pure resistance depends only on the value of $|X|$, and hence on a resonance-curve width. The resonant length of the line remains constant at l_r for resistances less than Z_0, and is shifted one-quarter wave-length for resistances greater than Z_0.

2. The measurement of pure reactance is in terms solely of the phase angle ϕ', or of the resonant length of the line. The value of $|X|$ remains unity. This case is illustrated by Fig. 3 which shows the variation of the resonant length of a line for various pure reactance terminations. The reference length (for short-circuit termination of zero reactance) is indicated as one-half-wave-length.

3. If any two impedances Z_i and Z_i' are related by $Z_iZ_i'=Z_0^2$, and $|X|e^{j\phi'}$ is the reflection coefficient of Z_i, it can be shown by Eq. (18) that the reflection coefficient of Z_i' is $|X|e^{j(\phi'-\pi)}$. Since Fig. 2 is symmetrical in positive and negative values of ϕ', this means that the point $|X|e^{j(\pi-\phi')}$ will give the components of Z_i'. This point is the mirror image about the axis $\phi'=90°$ of the point $|X|e^{j\phi'}$, corresponding to the components of Z_i.

It follows that the impedances Z_i and Z_i' will have resonance curves identical in shape, and that the possible accuracy of measurement of magnitude and phase angle will be the same for both.

IV. The Experimental Procedure for Determining Reflection Coefficients

The simple line-circuit designed in the light of the requirements of the above theory is illustrated in Fig. 4.

The oscillator shown at A supplies the high frequency e.m.f. $BCDEF$ is a parallel conductor system of telescoping brass tubes. Unknown impedances Z_i are connected at B. The thermocouple termination is connected at C to the ends of the *outer* tubes of the line. D and F are heavy brass "tandem" bridges, D about one-quarter wave-length from C and F about three-quarters wave-length from D. The point G is connected to the carriage of a rigidly mounted comparator. The length of the line is varied continuously by turning the comparator screw and changes of line-length are read on the comparator vernier.

The important features of the circuit are:

1. The line supports consist of strips of Victron-G held by Bakelite screws to 3″ steatite stand-off insulators, as shown in Fig. 5. One of these holds the line rigidly near B. A second between D and E allows the outer tube of the line to slide through it as the line length is varied from G. For high impedances the support near B must be placed always at a voltage antinode to minimize the effect of its shunt capacity on the impedance being measured (see Section VIII).

2. The line dimensions are maintained constant along the length of the line by means of the support at B, the bridges at D and F, and a Victron clamp near C.

3. The conductors are brass tubes of external diameter 0.476 cm. The value of α for these at the frequency of 377 mc/sec. used is small enough to be negligible in all calculations.

4. The terminals at the end B of the line are illustrated in Fig. 6. These ensure that the reflection coefficient X at this point is determined only by the connected unknown impedance Z_i.

5. The oscillator A, designed to give steady potential at constant frequency, uses the circuit of Fig. 7. The tubes are type WE316A, operated with 400 volts on the plate from an electronically regulated power supply.[10]

The combination of a three-quarter wave-length grid circuit with a five-quarter wave-length plate circuit allows precise tuning of the grid circuit at the shortest wave-lengths obtainable from the tubes. A one-quarter wave-length

[10] F. V. Hunt and R. W. Hickman, *On Electronic Voltage Stabilizers*, to be published shortly.

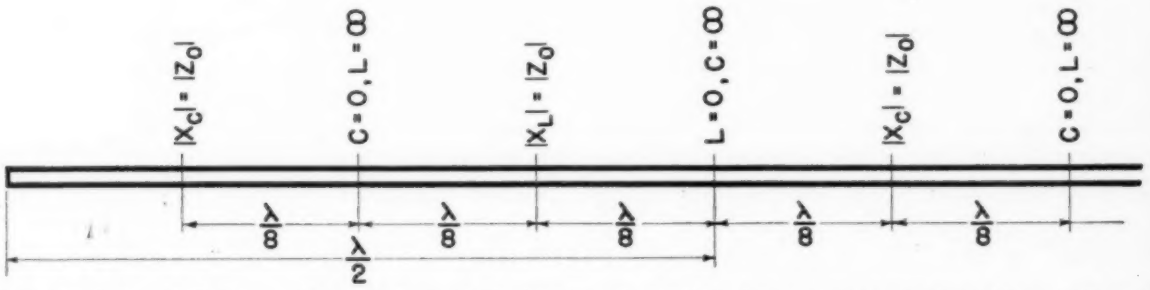

FIG. 3. Variation of the resonant-length of a parallel-wire transmission line when one end is terminated in a short circuit and the other end is terminated in various pure reactances.

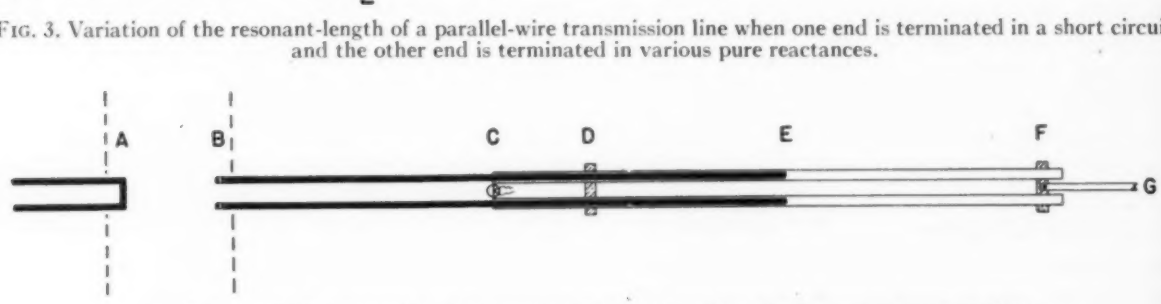

FIG. 4. The line circuit used in measuring impedances by the resonance-curve method.

A —oscillator supplying high frequency e.m.f.
BCDEF—parallel-wire telescoping transmission line
B —point where unknown impedances are connected
C —thermocouple
D,F—brass "tandem" bridges
G —point where comparator is connected for varying line length
BE —maximum possible resonant line length

grid circuit at these wave-lengths is too short to permit such tuning.

The concentric-line type of filament chokes, while not critically important in this push-pull circuit, increase the circuit output by several percent at optimum adjustment.

It is evident that with simple coupling of A and B as indicated in Fig. 4, e.m.f. is being induced in the parallel wires of the line as well as in the termination. Experiment shows that the theory apparently remains applicable. Large parallel copper sheets placed at A and B (dotted lines in Fig. 4) with the ends of the lines projecting slightly through small holes in the sheets had negligible effect on the measured value of typical impedances.

Strong odd harmonics in the oscillator output

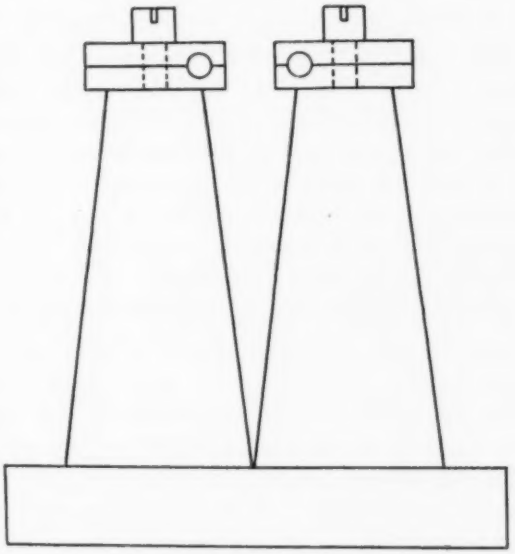

FIG. 5. Detail of line supports.

(the line circuits would maintain only odd harmonics) might seriously affect the shape of the desired current resonance curves. Such harmonics can be detected by sharp rises of thermocouple output as the line length is varied continuously from zero to one-half-wave-length. None were detectable in the present work.

V. The Effects of Distributed Line Resistance

It was pointed out in connection with Eqs. (14) and (15) and Fig. 1 that

(a) The value of $|XY|$ calculated for any observed resonance curve width varies somewhat with α, and

(b) For large values of α the current resonance curves become not quite symmetrical, so that the

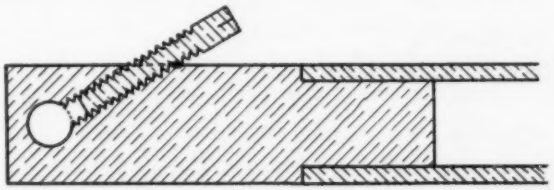

FIG. 6. Detail of line termination where unknown impedances are connected.

resonant line length cannot in such a case be accurately calculated as the average of the two line lengths for half-maximum current, which is normally a much more precise means than direct measurement for locating the position of the peak of a resonance curve.

A brief consideration indicates that neither of these effects is of importance in practical measurements when accuracy of 1 to 2 percent is sufficient.

(a) In the experimental measurement of an unknown impedance, *two* resonance curve widths are measured, one for the determination of $|XY|$ and one for the determination of $|Y|$. The ratio $|XY|/|Y|$ is the quantity used in the final impedance calculation. It is found by trial that regardless of which of the curves of Fig. 1 the two measured resonance-curve widths are referred to, this ratio is very accurately constant. The error might be appreciable for a sufficiently high value of α, but values higher than that chosen for the dotted curve of Fig. 1 (10^{-4}/cm) are never to be expected experimentally.

(b) Calculations of the asymmetry of current resonance curves for the same values of α and l_0 as above show that in an extreme case of a resonance curve 30 cm wide at half-maximum current the resonant length of line differs from the length to the center of the curve at half-maximum height by 2 mm. The value of $|XY|$ in this case is 0.20, and this 2 mm corresponds to an error in its phase angle of about 2°. Fig. 2 shows that as $|XY|$ decreases, ϕ need be known less accurately for any desired accuracy in the calculation of R_i and X_i. For values of α up to the value used above, at a frequency of 377 mc/sec.,

this asymmetry effect does not introduce an error as great as the probable experimental error in the resonance-curve measurements.

For line dimensions likely to be chosen in practice the increase of line resistance caused by the proximity of the two line conductors[11] is also not important.

VI. Radiation Resistance

Radiation can occur from both the linear portions of a parallel-wire transmission line, and the terminations of the line, and must be taken into account theoretically by a properly located radiation resistance. If there is radiation from the length of a line, the appropriate radiation resistance will influence the value of α, and may aggravate the effects described in Section V. Radiation from the terminations is easily allowed for as a small equivalent resistance in series with each of the line's terminal impedances, modifying the reflection coefficients.

A discussion of the problem of radiation from a parallel-wire line, together with a few experimental measurements of linear and terminal radiation resistances, is given in Appendix I. The measurements indicate that the equivalent *distributed* radiation resistance for the experimental line used in the present work is small enough that α can still be neglected. They suggest that the radiation resistance of a termination can be estimated from the classical formula for a current filament[12]

$$R_{\text{rad}} = 80\pi^2 l^2/\lambda^2, \qquad (20)$$

where l is the center-spacing of the conductors of the line.

To permit accurate measurement of low resistance-component impedances, this terminal radiation resistance must be kept at a minimum, by using a small line spacing. This in turn limits the physical dimensions of impedances that can be measured by the line. However, this effect is not likely to become objectionable, because at very high frequencies only impedances of small dimensions can accurately be regarded as "lumped" impedances.

[11] E. J. Sterba and C. B. Feldman, Proc. I.R.E. **20**, 1163 (1932), Fig. 8.

[12] M. Abraham, *Classical Electricity and Magnetism* (New York, 1932), p. 228.

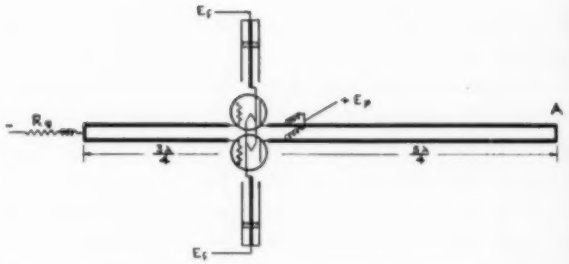

Fig. 7. Circuit of the oscillator used to supply the high frequency e.m.f. The tubes are type WE316A.

VII. The Calculation of High Frequency Resistance and Reactance

A straight wire is the only form of conductor for which the high frequency resistance and reactance may be calculated with any accuracy, and is therefore the only available "standard" for checking an impedance-measuring method.

Rigorous calculations for the resistance of such a conductor as a function of frequency have been made by Rayleigh[13] and Kelvin[14] with apparently identical results. Formulas commonly used are approximations to these rigorous derivations[15] or represent their limiting form at infinite frequency.[16] Only Rayleigh has taken account of the permeability of a conductor.

The inductance of such a conductor has been calculated using independent methods by Rayleigh,[13] Russell,[17] and Gray,[18] with results that differ appreciably only for conductors of high permeability, or conductors whose length is less than one hundred or so times the cross-section dimensions. Rayleigh's formula, taking account of permeability, can be applied easily and exactly to any conductor, using tables that have been prepared.[19]

The formulas for the high frequency resistance of a linear conductor have received considerable

[13] Lord Rayleigh, Phil. Mag. **21**, 381 (1886).

[14] Lord Kelvin, *Mathematical and Physical Papers*, Vol. III (1889), p. 491.

[15] E. B. Moullin, *Radio Frequency Measurements* (London, 1931), Eqs. (1) and (1a), p. 238.

[16] F. Vilbig, *Lehrbuch der Hochfrequenztechnik* (Leipzig, 1937), p. 85.

[17] A. Russell, *Alternating Currents* (Cambridge, 1914), Vol. I, p. 78.

[18] A. Gray, *Absolute Measurements in Electricity and Magnetism* (London, 1921), pp. 494–496.

[19] National Bureau of Standards Circular **74**, pp. 244 and 282.

experimental verification,[20] those for inductance very little. Inductance at high frequencies is a function almost exclusively of the field external to a conductor. It may be expected therefore that, especially for short conductors, the effect on the field of the terminal connections to a conductor will materially influence its inductance. It is probable that the formulas for inductance referred to above cannot for this reason be considered to have as high accuracy as the resistance formulas, under experimental conditions.

For capacitive reactance standards, King[21] has recently discussed in detail the calculation of the capacity of parallel-plate condensers at very high frequencies.

In considering the possibility of "standard" resistances having values of the order of a thousand ohms and more for high frequency use, it is necessary to take account of the effect of small parallel capacities.[22] This effect increases rapidly with frequency and the value of the resistance, and is of such magnitude that there is no commercial type of resistance available in the very high ranges whose steady current value gives any indication of the value at very high frequencies. A megohm resistance may, for example, be reduced to an effective value of a few thousand ohms by the shunt capacity of its glass-rod core, or of its insulation sheath.

VIII. Examples of Impedance Measurements

The present impedance measuring method is symmetrical for two impedances Z_i and Z_i' related by $Z_i \cdot Z_i' = Z_0^2$, as shown in Section III. Hence measurements made by the method on "known" impedances less than Z_0 can serve as a check on the accuracy and applicability of the method over the entire impedance range. The fact that calculable high resistance-component impedances do not exist becomes unimportant so far as checking the method is concerned.

Test measurements have been made on a number of wire samples varying in length, diameter, resistivity and conductivity, and on "metallized" glass rods with their terminals removed. Because of the doubts concerning radiation resistance and the unknown permeability of high resistivity ferric alloy wires at these frequencies, however, there is an unavoidable indeterminacy in the "known" values of any of these samples. The stated optimum accuracy of one to two percent for the present method is not based primarily on the agreement of measurements with calculations, but rather on an estimate of possible errors. The percentage indeterminacy caused by radiation resistance of course decreases as the resistive component of an impedance increases, for the same measuring line.

Table I shows typical results of measurements on linear resistance wires. The frequency throughout is 377 mc/sec.

Table II gives the results of measurements made on a number of different sizes of IRC type F½ metallized resistors, with various forms of connection to the line. The resistance component only is given in each case, the reactance component being small.

Some of these measurements are made from resonance-curve widths, others from maximum

Table I.*

The line constants are:	For (1) and (2)	For (3)
Conductor diameter	0.476 cm	0.476 cm
Center-spacing of conductors	2.00 "	1.60 "
Characteristic impedance of line	255.5 ohms	229.0 ohms
Reference resonance-curve width (see Table III in Appendix)	3.98 mm	4.20 mm
Reference resonant line length, l_r (see Table III in Appendix)	35.83 cm	36.12 cm

Sample (see identification below)	(1)	(2)	(3)
Diameter (cm)	0.00456	0.00472	0.00442
Length (cm)	1.58	1.54	1.135
D.c. resistance (ohms)	4.73	9.69	12.28
Resistivity (μ-ohms-cm)	49	112	167
Measured resonance-curve width (mm)	9.69	14.85	48.63
Measured resonant line length (cm)	33.52	33.58	33.00
Measured resistance component (ohms)	5.98	11.29	42.8
Measured reactance component (ohms)	47.2	45.9	55.8
Radiation resistance (Eq. (20), ohms)	0.50	0.50	0.3
Measured resistance corrected (ohms)	5.48	10.79	42.5
Calculated resistance for $\mu = 1$ (ohms) (Eq. (1) of reference 16)	4.98	9.81	12.33
Value of μ required to make calculated resistance and corrected measured resistance agree	1.7	3.5	92
Calculated reactance for $\mu = 1$ (ohms) (Eq. (128) of reference 19)	47.7	46.1	32.3
Reactance calculated for the value of μ obtained from the resistance calculation (ohms) (Eq. (132) of reference 19)	49.2	49.8	71.7
Deviation of last calculated reactance from measured reactance (percent)	4	8	28
Nickel content of conductor material	2–10%	16%	small
Iron content of conductor material	trace	28%	70%

* Sample (1)—size 44 Manganin: Sample (2)—size 44 Nichrome: Sample (3)—size 44 Ohmax.

[20] A. E. Kennelly and H. A. Affel, Proc. I.R.E. **4**, 523 (1916).
[21] R. King, Phil. Mag. **25**, 339 (1938).
[22] A. Hund, *High Frequency Measurements* (New York, 1933), Eq. (6), p. 5.

TABLE II. *The frequency is again 377 mc/sec.*

Nominal Value of Resistance (Ohms)	Connection at Termination	Measured Resistance Component (Ohms)	d.c. Resistance (Ohms)	Ratio of Measured to d.c.
50	Full original lead length	55.2	49.5	1.11
—	Metallized rod removed from case; Ni tubes fitted for terminations	69.9	63.3	1.10
100	Leads cut short only	104.6	95.6	1.09
150	Leads cut short only	175	156	1.12
200	Leads cut short only	208	195	1.07
250	Leads cut short only	309	277	1.11

and minimum currents. So long as the phase angle of $|XY|$ is small, and radiation resistance small compared with the measured impedance, the latter method gives the resistance component of a termination with sufficient accuracy.

IX. Conclusions

This impedance measuring method can be said to give results agreeing with calculations only if Manganin and Nichrome have permeabilities greater than unity at a frequency of 377 mc/sec. A final conclusion about the accuracy of the method will depend on some independent evidence about this fact, or further measurements on impedances that may be considered more accurately known. Such permeabilities are conceivable on the basis of the nickel and iron content of these alloys. Ohmax, with a very high iron content, shows the increase of resistance and reactance much more markedly.

For each wire it is notable that the value of μ required to produce agreement between the calculated and measured resistance values makes the calculated value of the reactance greater than the measured value. The deviation cannot with any certainty be localized in either of the measurements or either of the calculations, but most probably is due to inaccuracy of the reactance calculation as suggested in Section VII.

The fairly constant deviation of about 10 percent in the measurements of Table II is compatible with other independent unpublished measurements that have been made on IRC type F resistances at frequencies of the same order. The increase of the value of these resistances with frequency is perhaps due to a true "skin-effect" in their thin resistance layer, or may be caused by nonhomogeneous granular structure of the layer.

In general it has been found that measurements with this impedance measuring method of resonance-curve width and resonant line length for any impedance termination are repeatable with a very high degree of accuracy (much better than 1 percent), unless the impedance approximates a resistance equal to the characteristic impedance of the line. In such a case the resonant line length is difficult to locate, and the value of $|XY|$ must be determined from measurement of maximum and minimum currents. For best accuracy it is advisable to always avoid this situation by varying the characteristic impedance of the line (i.e. the spacing) when necessary.

It is hoped in a later paper to present a series of measurements of the resistance and reactance of a number of types and ranges of impedance at very high frequencies, indicating the properties and the usefulness of the different types at these frequencies.

X. Acknowledgments

This work has been made possible by the grant of a Fellowship from the Cruft Laboratory of Harvard University in cooperation with the General Radio Company of Cambridge. Many helpful suggestions have been received from several men at Harvard, at the General Radio Company, and at the Massachusetts Institute of Technology. They will recognize their contributions throughout the paper. It is a pleasure to express my gratitude to all of them.

Appendix I

Radiation Resistance in Parallel-Wire Transmission Lines

It has been generally accepted that the terminations of a parallel-wire transmission line radiate energy, and that the equivalent radiation resistance is given by the formula for the radiation resistance of a current filament.

Whether or not there is radiation from the *length* of a parallel-wire line, however, has been a point of controversy. Carson,[23] for example, has held that there is not, quoting Macdonald[24] and Mie[25] in his support. Sterba and Feldman[26] have implied this when they show radiation resistance as independent of the length of a line. Hund[27] gives a formula for radiation resistance that involves length, but indicates no source for this.

It seems probable that so long as the wave front traveling along a line remains plane there will be no distributed dissipation along the line. This is never true near the terminations, however, and if the line spacing is as much as a few percent of the wave-length (which cannot be avoided at very high frequencies) there are also distortions of the wave front at all nodes and loops along a line. This would imply that radiation resistance should be regarded as non-uniformly distributed.

Some of the data obtainable with the apparatus described in Section IV are explicable only on the basis of radiation occurring from both the terminals *and* the length of a parallel-wire line.

(1) The peak currents at C (Fig. 4) were measured at two successive resonant line lengths differing by half a wave-length, for the cases of the line open-circuited at B and the line short-circuited at B. The results were the following:

(a) Line open-circuited at B.
  Peak current at C for resonant line $\frac{1}{4}$ wave-length long—6.35 arbitrary units
  Peak current at C for resonant line $\frac{3}{4}$ wave-length long—3.56 same units
(b) Line short-circuited at B.
  Peak current at C for resonant line $\frac{1}{2}$ wave-length long—5.77 arbitrary units
  Peak current at C for resonant line 1 wave-length long—5.56 same units

The peak resonant current at C is given by Eq. (13), and is approximately inversely proportional to (αl_0+p) when this quantity is small as in the present case. p has a constant value for the two measurements in (a) and another constant value for the two in (b), hence the differences in each case must be attributed to a variation in αl_0, l_0 having varied by half a wave-length or about 40 centimeters. The value of α required to account for the observations (a) is equivalent to a resistance of about 4 ohms distributed over the added half-wave-length of line, almost 10 times the calculated high frequency ohmic value. (This is considerably lower than the value of α used in the calculations of Section VI and hence will not affect experimental impedance measurements.) For case (b) the value of α required is approximately the same as the ohmic value.

No theoretical justification for the large difference in the increase of equivalent distributed radiation resistance in these two cases is known, though the data are somewhat reminiscent of Ballantine's curve[28] for the radiation resistance of a grounded vertical antenna as a function of height.

(2) The value of XY in magnitude and phase angle, represented by resonance-curve width and resonant line length respectively, was measured for several possible "reference" terminations at B. The results are given in Table III. Since the phase angle of XY is small in each case, the resonance-curve width is with high accuracy dependent only on the resistance in the circuit, and the resonant line length dependent only on the reactance components of the terminations, in each case.

The magnitude of the resonance-curve width in each case is of course largely due to the resistance of the thermocouple terminations at C, but the *variations* in width are due entirely to differences in terminal radiation resistance or distributed ohmic and radiation resistance among the various cases. Where either the terminal or the linear resistances are constant in two cases, the variation of the other can be observed. The terminal ohmic resistances are negligible in each of the short-circuit cases.

Of the short-circuit cases, the copper-plate termination is shown to have the smallest radiation resistance suggesting, as might be expected, that it more perfectly reflects the traveling waves on the line. If the copper wires be assumed to produce the asymptotic maximum radiation for a short-circuit termination, and the copper plate be assumed to produce zero radiation (i.e. perfectly reflecting), the experimental radiation resistance for the wire terminations is found to be equal to the value given by Eq. (20), within an experimental accuracy of about 10 percent. In the equation a current-filament length equal to the center-spacing of the line conductors is used.

The brass-block termination has a radiation resistance less than the wires, being a somewhat better reflector.

Comparing the resonance-curve width for the copper plate with that for open termination of the quarter wave-length line, the greater value of the latter must be due either to higher distributed radiation resistance, which seems improbable, or to radiation from the open end of the line, about which nothing is known.

The increase in resonance-curve width from a $\frac{1}{4}$ wave-length circuit to a $\frac{3}{4}$ wave-length circuit is consistent with the sharp decrease of resonant current noted earlier in

TABLE III. *The frequency is 377* mc/sec. *throughout;* $\lambda = 79.20$ cm.

TERMINATION AT B	RESONANT LINE LENGTH (cm)	RESONANCE-CURVE WIDTH (mm)
Large copper sheet	$35.83 \doteq \frac{1}{4}\lambda$	3.98
Copper wire diameter 1.05 mm	$34.82 \doteq \frac{1}{4}\lambda$	4.44
Copper wire diameter 0.384 mm	$34.48 \doteq \frac{1}{4}\lambda$	4.43
Brass block $\frac{1}{4}$" square	$35.71 \doteq \frac{1}{4}\lambda$	4.22
" " " "	$75.31 \doteq \lambda$	4.39
Open circuit	$15.47 \doteq \frac{1}{4}\lambda$	4.13
" "	$55.07 \doteq \frac{3}{4}\lambda$	4.48

[23] J. R. Carson, Journal A.I.E.E. **43**, 908 (1924).
[24] H. M. Macdonald, *Electric Waves* (Cambridge, 1902), pp. 106–133.
[25] G. Mie, Ann. d. Physik **2**, 201 (1900). See page 248.
[26] E. J. Sterba and C. J. Feldman, reference 11, Fig. 9.
[27] A. Hund, reference 22, Eq. (1), p. 2.
[28] S. Ballantine, Proc. I.R.E. **15**, 245 (1927).

this appendix, but is not as large as would be expected from the linearly distributed resistance needed to account for the previous figures. The discrepancy could be caused by a nonlinear radiation resistance distribution.

The increase in resonance-curve width from a $\frac{1}{2}$ wave-length line to a one wave-length line is approximately the amount to be expected from the calculated ohmic value of α, thus again suggesting that the total effective distributed radiation resistance is nearly the same for these two line lengths.

The two resonant line lengths for the brass block termination, and the two for open-circuit termination differ by exactly the same amount, i.e. one-half-wave-length. The resonant length for copper sheet termination does not lie exactly half-way between the two open-circuit resonant lengths, however, implying that there is some phase shift (reactance component) in one or the other of these terminations. The angle of difference is about 5°. The fact that reactance measurements on straight copper wires have checked with theory quite accurately when referred to the copper plate termination suggests that the phase shift may be inherent in the open-circuit termination, possibly due to the abrupt cut-off of the cylindrical conductors. No ambiguity in measurements is caused by this discrepancy, however, over most impedance ranges likely to be encountered experimentally.

On the Resonant Frequency of Closed Concentric Lines

W. W. Hansen
Stanford University, California

(Received August 8, 1938)

A new and more exact method of calculating the resonant frequency of closed concentric line resonators of the type shown in Fig. 1 is developed. The method becomes more accurate as the length of the line becomes small by comparison with a quarter wave-length.

Introduction

In a certain new type of oscillation generator under development at Stanford we find it convenient to use resonators of the general type sketched in Fig. 1. There is, of course, nothing new about such a resonator and some approximation to the resonant frequency may be obtained by considering the resonator as a concentric line terminated by the capacity between the end of the re-entrant central tube and the disk closing the outer tube. Though often of sufficient precision, the formula so obtained is obviously pretty crude as it corresponds to assuming that the lines of E are distributed more or less as in Fig. 2a whereas it is plain that this is far from the truth, Fig. 2b giving a much better picture of the real distribution. Even if one ignores this difficulty other trouble appears, for the resulting formula contains the length of the concentric line and this is not well defined.

Now it so happens that in the application referred to, it is of prime importance to be able to predetermine the frequency with extreme accuracy. So we have devised a more exact calculation which is presented here both because others may have use for the results and also because certain points of the mathematical technique involved seem quite interesting.

The Analysis

The analysis proceeds according to the following plan. We divide the interior into two parts,[1] labeled I and II in Fig. 1. Then we make two vector functions corresponding to the electric field in the two sections. For any arbitrary frequency both functions are constructed to be exact solutions of the wave equation and to satisfy the proper boundary conditions. The functions are adjusted to have the same value over the joining surface but will then, in general, have discontinuous derivatives there. But the frequency is, as yet, a disposable constant and

[1] This division is a suitable one if $\delta \ll \rho_2 - \rho_1$. As this is so in the practical cases of interest to us, we have used this division. It should be noted, however, that if the sign of the inequality is reversed it would be better to make the division on the disk $z = \delta$. If this is done the analysis can be carried through in a way quite similar to that here reported.

by proper choice of this it is possible to make the functions join smoothly on at least one line on the dividing surface. In this way the frequency is determined.

As a first step, then, we seek a suitable wave function for use in region I. This must be built up in the form of an infinite series. Thus let us define the sequence of functions

$$\mathbf{E}_n{}^I = \mathbf{k}_\rho \frac{a_{I,n}}{b_{I,n}} \sin(a_{I,n}z) L_1{}^I(b_{I,n}\rho) + \mathbf{k}_z \cos(a_{I,n}z) L_0{}^I(b_{I,n}\rho) \tag{1}$$

with
$$a^2{}_{I,n} + b^2{}_{I,n} = k^2 = (2\pi/\lambda)^2, \tag{2}$$

$$a_{I,n} = n\pi/z_0, \quad n = 0, 1, 2\cdots, \tag{3}$$

$$L_0{}^I = \frac{N_0(b_{I,n}\rho_2)J_0(b_{I,n}\rho) - J_0(b_{I,n}\rho_2)N_0(b_{I,n}\rho)}{N_0(b_{I,n}\rho_2)J_0(b_{I,n}\rho_1) - J_0(b_{I,n}\rho_2)N_0(b_n\rho_1)}, \tag{4}$$

$$L_1{}^I = \frac{N_0(b_{I,n}\rho_2)J_1(b_{I,n}\rho) - J_0(b_{I,n}\rho_2)N_1(b_{I,n}\rho)}{N_0(b_{I,n}\rho_2)J_0(b_{I,n}\rho_1) - J_0(b_{I,n}\rho_2)N_0(b_{I,n}\rho_1)}, \tag{5}$$

ρ, ϕ, z = standard cylindrical coordinates, with unit vectors $\mathbf{k}_\rho, \mathbf{k}_\phi, \mathbf{k}_z$.

Inspection will show that these satisfy the wave equation, and that $E_\rho = 0$ at $z = 0$, z_0, and $E_z = 0$ at $\rho = \rho_2$, i.e., the proper boundary conditions are fulfilled over these surfaces.

Before going on to use these functions, we will interpolate a remark on a minor point in connection with numerical work. That is, we observe that since z_0 is ordinarily less than $\lambda/4$ and certainly less than $\lambda/2$, only b_{I0} is real; all the higher $b_{I,n}$ are purely imaginary. As suitable tables of the N_0 and N_1 functions are not common, it is convenient to substitute for the J and N functions the functions I and K which are essentially equivalent and are well tabulated. (Watson's *Bessel Functions*.) Unfortunately, these functions do not satisfy the same recursion formula as the ordinary Bessel functions, so that the equations defining L_0 and L_1 in terms of I and K differ slightly from (4) and (5). To avoid possible confusion and bother we write out the proper formulae which are to be used when $b_{I,n}$ is imaginary.

$$L_0{}^I = \frac{K_0(-ib_{I,n}\rho_2)I_0(-ib_{I,n}\rho) - I_0(-ib_{I,n}\rho_2)K_0(ib_{I,n}\rho)}{K_0(-ib_{I,n}\rho_2)I_0(-ib_{I,n}\rho_1) - I_0(-ib_{I,n}\rho_2)K_0(-ib_{I,n}\rho_1)}, \tag{4'}$$

$$L_1{}^I = i\frac{K_0(-ib_{I,n}\rho_2)I_1(-ib_{I,n}\rho) + I_0(-ib_{I,n}\rho_2)K_1(-ib_{I,n}\rho)}{K_0(ib_{I,n}\rho_2)I_0(-ib_{I,n}\rho_1) - I_0(-ib_{I,n}\rho_2)K_0(-ib_{I,n}\rho_1)}. \tag{5'}$$

Also, the positive root is taken so that $-ib_{I,n}$ is real and positive.

We have now to combine the $\mathbf{E}_n{}^I$ into an infinite series that will make the z component of the electric field take on the proper values on the cylinder $\rho = \rho_1$. But what are the proper values? Of course, in the range $\delta < z < z_0$ the z component should be zero. But in $0 < z < \delta$ the proper values are not known, and one must make some assumption. Now, if we made exactly the right assumption, and were able to carry the analysis through, we would find that, if we matched the functions valid in regions I and II along the cylinder dividing the two regions, then a proper choice of frequency would result in the derivatives also matching and we should have an exact solution. Actually, however, the proper function is not known, with the result that the derivatives can only be matched on a single line (ring). At other places the derivative will be discontinuous by an amount depending on how well the chosen function for the component of the electric field approximates the truth.

The above sounds discouraging as it would seem that all depends on a good guess as to a certain function. But in actual fact the situation is very good because: (a) Errors in choice of the proper function change only the higher terms in

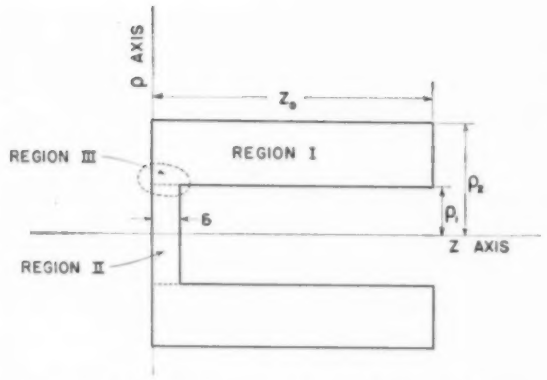

FIG. 1. This shows a cross section of the type of resonator considered, along with the coordinate axes and some of the notation used. The inside is divided into two mutually exclusive regions labeled I and II; the (hypothetical) cylinder dividing the regions being shown dotted. There is also shown a small region III which contains some of both I and II.

the approximation for the frequency and only change these slowly, so that the simplest possible choice of function gives good accuracy on the frequency and (b) we have had the enormous good fortune to discover a function which can be demonstrated to be very nearly correct and for which the analysis can be carried through.

To justify the above statements we start by considering how we may guess a likely function. This may be done by remembering that, in a sufficiently small region, solutions of Laplace's equation and the wave equation may be found that are almost identical. Thus, provided $\delta \ll \lambda$, an appropriate exact solution of the electrostatic problem in the region designated by III in Fig. 1 will give values for the electric field that are almost exactly right.

Now the electrostatic problem is soluble if we also have $\delta \ll \rho_1$, for then we may, without appreciable error, consider the problem as a two-dimensional one in which case it can be solved by using the Schwarz-Christoffel transformation.

Since a solution is much simplified if $\delta \ll \rho_2 - \rho_1$, and as this condition is well fulfilled in the practical cases which interest us, we have assumed that this inequality is satisfied. Doing this we find the electric field that would exist on the line $\rho = \rho_1$, $0 < z < \delta$ if the conductors on opposite ends of this line were maintained at a fixed potential difference. A graph of field strength could be constructed, but for our purposes the following statements furnish a better characterization. First, for unit difference of potential between the boundaries, the field at $z=0$, $\rho = \rho_1$ has the value $0.833/\delta$. Also, obviously, $\partial E_z/\partial z = 0$ there. Second, for the same p.d., the field at $z=\delta$, $\rho = \rho_1$, i.e., near the corner, is $0.515/(\delta^{\frac{1}{2}}(\delta - z)^{\frac{1}{2}})$.

Now the two-parameter formula constant $\times(\delta^2 - z^2)^{-\frac{1}{2}}$ + constant has the same general behavior as the exact function described above and by proper adjustment of the constants any two of three quantities p.d., magnitude of singularity at $z=\delta$, and magnitude at $z=0$ can be made exactly right, after which the discrepancy in the remaining quantity will be some measure of how well this function approximates the truth. Not knowing which are the best two we have arbitrarily made the potential difference and the magnitude of the singularity at the corner the same as for the exact function, with the result that we assume

$$E_z = \frac{1.03}{\delta^{\frac{1}{2}}(\delta^2 - z^2)^{\frac{1}{2}}} - \frac{0.32}{\delta} \qquad 0 < z < \delta \qquad (6)$$

$$= 0 \qquad \delta < z < z_0.$$

It will be found that this choice of constants makes the field at $z=0$ about 10 percent too low. Inasmuch as (6) must cross the true function in the range $0 < z < \delta$ we see that besides having a shape very similar indeed to the true function (6) can never be very far off in actual value.

Though we will actually use (6), which must be very close to correct, it can be shown that even using such a crude formula as $E_z = (1/\delta)$ gives very good results, i.e., the final answer is very insensitive to the choice of field on the boundary between regions I and II.

Using (6) we can expand the field along the cylinder $\rho = \rho_1$ in the ordinary Fourier manner and so find the field throughout region I. A small

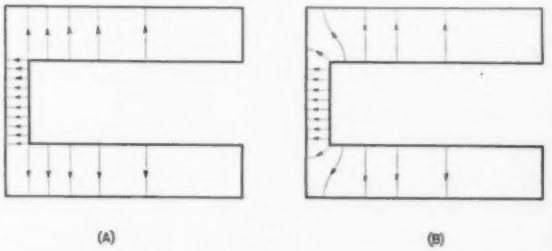

FIG. 2a. Qualitative drawing of an assumed field distribution. 2b. Another, and better, field distribution.

difficulty arises in the integration of the first term of (6) but it is found that this can be done in terms of Bessel's functions. On carrying through the calculation we find for the electric field

$$\mathbf{E}=\sum c_{I,n}\mathbf{E}_{I,n}$$

$$=\mathbf{k}_\rho\sum c_{I,n}\frac{a_{I,n}}{b_{I,n}}\sin(a_{I,n}z)L_1^I(b_{I,n}\rho)$$

$$+\mathbf{k}_z\sum c_{I,n}\cos(a_{I,n}z)L_0^I(b_{I,n}\rho) \quad (7)$$

with

$$c_{I,n}=c'_{I,n}+c''_{I,n}, \quad (8)$$

$$c'_{I,n}=\frac{1}{z_0}2.06\frac{3\pi^{\frac{1}{2}}}{2^{11/6}}(2/3)!\frac{J_{1/6}(n\pi\delta/z_0)}{(n\pi\delta/z_0)^{1/6}}, \quad n\neq 0, \quad (9)$$

$$c''_{I,n}=-\frac{1}{z_0}0.64\frac{z_0}{n\pi\delta}\sin\frac{n\pi\delta}{z_0}, \quad n\neq 0. \quad (10)$$

As to $n=0$, $c_{I,0}=1/z_0$.

Now in exactly the same way we can find the field in region II. The functions needed are rather simpler, being

$$\mathbf{E}_n^{II}=\mathbf{k}_\rho\frac{a_{II,n}}{b_{II,n}}\sin(a_{II,n}z)L_1^{II}(b_{II,n}\rho)$$

$$+\mathbf{k}_z(\cos a_{II,n}z)L_0^{II}(b_{II,n}\rho) \quad (11)$$

with

$$a^2_{II,n}+b^2_{II,n}=k^2, \quad (12)$$

$$a_{II,n}=n\pi/\delta, \quad (13)$$

$$L_0^{II}=(J_0(b_{II,n}\rho)/J_0(b_{II,n}\rho_1)), \quad (14)$$

$$L_1^{II}=(J_1(b_{II,n}\rho)/J_0(b_{II,n}\rho_1)). \quad (15)$$

Here, as before, supplementary definitions are useful when $b_{II,n}$ is imaginary. Thus we write

$$L_0^{II}=I_0(-ib_{II,n}\rho)/I_0(-ib_{II,n}\rho_1), \quad (14')$$

$$L_1^{II}=iI_1(-ib_{II,n}\rho)/I_0(-ib_{II,n}\rho). \quad (15')$$

In terms of these the field in region II that satisfies the proper boundary conditions and has the value (6) on the boundary cylinder $\rho=\rho_1$ is found to be

$$\mathbf{E}=\sum c_{II,n}\mathbf{E}_{II,n}, \quad (16)$$

$$c_{II,n}=\frac{1}{\delta}2.06\frac{3\pi^{\frac{1}{2}}}{2^{11/6}}(2/3)!\frac{J_{1/6}(n\pi)}{(n\pi)^{1/6}}, \quad n\neq 0, \quad (17)$$

$$=1/\delta, \quad n=0.$$

It will be observed that the coefficients (17) may be derived from those of (8), (9), (10) by replacing z_0 by δ.

Having thus found suitable fields in the regions I and II that have the same tangential component on the common boundary, we can now determine the frequency. To do this any one of a number of the characteristics of E might be made continuous on crossing the boundary between I and II but perhaps the simplest is to match values of the magnetic field. To do this we need expressions for the magnetic field in the two regions. These are easily found to be

$$\mathbf{B}=\mathbf{k}_\phi k\sum c_{I,n}\frac{1}{b_{I,n}}$$

$$\times\cos(a_{I,n}z)L_1^I(b_{I,n}\rho) \text{ in region I} \quad (18)$$

and

$$\mathbf{B}=\mathbf{k}_\phi k\sum c_{II,n}\frac{1}{b_{II,n}}$$

$$\times\cos(a_{II,n}z)L_1^{II}(b_{II,n}\rho) \text{ in region II.} \quad (19)$$

Now we might try to make these expressions equal on any ring on the boundary between I and II, but it is plain that by far the easiest will be that at $z=0$. We therefore seek to make the two expressions

$$\mathbf{B}(\rho=\rho_1,\ z=0)=\mathbf{k}_\phi k\sum c_{I,n}\frac{1}{b_{I,n}}L_1^I(b_{I,n}\rho_1) \quad (20)$$

and

$$\mathbf{B}(\rho=\rho_1,\ z=0)$$

$$=\mathbf{k}_\phi k\sum c_{II,n}\frac{1}{b_{II,n}}L_1^{II}(b_{II,n}\rho_1) \quad (21)$$

equal.

But at this point we meet a most depressing difficulty in that the series, though by test convergent, converge so slowly as to be useless for calculation. To get a qualitative idea we note that, for any but very small n, $1/b_{I,n}$ decreases

as $1/n$ while $c''_{I,n}$, for example, decreases as $(z_0/n\pi\delta)\sin n\pi\delta/z_0$ and $-L_1{}^I$ rapidly approaches unity. Thus the terms start out by being all of one sign and decreasing like $1/n$, i.e., not fast enough to converge at all. Of course when n becomes larger than z_0/δ the absolute values of the terms decrease, on the average, as $1/n^2$, and one has in addition reversals of sign every z_0/δ terms. Either of these considerations alone would suffice to make the series convergent, but both together do not render it in any sense suitable for numerical calculation.

This matter is really the crucial point in the whole analysis and must be surmounted if progress is to be made.

This may be done as follows. We find a series satisfying the following two requirements: (a) its sum is known and (b) in the limit of large n its terms become equal to the terms of the series in (20), for instance. Then from the series to be summed we subtract, term by term, the series of known sum and also add the value of the known series. The series resulting from this transformation will, of course, converge with greater rapidity than the original series, the degree of increase of convergence depending on how rapidly the terms of the two series that are subtracted approach equality. A transformation of this type is sometimes known as Kummer's transformation.

To apply this transformation in the present case we introduce the following functions which really combine two series.

$$\sigma_m(x)=\sum_1^\infty {}_n\frac{1}{n^m}\left[2.06\frac{3\pi^{\frac{1}{2}}}{2^{11/6}}(2/3)!\frac{n^{5/6}}{x^{1/6}}\times J_{1/6}(nx)-0.64\frac{1}{x}\sin nx\right]. \quad (22)$$

We postpone for a time the not inconsiderable question of how these series are to be summed when actual values of the σ_m are needed.

Also we need to describe the behavior of $L_1{}^I(b_{I,n}\rho_1)/b_{I,n}$ for large values of n. It will be found that for large imaginary values of the argument, which correspond to large values of n, the function $L_1{}^I$ approaches -1 while $L_1{}^{II}\rightarrow+1$. Moreover, higher terms in the expansion in powers of $(1/n)$ are easily found from the known asymptotic expansions of the Bessel's functions involved. Thus we can write the exact expressions

$$\frac{L_1{}^I(b_{I,n}\rho_1)}{b_{I,n}}=-\frac{z_0}{\pi n}\left[1+\frac{\alpha_1{}^I}{n}+\cdots\frac{\alpha_k{}^I}{n^k}+\Delta_k{}^I(n)\right], \quad (23)$$

$$\frac{L_1{}^{II}(b_{II,n}\rho_1)}{b_{II,n}}=\frac{\delta}{\pi n}\left[1+\frac{\alpha_1{}^{II}}{n}+\cdots\frac{\alpha_k{}^{II}}{n^k}\Delta_k{}^{II}(n)\right], \quad (24)$$

which define the quantities Δ. Any desired number of powers of $1/n$ may be used, the choice being governed by the following considerations. As the number is increased the sequence $\Delta_k(n)$ becomes more tedious to compute and may need more terms before beginning to run smoothly. On the other hand the sequence eventually converges the more rapidly the more powers of $1/n$ are carried.

We may note at this point that the possibility of using Kummer's transformation depends entirely on the ability to determine the quantities α correctly, i.e., on the knowledge of the asymptotic expansions of L_1.

Now we introduce another bit of notation

$$\sum_k{}^I(x)=\sum\frac{\Delta_k{}^I(n)}{n^2}\left(2.06\frac{3\pi^{\frac{1}{2}}}{2^{11/6}}(2/3)!\frac{n^{5/6}}{x^{1/6}}\times J_{1/6}(nx)-0.64\frac{1}{x}\sin nx\right) \quad (25)$$

with $\sum_k{}^{II}$ defined in a similar way.

Then on equating magnetic fields we find

$$\sigma_2(x)+\cdots\alpha_k{}^I\sigma_{k+2}(x)+\sum_k{}^I(x)+\sigma_2(\pi)+\cdots\alpha_k{}^{II}\sigma_{k+2}(\pi)+\sum_k{}^{II}(\pi)+\frac{\pi^2}{kz_0}\left(\frac{1}{x}L_1{}^{II}(k\rho_1)-\frac{1}{\pi}L_1{}^I(k\rho_1)\right)=0, \quad (26)$$

where $x=\pi\delta/z_0$.

Till now we have spoken as if this equation is to be satisfied by properly adjusting k, the various dimensions remaining fixed. In actual practice, however, because k enters in so many ways, both explicit and implicit, it is easier to assume fixed values of k, z_0, ρ_1 and ρ_2 and vary δ until the equation is satisfied. We will find that this

is quite easy, provided we can consider the functions σ_m as known and provided also the sequence of Δ_k decreases rapidly.

Thus if these provisos are fulfilled, as in fact they are, the problem is essentially solved.

We conclude the analysis therefore by showing how the functions σ_m are to be determined from the defining series. In the next section it will be shown by numerical trial, for a typical case, that the Δ_k decrease very rapidly indeed.

To evaluate the σ_m it is convenient to break them up into two series: thus we define

$$\mathbf{S}_m(x)=\sum_1^\infty (1/n)^m \sin(nx), \tag{27}$$

$$\mathbf{J}_m(x)=\sum_1^\infty (1/n)^{m-5/6} J_{1/6}(nx). \tag{28}$$

Consider then the first of the functions $\mathbf{S}_m$ that we need, the one for which $m=2$. This can be summed in a variety of ways, perhaps the simplest of which is to differentiate it, when the resulting series will be recognized as known.

Thus

$$(d/dx)\mathbf{S}_2(x)=\sum_1^\infty (1/n)\cos(nx)=\log 2 \sin(x/2). \tag{29}$$

The right-hand side is now expanded in power series, either about the point $x=0$, or about $x=\pi$, and the series integrated term by term. If the expansion is about $x=0$ the result is

$$\mathbf{S}_2(x)=-x\log\frac{x}{e}+\frac{1}{72}x^3+\frac{1}{14400}x^5+\frac{1}{1{,}270{,}080}x^7. \tag{30}$$

Although this series is easy to compute, even when $x=\pi$, it is convenient to have also the expansion about π.

This is found to be

$$\mathbf{S}_2(\pi+y)=-y\log 2+\frac{1}{24}y^3+\frac{1}{960}y^5+\frac{1}{20{,}160}y^7\cdots. \tag{31}$$

The function $\mathbf{S}_3$ is a known series being in fact

$$\mathbf{S}_3(x)=\sum_1^\infty \frac{\sin nx}{n^3}=\frac{x}{12}(\pi-x)(2\pi-x)=\frac{1}{12}x(x-\pi)(x-2\pi). \tag{32}$$

We have not used any of the $\mathbf{S}_m$ beyond $\mathbf{S}_3$, but they can be found if needed by integration. Thus $\mathbf{S}_4$ would be obtained by integrating $-\mathbf{S}_2$ twice. We conclude that the $\mathbf{S}_m$ can be regarded as known functions.

We come now to the function $\mathbf{J}_2$, or what is a little more convenient for the moment,

$$(2/x)^{1/6}\mathbf{J}_2(x)=\sum_1^\infty (1/n)(2/nx)^{1/6}J_{1/6}(n/x). \tag{33}$$

This series is known as a Schlömilch series and a useful discussion will be found in Watson, *Theory of Bessel Functions*, Chapter XIX. The analysis there suggests that we introduce an auxiliary function $g(x)$ (we follow Watson's notation).

$$g(x)=\sum_1^\infty (1/n)\cos(nx). \tag{34}$$

Then Watson shows that the series (33) may be evaluated from $g(x)$ by the following formula:

$$\left(\frac{2}{x}\right)^{1/6}\mathbf{J}_2(x)=\frac{2}{\Gamma(2/3)\Gamma(1/2)}\times\int_0^{\pi/2}\cos^{\frac{1}{2}}\theta\, g(x\sin\theta)\,d\theta. \tag{35}$$

Now we have already determined g; see (29) above. This can be expanded in power series and put in the integrand of (35) when it will be found that except for one term the series can be integrated using B integrals. The single remaining integration is done numerically. In this way we find

$$\frac{1}{x^{1/6}}\mathbf{J}_2(x)=-\frac{2^{5/6}}{3}\frac{2}{(2/3)!\pi^{\frac{1}{2}}}\int_0^{\pi/2}\cos^{\frac{1}{2}}\theta\cos\sin\theta\,d\theta-\frac{(2\pi)^{\frac{1}{2}}}{3}\frac{(1/3)!}{(2/3)!(1/6)!(1/6)!}\times\left[\log x-\frac{1}{56}x^2-\frac{3}{29{,}120}x^4\frac{1}{774{,}592}x^6\cdots\right]. \tag{36}$$

The numerical value of the integral is found to be 1.060. This series converges rapidly, three terms giving better than one percent accuracy at the highest value of x, namely π. The similarity between this series and that for $(1/x)\mathbf{S}_2$ should be noted.

The function $\mathbf{J}_3$ is evaluated in an exactly similar manner. The results are somewhat simpler however because the auxiliary function $g(x)$ can be expressed in a finite number of powers of x. In fact we find

$$\frac{1}{x^{1/6}}\mathbf{J}_3(x)=\frac{\pi^{\frac{1}{2}}}{3(2)^{\frac{1}{2}}}\frac{(1/3)!}{(2/3)!(1/6)!}\left[\frac{\pi^2}{3}\frac{1}{(1/6)!}-\frac{\pi}{2}\frac{1}{(1/2)!(2/3)!}x+\frac{3}{14(1/6)!}x^2\right]. \quad (37)$$

The higher $\mathbf{J}$ can be evaluated in a similar manner so that all the $\mathbf{J}$ can be regarded as known.

Using the above results, the σ_m functions are easily determined. We have only used the first two; these are plotted in Fig. 3.

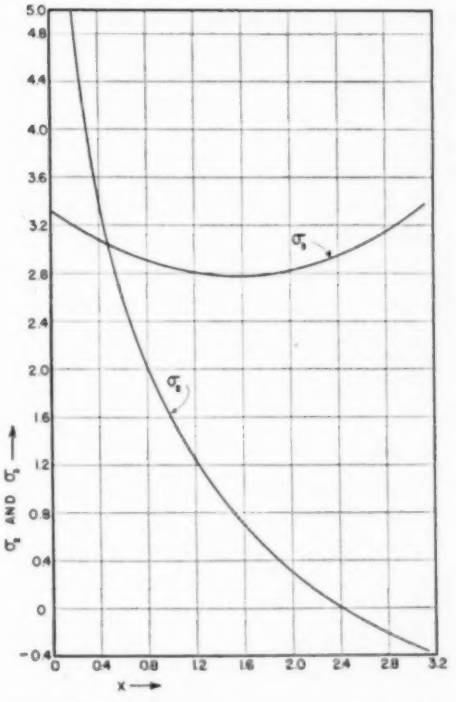

FIG. 3. Plot of the functions $\sigma_2(x)$ and $\sigma_3(x)$.

NUMERICAL EXAMPLE AND ESTIMATE OF ERRORS

In this section we show by example that Eq. (26) is not difficult to use in practice and also make some estimate of the accuracy of our method.

First we must decide what is the easiest thing to solve for. A little reflection will show that ρ_1, ρ_2 should certainly be given because they enter in such complex ways in the L. Also it will be found that k and z_0 should be given and x should be solved for. This solution will be of the cut and try type, but this seems unavoidable. In any case, we will soon see that the "cut and try" part does not involve any appreciable labor.

Let us assume, for a specific example, that we have given the values $k=0.35$ cm^{-1}, $\rho_1=1.27$ cm, $\rho_2=3.81$ cm, $kz_0=0.1$. Now we need a trial value of x. This we obtain by noting that all the various functions involved are of the order of magnitude unity and that $\pi^2/kz_0\sim 100$, so that an approximate solution may be obtained by equating the expression in the round brackets to zero. Calculating this out we find $L_1^{II}(k\rho_1)=0.228$, $(1/\pi)L_1^I \times(k\rho_1)=0.857$ so that x is approximately 0.266.

We now proceed to substitute the above value of x throughout the equation. Before doing so we must decide how many terms of the asymptotic expansion to use. We arbitrarily decided to keep two, i.e., we use only σ_2 and $\alpha_1\sigma_3$ etc. Now we go through the equation from the beginning. term by term. From Fig. 3 we find $\sigma_2(x)=4.24$, Next we find $\alpha_1{}^I=z_0/2\pi\rho_1=0.036$. Getting $\sigma_3(x)=3.15$ from Fig. 3 we find the second term to be 0.11. As for $\sum_1{}^I$ it is found that all terms of this are negligible, because with small z_0, $b_{I,1}$ is large and $L_1{}^I(b_n\rho_1)$ is very well given by its asymptotic expansion. Next we read from Fig. 3 $\sigma_2(\pi)=-0.370$. The quantity $\alpha_1{}^{II}\sigma_3(\pi)$ turns out to be negligible, because $\alpha_1{}^{II}$ is small. The sum $\sum_1{}^{II}$ is negligible for the same reasons that $\sum_1{}^I$ is. Finally the term in brackets has been made zero by the choice of x.

Now on adding all the above up, it will be found that the sum is 3.98 instead of zero. In principle we should try another value of x throughout the equation in an endeavor to get the sum of the terms to come to zero. But actually this is not necessary because if we were to differentiate with respect to x, the term coming from $(\pi^2/kz_0)L_1{}^{II}(x)(1/x)$ would be much larger than

any of the others. Thus to a high approximation we can estimate from this term alone how much to alter our assumed x. Doing this we find that x should be increased by 0.0125, so that, to three figures, our final answer for x is $x = 0.278$.

To sum up the above calculation we may say that, for this value of kz_0, only five terms in (26) need be counted and these are all very easily computed or are looked up on curves.

If now we repeat the above calculation for a higher value of kz_0, say $kz_0=0.2$, the following changes occur. First, the coefficient in front of the last bracket will be half as big as before, so that a good trial value of x is slightly more important. On the other hand a good guess is now easily obtained by extrapolation from the known values at $kz_0=0$, 0.1. For still higher values of kz_0 the above remarks apply with increasing force. Aside from this, there is no great change in the calculation until one reaches about $kz_0=1$ when one finds that $\sum_1{}^I$ is no longer negligible. This adds a certain amount of labor to the calculation but not much because the series for $\sum_1{}^I$ converges so rapidly that we need only one term!

In fact, after trying the above calculation up to $kz_0=1.3$, we have concluded that (26) is indeed very easy and practical to compute with. All of the quantities except the $\sum$ are easily computed or can be found from graphs. The $\sum$ are given by infinite series and this might be some bother except that it is found that the series converge in one term.

Finally, we should like to give some estimate of the magnitude of errors. Perhaps the biggest weakness of the present method is that we have not been able to formulate a really convincing estimate of the errors for all cases. But in one case, which happens to be the one of greatest interest to us, a good estimate is possible. Thus, let us suppose that δ is small compared to ρ_1, $\rho_2-\rho_1$ and of course to λ. Then replacing the true solution of the cylindrical wave equation by a two-dimensional solution of Laplace's equation, as we have done, will be an enormously good approximation. In this case there is no doubt that practically all the errors in the calculation arise when this exact solution of Laplace's equation is approximated by the function of Eq. (6). Now, the magnitude of the errors from this cause can be estimated by varying the coefficients in (6) and observing the results on the final answer. Now, it is convenient in doing this to keep the integral of E_z from 0 to δ unity because this keeps the $n=0$ terms, which are treated separately, constant. Thus all the changes occur in the σ and $\sum$ terms. But as a consequence of the above, any change in one of the coefficients in (6) requires a change in the other and as the two appear in about the same way in the expression for σ as in (6) it is plain that the σ will not change much. In fact, it is found that the ten percent uncertainty in the first coefficient results in less than one percent uncertainty[2] in the σ. Thus the final errors in x are quite small indeed, and our assertion, that large errors in the field on the surface, separating I and II make little difference in the frequency, is justified. Also, we note that the percentage error in x, and so in δ, decreases linearly with kz_0, so that in the limit $kz_0\to 0$ the result is exact. On the other hand even when $kz_0=1$ the uncertainties will be less than one-tenth percent.

This represents an enormous advance over formulae that consider such a resonator as a concentric line terminated by a condenser. In addition to neglecting fringing in computing the capacity such formulae suffer from uncertainty as to whether to take z_0 or $z_0-\delta$ as the length of the line. That this may be serious is illustrated by the present case where the uncertainty is about four percent at $kz_0\to 0$, and rises to 30 percent at $kz_0=1$ and becomes infinite at $kz_0=1.57$ (corresponding to $z_0=\lambda/4$).

[2] One can be even more extreme and try the effect of using $E_z=1/\delta$ instead of (6). Although this is surely about the poorest approximation that might be used, the value of the main correction term σ_2 is changed by less than ten percent. This justifies various assertions made earlier in the paper.

Studies in Lubrication

III. The Theory of the Thick Film Lubrication of a Complete Journal Bearing of Finite Length with Arbitrary Positions of the Lubricant Source

M. Muskat and F. Morgan
Gulf Research & Development Company, Pittsburgh, Pennsylvania

(Received August 13, 1938)

A successive approximation theory is developed for the thick film lubrication of complete journal bearings of finite length for arbitrary positions of the lubricant source. It has been carried through in detail up to the third approximation, which permits studies of systems having journal eccentricities up to the value of $\frac{1}{2}$. The range of bearing length for which the theory is valid includes such as are of the order of, or greater than, half the bearing perimeter. Detailed calculations are reported on the interrelationships between the attitude of the line of centers of the journal and bearing, the journal eccentricity, the lubricant source strength, the "Sommerfeld variable," $(r^2/c^2)\mu N/P$—where r=journal radius, c=radial clearance, μ=lubricant viscosity, N=journal speed and P=bearing load per unit projected bearing area—and the coefficient of friction, both for lubricant sources set at the crown and base of the bearing. Most of the numerical results refer to the case where the bearing length equals the bearing perimeter. In general it is found that when the lubricant source is at the crown or unloaded portion of the bearing, it tends to increase the journal eccentricities, oppose the journal supporting forces caused by the journal rotation, and increase the friction coefficients. When the source is set at the base, or loaded side, of the bearing, and has a strength less than the "critical value," determined by the bearing length, it tends to decrease the journal eccentricities, to aid in supporting the load, and to decrease the friction coefficients on the journal. At the "critical values" of source strength the journal becomes concentric with the bearing and the lubricant source alone supports the load. For higher values of source strength the journal is raised above the center of the bearing so that the journal rotation detracts from the load-carrying power of the film, and the friction coefficient on the journal begins to rise. Moreover, when the source is set at the base of the bearing, the friction coefficient curves for both the bearing and journal, when plotted against the Sommerfeld variable, all go through the origin in contrast to the infinitely long bearing theory where the coefficient of friction on the journal has a unit friction axis intercept. From the hydrodynamic point of view there are therefore no minima in the curves, or suggestions of thin film friction rises when the lubricant source is at the base of the bearing.

IN PART I[1] of this series was developed a theory of the thick film lubrication of a complete journal bearing of finite length under the assumptions that the bearing length was of the order of, or greater than, the bearing perimeter, and that the lubricant source was set 90° in advance of the maximum film thickness. In the present paper this theory will be extended and generalized so as to include bearing lengths as short as one-half the bearing perimeter, and so as to apply to arbitrary positions of the source of lubricant. While the general method of analysis will be the same, the details of the calculations will differ from the previous development.

General Theory

As before, the fundamental starting point for the theory will be the generalized Reynolds equation for the pressure distribution in the film of the lubricant, namely,

$$\nabla\cdot\left(\frac{h^3}{12\mu}\nabla p\right)=\frac{U}{2r}\frac{\partial h}{\partial\theta}, \tag{1}$$

where h is the film thickness, μ the lubricant viscosity, p the pressure in the film, U the surface velocity of the journal, r the journal radius, and θ the azimuthal coordinate (cf. Fig. 1). In order to derive results valid for any position of the lubricant source, it will be convenient to consider the lubricant source as fixed, so as to define the origin of the coordinates, and to suppose that the line of centers of the journal and bearing is tilted with respect to the source by the arbitrary angle α. In this system the film thickness will be given by

$$h=c+e\cos(\theta-\alpha), \tag{2}$$

where c is the radial clearance and e the journal

[1] M. Muskat and F. Morgan, J. App. Phys. **9**, 393 (1938). A brief review of the literature on theoretical studies of the hydrodynamics of lubrication will be found in this paper.

displacement. It will also be supposed that the load is applied to the journal.

Introducing the notation

$$\eta=e/c; \quad w=z/r; \quad \beta=6\mu Ur/c^2, \tag{3}$$

where η represents the journal eccentricity[2] and z is the coordinate along the journal bearing axis, and assuming that the viscosity μ is the same everywhere throughout the film,[3] Eq. (1) takes the dimensionless form

$$\frac{\partial}{\partial\theta}\left\{(1+\eta\cos(\theta-\alpha))^3\frac{\partial p}{\partial\theta}\right\}+(1+\eta\cos(\theta-\alpha))^3\frac{\partial^2 p}{\partial w^2}=-\beta\eta\sin(\theta-\alpha), \tag{4}$$

where p is supposed to be expressed in terms of a unit pressure (atmospheric). This equation and the subsequent analysis reduces to that developed in Part I of this series if α be set equal to $\pi/2$.

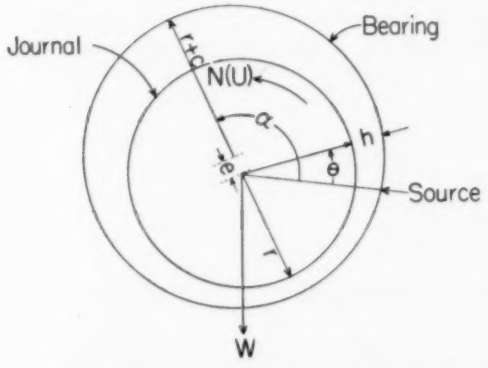

FIG. 1. Cross section of a complete journal bearing system.

To solve Eq. (4) we again use a successive approximation method in which all the physical quantities of interest are expanded in powers of the eccentricity η. That is, we assume that the pressure distribution $p(\theta, w)$ can be expanded in the form:

$$p(\theta, w)=\sum\eta^m p_m(\theta, w). \tag{5}$$

This is inserted in Eq. (4), and after the expansion of the various terms the coefficients of like powers of η are equated. We thus find a series of equations for the p_m given by

$$\left.\begin{aligned}
&\nabla^2 p_0=\partial^2 p_0/\partial\theta^2+\partial^2 p_0/\partial w^2=-\beta\eta\sin(\theta-\alpha),\\
&\nabla^2 p_1=-3\cos(\theta-\alpha)\nabla^2 p_0\\
&\qquad\qquad +3\sin(\theta-\alpha)\partial p_0/\partial\theta,\\
&\cdots\cdots\cdots\cdots\cdots\cdots\\
&\nabla^2 p_m=-3\{\cos(\theta-\alpha)\nabla^2 p_{m-1}\\
&\qquad -\sin(\theta-\alpha)\partial p_{m-1}/\partial\theta\}\\
&\qquad -3\cos(\theta-\alpha)\{\cos(\theta-\alpha)\nabla^2 p_{m-2}\\
&\qquad -2\sin(\theta-\alpha)\partial p_{m-2}/\partial\theta\}\\
&\qquad -\cos^2(\theta-\alpha)\{\cos(\theta-\alpha)\nabla^2 p_{m-3}\\
&\qquad\qquad -3\sin(\theta-\alpha)\partial p_{m-3}/\partial\theta\}.
\end{aligned}\right\} \tag{6}$$

It is thus seen that formally the solution of Eq. (4) has been reduced to that of a series of equations of a known type, namely, the Poisson equation. It should be noted that in this reduction the term $\beta\eta\sin(\theta-\alpha)$ has been considered as a zero-order term in spite of the coefficient η. This has been done in order to permit the asymptotic behavior of the system, where η approaches zero, to correspond to one where the load is nonvanishing, since in the limit of very small values of η, $\beta\eta$ becomes proportional to the load.[4] In Part I it was assumed that the limit $\eta\to 0$ corresponds to a vanishing load, whereas here it is supposed that this limit is to be attained by making β very large. Either assumption may be used without changing the essentials of the analysis. All that will be affected will be the power of η having β as the coefficient which will be retained in any particular order of the approximation.

In constructing the solutions of Eq. (6) we shall denote the dimensionless half-length of the bearing by w_0. The assumption that the bearing length is equal to or greater than half the bearing perimeter will therefore imply that $w_0\geqslant\pi/2$ in the solutions. Terms of the order of e^{-2w_0} will be

[2] For simplicity, η is being called throughout this paper the journal "eccentricity," rather than the "eccentricity ratio."

[3] While the variation of the viscosity with the film temperature would be quite difficult to take into account, the effect of pressure can be taken care of by simply making the change of variable: $\Psi=\int dp/\mu$, which will reduce Eq. (1) to the same form as Eq. (4). This possibility was pointed out for an exponential variation of μ with p, by S. Skinner, J. App. Phys. **9**, 410 (1938).

[4] This will break down in the special case where the lubricant source is set at the base (loaded side) of the bearing and has a strength equal to the "critical" value (cf. below).

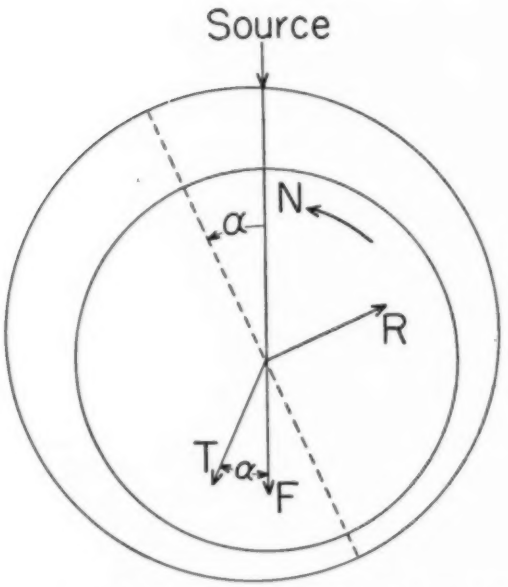

FIG. 2. Forces acting on the journal as the result of the pressure distribution in the lubricating film when the source is at the crown of the bearing.

dropped. The general conditions to be imposed upon the pressure distributions $p_m(\theta, w)$ are that

(1) They shall be even in w, corresponding to a source placed midway between the ends of the bearing.

(2) That p and $\partial p/\partial\theta$ reproduce themselves as θ makes the circuit of 2π around the circumference of the bearing.

(3) That p reduces to the value 1 at the ends of the bearing.

This last requirement will be satisfied by making p_0 equal to 1 at the ends of the bearing, and $p_m=0$ at the ends for $m>0$.

Proceeding now to the solutions of Eq. (6), we find for the zeroth approximation:

Zeroth approximation

$$p_0=1+\beta\eta\sin(\theta-\alpha)\left\{1-\frac{\cosh w}{\cosh w_0}\right\}$$

$$-q\left\{\log\frac{\cosh w-\cos\theta}{\cosh w_0}+\frac{\cos\theta\cosh w}{\cosh^2 w_0}\right\}. \quad (7)$$

It will be noted that Eq. (7) is the solution of the first of Eqs. (6). It is even in w, and periodic in θ; $\partial p/\partial\theta$ is also periodic in θ. At the ends of the bearing $w=\pm w_0$, p_0 reduces to 1 except for terms equal to or less than e^{-2w_0}. Furthermore, p_0 has a singularity at $\theta=w=0$, and therefore represents a source placed at that point. Its flux strength is q, and is related to the actual inflow Q through the source or leakage from the ends of the bearing by

$$q=\frac{3\mu Q}{\pi c^3(1+\eta\cos\alpha)^3}. \quad (8)$$

First approximation

Combining Eq. (7) with the second of Eqs. (6), we have for the Poisson equation giving p_1:

$$\nabla^2 p_1=3\beta\eta\sin 2(\theta-\alpha)\left\{1-\frac{\cosh w}{2\cosh w_0}\right\}-3q\sin(\theta-\alpha)\sin\theta\left\{\frac{1}{\cosh w-\cos\theta}-\frac{\cosh w}{\cosh^2 w_0}\right\}. \quad (9)$$

Its solution, which is free of singularities and satisfies the requirements previously listed, may be shown to be

$$p_1=\frac{\beta\eta}{2}\sin 2(\theta-\alpha)\left\{-\frac{3}{2}+\frac{\cosh w}{\cosh w_0}+\frac{\cosh 2w}{2\cosh 2w_0}\right\}+3q\left[\cos\left(\alpha-\frac{\theta}{2}\right)\cosh\frac{w}{2}\log\frac{\cosh w/2-\cos\theta/2}{\cosh w/2+\cos\theta/2}\right.$$

$$-\cos\alpha\log\frac{\cosh w-\cos\theta}{\cosh w_0}+\cos\alpha+\cos(\theta-\alpha)$$

$$\left.+\frac{\cosh w}{2\cosh^2 w_0}\{\cos\alpha+\tfrac{1}{3}\cos(2\theta-\alpha)\}-\frac{\cosh w\cos(\theta+\alpha)}{3\cosh^2 w_0}\right]. \quad (10)$$

Second approximation

Inserting the expressions for p_0 and p_1 into the Poisson equation for p_2, it is readily found that p_2 must satisfy the equation

$$\nabla^2 p_2=\frac{3}{2}\beta\eta\left[3\sin 3(\theta-\alpha)\left\{-1+\frac{\cosh w}{2\cosh w_0}+\frac{\cosh 2w}{6\cosh 2w_0}\right\}-\frac{1}{2}\sin(\theta-\alpha)\left\{\frac{\cosh w}{\cosh w_0}+\frac{\cosh 2w}{\cosh 2w_0}\right\}\right]$$

$$+9q\sin(\theta-\alpha)\left[\frac{1}{2}\cosh\frac{w}{2}\sin\left(\alpha-\frac{\theta}{2}\right)\log\frac{\cosh w/2-\cos\theta/2}{\cosh w/2+\cos\theta/2}+\frac{1}{2}\sin\alpha-\frac{1}{2}\sin(\theta-\alpha)\right.$$

$$\left.+\frac{\sin\theta\{5\cos(\theta-\alpha)-3\cos\alpha\}}{6(\cosh w-\cos\theta)}+\frac{\cosh w}{3\cosh^2 w_0}\{\sin(\alpha+\theta)-\sin(2\theta-\alpha)-\sin\theta\cos(\theta-\alpha)\}\right]. \quad (11)$$

A solution of this equation which is symmetrical in w, periodic in θ, free of singularities, and vanishes at $w=\pm w_0$, is

$$p_{20}=\frac{\beta\eta}{160}\sin 3(\theta-\alpha)\left\{80-45\frac{\cosh w}{\cosh w_0}-24\frac{\cosh 2w}{\cosh 2w_0}-11\frac{\cosh 3w}{\cosh 3w_0}\right\}$$

$$-\frac{\beta\eta}{4}\sin(\theta-\alpha)\left\{\frac{3}{2}\frac{w\sinh w}{\cosh w_0}-\frac{3}{2}\frac{w_0\tanh w_0\cosh w}{\cosh w_0}+\frac{\cosh 2w}{\cosh 2w_0}-\frac{\cosh w}{\cosh w_0}\right\}+\frac{9}{2}q-\frac{9}{4}qw_0$$

$$+3q\cos 2\alpha-\frac{9}{4}q\sin\alpha\sin(\theta-\alpha)\left\{1-\frac{\cosh w}{\cosh w_0}\right\}-\frac{3}{2}q\cos 2(\theta-\alpha)$$

$$+\frac{27}{4}q\cos\alpha\cos(\theta-\alpha)\left\{1-\frac{\cosh w}{\cosh w_0}\right\}-\frac{3}{4}q\left\{\cos(\theta-2\alpha)-\frac{1}{\cosh^2 w_0}(\cos\theta+\tfrac{1}{2}\cos(\theta-2\alpha))\right\}$$

$$\cdot\{w_0\tanh w_0\cosh w-w\sinh w\}+\frac{9}{2}q\frac{\cosh w}{\cosh w_0}\{\cos\theta+\tfrac{1}{2}\cos(\theta-2\alpha)\}$$

$$-\frac{3}{4}q\{\cosh w\cos(\theta-2\alpha)-\cos 2\alpha+6\cos^2\alpha\}\log\frac{\cosh w-\cos\theta}{\cosh w_0}$$

$$-\frac{9}{4}q\left[\{\cos(\theta-\alpha)-3\cos\alpha\}\cos\left(\frac{\theta}{2}-\alpha\right)\cosh\frac{w}{2}+\frac{1}{2}w\sinh\frac{w}{2}\cos\frac{\theta}{2}\right]$$

$$\cdot\log\frac{\cosh w/2-\cos\theta/2}{\cosh w/2+\cos\theta/2}-\frac{9}{8}q\cos\frac{\theta}{2}\sinh\frac{w}{2}\int_0^w\log\frac{\cosh v/2-\cos\theta/2}{\cosh v/2+\cos\theta/2}dv$$

$$-\frac{9}{4}qw\sin\frac{\theta}{2}\cosh\frac{w}{2}\tan^{-1}\frac{\sinh w/2}{\sin\theta/2}+\frac{9}{8}q\pi w_0\frac{\sin\theta/2\cosh w/2}{\cosh^2 w_0/2}$$

$$+\frac{q\cos\theta\cosh w}{\cosh^2 w_0}\left\{\frac{3}{4}w_0-\frac{5}{2}-\frac{9}{16}\cos 2\alpha\right\}+\frac{3q}{2\cosh w_0}\left[\frac{\cos 2\alpha\cosh w}{\cosh w_0}\right.$$

$$+\frac{1}{3}\cos 2\theta\left(\frac{\cosh w}{\cosh w_0}-\frac{3}{4}\frac{\cosh 2w}{\cosh 2w_0}\right)-\frac{1}{4}\frac{\cosh 2w\cos 2(\theta-\alpha)}{\cosh 2w_0}-\frac{3}{16}\frac{\cosh w\cos(3\theta-2\alpha)}{\cosh w_0}$$

$$\left.-\frac{3}{16}\frac{\cosh w\cos(\theta-2\alpha)}{\cosh w_0}+\frac{\cos\alpha\cosh w\cos(\theta-\alpha)}{\cosh w_0}+\frac{1}{2}\frac{\cos\alpha\cosh 2w\cos(2\theta-\alpha)}{\cosh 2w_0}\right]$$

$$+\frac{9}{8}\pi\tanh\frac{w_0}{2}\left[(\theta-\pi)\cos\frac{\theta}{2}\cosh\frac{w}{2}+w\sin\frac{\theta}{2}\sinh\frac{w}{2}\right]. \quad (12)$$

Unfortunately, however, this expression for p_2 still fails to meet the requirement that its first derivative repeat at $\theta=0$ and $\theta=2\pi$. Thus it may be shown that the difference in the derivatives at $\theta=0$ and 2π is given by

$$\left.\frac{\partial p_{20}}{\partial\theta}\right|_{\theta=0}-\left.\frac{\partial p_{20}}{\partial\theta}\right|_{\theta=2\pi}=\frac{9q\pi}{4}\left[\left(1-\frac{|w|}{2}\right)e^{-|w|/2}+2e^{-w_0}(w_0-1)\cosh\frac{w}{2}-we^{-w_0}\sinh\frac{w}{2}\right]. \tag{13}$$

To remove this discontinuity we add on the Fourier series harmonic solution,

$$\bar{p}_2=\frac{2w_0}{\pi}\sum_{\text{odd}}\frac{A_m\cos(m\pi w/2w_0)\cosh(m\pi(\theta-\pi)/2w_0)}{m\sinh m\pi^2/2w_0}, \tag{14}$$

where

$$A_m=\frac{9\pi\gamma_m q}{2w_0(1+\gamma_m{}^2)^2}\left[2\gamma_m+\sin\frac{m\pi}{2}e^{-3w_0/2}\left\{(1+\gamma_m{}^2)\left(\frac{3w_0}{2}+1\right)-2\right\}\right], \tag{15}$$

and $\gamma_m=w_0/m\pi$.

The final solution to the second approximation is now given by

$$p_2=p_{20}+\bar{p}_2. \tag{16}$$

In a similar manner the third-order approximation pressure distributions could be derived. However, as these will be even more complicated than the second-order terms, we shall carry the approximations no further than the latter. Rather, we shall proceed at once to the determination of the load-carrying power of the film.

Load-Carrying Power of the Lubricating Film

The load-carrying power of the lubricant film corresponding to the pressure distributions developed above may be found by integrating the pressure components over the bearing surface. The results of such integrations are, for the components normal and parallel to the polar axis,

$$P_n\equiv\int_{-w_0}^{w_0}dw\int_0^{2\pi}p\sin\theta d\theta=2\pi\beta\eta(w_0-\tanh w_0)\cos\alpha-\pi q\eta(3-8e^{-w_0})\sin\alpha+\pi\beta\eta^3\cos\alpha$$
$$+\pi q\eta^2\left\{-\frac{7}{2}+\frac{33}{4}e^{-w_0}+3w_0e^{-w_0}\right\}\sin 2\alpha. \tag{17}$$

$$P_p\equiv\int_{-w_0}^{w_0}dw\int_0^{2w}p\cos\theta d\theta=4\pi q(1-2e^{-w_0})-2\pi\beta\eta(w_0-\tanh w_0)\sin\alpha+\pi q\eta(3-8e^{-w_0})\cos\alpha$$
$$-\pi\beta\eta^3\sin\alpha+\pi q\eta^2\left\{-\frac{9}{2}-\frac{5}{2}\cos 2\alpha+16e^{-w_0/2}-12w_0e^{-w_0/2}-\left(8-\frac{15}{4}\cos 2\alpha\right)e^{-w_0}\right.$$
$$\left.+3w_0(2+\cos 2\alpha)e^{-w_0}-4(4-9w_0)e^{-3w_0/2}\right\}+\eta^2P_2, \tag{18}$$

where

$$P_2=144\bar{w}^3q\sum_{\text{odd}}\frac{\sin m\pi/2}{(m^2+\bar{w}^2)^2(m^2+4\bar{w}^2)}\left[2\bar{w}m+\exp(-3\pi\bar{w}/2)\sin\frac{m\pi}{2}\left\{(m^2+\bar{w}^2)\left(\frac{3\pi\bar{w}}{2}+1\right)-2m^2\right\}\right], \tag{19}$$

and $\bar{w}=w_0/\pi$, and expresses the actual bearing length in units of the bearing perimeter.

It will be noted that these load components are functions of five variables, namely, w_0, β, α, q, η. For any given system, the bearing length w_0 and the position of the lubricant source will be fixed. On the other hand, α and η are essentially determined[5] by q and β, which involve the source strength, lubricant viscosity, and journal speed. To establish these relationships we impose on the load components the conditions that their resultant be along the vertical and have a magnitude equal to the journal load. In applying these conditions one must treat separately each position of the lubricant source. In this paper we shall consider only the cases where the source is either at the crown or base of the bearing.

Source at Bearing Crown

Since the polar axis is vertical for this case (cf. Fig. 2), the above-mentioned conditions to be imposed on the load components clearly become

$$P_n=0; \quad P_p=-W, \tag{20}$$

where r^2W is the actual load on the journal.

Eliminating β from these equations, and introducing the dimensionless flux strength,

$$q_0=(1+\eta\cos\alpha)^3 q/W=3\mu Q/\pi c^3 W, \tag{21}$$

one finds

$$\pi q_0\Big[4(1-2e^{-w_0})\cos\alpha+\eta(3-8e^{-w_0})\cos 2\alpha+\eta^2\Big\{-\frac{9}{2}-\frac{5}{2}\cos 2\alpha+16e^{-w_0/2}-12w_0e^{-w_0/2}$$

$$-\Big(8-\frac{15}{4}\cos 2\alpha\Big)e^{-w_0}+3w_0(2+\cos 2\alpha)e^{-w_0}-4(4-9w_0)e^{-3w_0/2}+P_2/\pi q\Big\}\cos\alpha$$

$$+\eta^2\Big\{-\frac{7}{2}+\frac{33}{4}e^{-w_0}+3w_0e^{-w_0}\Big\}\sin\alpha\sin 2\alpha\Big]=-(1+\eta\cos\alpha)^3\cos\alpha. \tag{22}$$

Fixing the values of w_0 and η, one may compute numerically[6] from this equation the relation between q_0 and α. The essential result is that α decreases with increasing q_0 and ultimately approaches an asymptotic value even though q_0 becomes indefinitely large.

Knowing α as a function of q_0 one can go back to Eq. (17) and find η as a function of β and q_0. Here it is convenient to introduce the "Sommerfeld variable": $S=(r^2/c^2)\mu N/P$, where P is the journal load per unit projected bearing area. In terms of S it is found, on referring to the definition of β in Eq. (3), that $\beta=3\pi SW/w_0$. Solving, then, Eq. (17) for S, it is found that

$$S=\frac{q_0w_0\tan\alpha[3-8e^{-w_0}-2\eta\cos\alpha\{-(7/2)+(33/4)e^{-w_0}+3w_0e^{-w_0}\}]}{\pi(1+\eta\cos\alpha)^3\{6(w_0-\tanh w_0)+3\eta^2\}}. \tag{23}$$

For small values of η where $\alpha\sim\pi/2$, S may be calculated more accurately by the equation

$$S=\frac{w_0[1+4\pi q_0(1-2e^{-w_0})]}{\pi^2\eta[6(w_0-\tanh w_0)+3\eta^2]}. \tag{24}$$

---

[5] From the strictly experimental point of view, q should also be considered as a "dependent parameter," since it is actually determined by the pressure at the lubricant source, i.e., the feed pressure. Analytically, however, it is more convenient to use q as the fundamental parameter, and compute the feed pressure from the assumed values of q.

[6] All the calculations for the various physical features of the lubricating system have also been carried through for the dimensionless bearing lengths: $\bar{w}=\frac{1}{2}$, 2, 5. For brevity, however, only the detailed results for $\bar{w}=1$ will be shown graphically, except where those for other cases can be indicated without adding to the number of diagrams.

Several plots of these equations for different bearing lengths and source strength are given in Fig. 3. The limiting curve for $q_0=0$, $\bar{w}=\infty$ corresponds to the Sommerfeld solution for the infinitely long bearing, and may be derived by letting w_0 approach ∞ in Eq. (24). It will be seen that the mere finiteness of the bearing leads to higher values of the eccentricity for given values of S. Moreover the increases in the eccentricity become larger as the bearing length

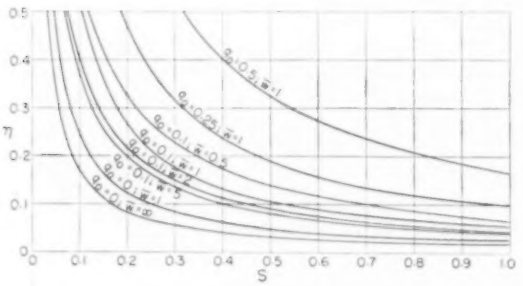

FIG. 3. The variation of the journal eccentricity η with the Sommerfeld variable, S, for journal bearings of finite length with the lubricant source at the crown of the bearing. q_0 = dimensionless source strength; $\bar{w}$ = (bearing length)/(bearing perimeter); $S=(r^2/c^2)\,\mu N/P$, where r = journal radius, c = radial clearance, μ = lubricant viscosity, N = journal speed (r.p.s.), and P = bearing load per unit projected bearing area.

becomes shorter. Finally, the lubricant source, when set at the crown of the bearing, leads to still further increases in the value of the eccentricity for given values of S.

The effect of the finiteness in the bearing length in increasing the value of η arises from the lower load-carrying capacity of the finite length bearing as compared to the infinitely long bearing. This latter difference is caused by the fact that in the finite length bearing the high film pressures at the center of the bearing must fall to the atmospheric value at the bearing ends, whereas in the infinitely long bearing there is no axial pressure fall. On the other hand, the effect of the lubricant source comes about through its action in tending to depress the journal, thus opposing the journal supporting force due to the journal rotation. Since the latter increases with increasing eccentricity, it is necessary to have a higher journal eccentricity in order to support a given load when the lubricant source opposes the load-carrying pressures caused by the rotation.

These variations of η with S, q_0 and $\bar{w}$ may also be interpreted in terms of individual forces acting on the journal because of the pressure distribution in the film. As indicated in Fig. 2, these may be resolved for small eccentricities into a force: $R=2\pi\beta\eta(w_0-\tanh w_0)$, which is caused by the rotation of the journal and acts normal to the line of centers; a force: $F=4\pi q(1-2e^{-w_0})$ acting in the direction of the lubricant inflow and representing the effect of the lubricant source on a journal which is concentric with the bearing; and finally a force: $T=\pi q\eta(3-8e^{-w_0})$ due to the lubricant source and the eccentricity of the journal, and which acts downward on the journal and is inclined to F by the angle α. From a study of these forces the qualitative features of the system can be predicted even without any numerical calculations.

This interplay between the lubricant source, the journal eccentricity, and the resultant carrying capacity of the film is shown more clearly in Fig. 4, where the ratio of the load-carrying capacity of the journal bearing of finite length to that of infinite length is plotted as a function of the eccentricity. This ratio is really nothing more than the ratio of abscissae of the finite bearing curves of Fig. 3 for given eccentricities to those of the infinitely long bearing curve for the same eccentricities.

While the detailed variations of the curves shown in Fig. 4 must be accepted simply as consequences of the numerical calculations, their general features do have direct physical interpretations. Thus all the curves show load-carrying capacities appreciably less than that for the infinitely long journal bearing, the deviation from the latter increasing as the bearing lengths are decreased. This is, of course, to be expected in view of the great importance of the "end effects," or fall in the pressure distribution to atmospheric at the bearing ends, as the bearings become shorter in length. Moreover, the source of lubricant is seen to cut the load-carrying capacity still further, this effect increasing as the source strength increases. The reason for this behavior lies in the journal depressing force F (cf. Fig. 2), which is proportional to the source strength and acts in the direction of the lubricant inflow. If the source were to be placed at the bottom of the bearing, the component F, as we shall see

later, will tend to support the journal, and thus increase the load-carrying capacity of the lubricating film, except at high source strengths.

It is to be understood, of course, that these curves do not imply an absolute limit to the load-carrying capacities of the journal bearings of finite length. Rather, they give only the relative values of the load-carrying capacity of the finite length bearings as compared to those for the infinitely long bearing for the same values of η, that is, *the same geometry*. All that would be necessary to attain in a finite length bearing any predetermined load-carrying capacity corresponding to an infinitely long bearing with fixed eccentricity would be to increase the eccentricity in the former. In principle, it will be possible to obtain arbitrarily large load-carrying capacities for the finite length bearing to the same extent that such would be possible with bearings of infinite length, although from a practical point of view the higher eccentricities that would be required in the case of the finite length bearing might lead to seizing or scoring of the bearing somewhat earlier than under the hypothetical case of the infinitely long bearing.

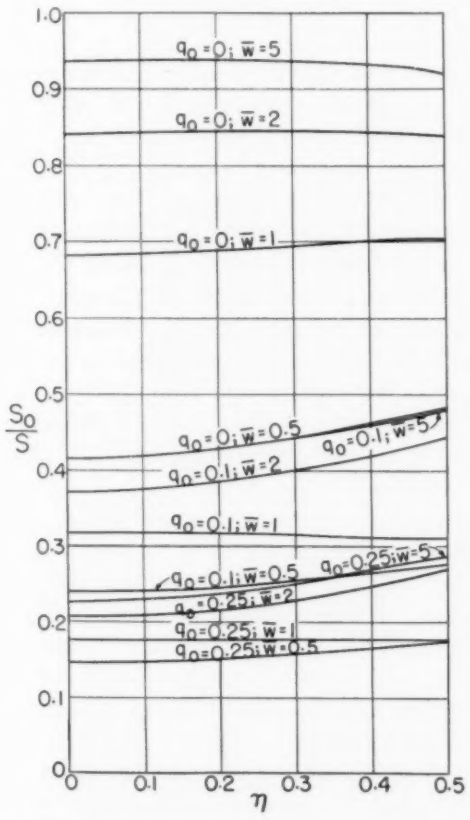

FIG. 4. Relative load-carrying capacities of finite length journal bearings with the lubricant source at the crown of the bearing. S_0/S = (load-carrying capacity of finite length bearing)/(capacity of infinitely long bearing of same eccentricity, η); $\bar{w}$ = (bearing length)/(bearing perimeter).

To determine finally the friction properties of the journal bearing system considered here, one must introduce the hydrodynamic expressions for the surface tractions acting on the journal bearing surfaces. These are given by:

$$\sigma=\mu U/h\pm(h/2r)\partial p/\partial\theta, \tag{25}$$

where the + refers to the traction on the journal and the − to that on the bearing. Integrating the right-hand side over the complete journal or bearing surfaces, one immediately finds for the total forces of friction the values:

$$K=\frac{r\mu UL}{c}\int_0^{2\pi}\frac{d\theta}{1+\eta\cos(\theta-\alpha)}$$
$$\pm\frac{c\eta r}{2}\int_{-w_0}^{w_0}dw\int_0^{2\pi}p\sin(\theta-\alpha)d\theta \tag{26}$$
$$=\frac{2\pi r\mu UL}{c(1-\eta^2)^{\frac{1}{2}}}\pm\frac{c\eta r}{2}\{P_n\cos\alpha-P_p\sin\alpha\},$$

after making use of the definition of h given by Eq. (2), and the notations of Eqs. (17) and (18).

Recalling that the coefficient of friction, f, is defined as the total frictional force per unit of total load, we have, making use of the previously introduced notation:

$$\frac{r}{c}f=\frac{2\pi^2S}{(1-\eta^2)^{\frac{1}{2}}}\pm\frac{\eta}{2}\left\{\frac{P_n}{W}\cos\alpha-\frac{P_p}{W}\sin\alpha\right\}. \tag{27}$$

Applying now Eq. (20) so as to specialize this relation to the present case where the source is at the crown of the bearing, we finally obtain for the coefficient of friction on the journal:

$$\frac{r}{c}f_j=\frac{2\pi^2S}{(1-\eta^2)^{\frac{1}{2}}}+\frac{\eta}{2}\sin\alpha. \tag{28}$$

Having previously determined the relation between η and S (Fig. 3), and between α and η, it is a simple matter to compute the friction coefficient as a function of the Sommerfeld

variable S, for different source strengths, q_0. Typical curves showing the results of these calculations for the friction coefficient for the journal and for small values of S are given in Fig. 5. The predominant feature of these curves

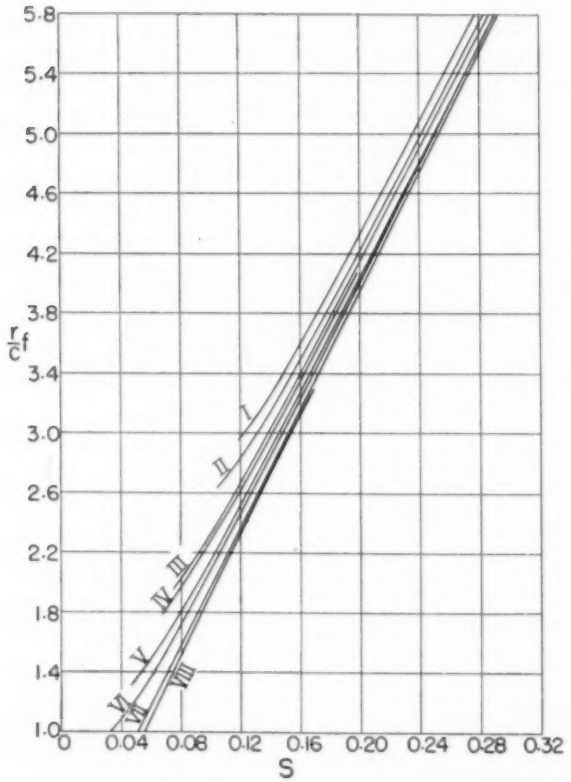

FIG. 5. Coefficients of friction, f, *vs.* S for finite length journal bearings fed with lubricant sources at the crown of the bearing. I: $\bar{w}=\frac{1}{2}$, $q_0=0.1$; II: $\bar{w}=1$, $q_0=0.1$; III: $\bar{w}=2$, $q_0=0.1$; IV: $\bar{w}=5$, $q_0=0.1$; V: $\bar{w}=1$, $q_0=0$; VI: $\bar{w}=\infty$, $q_0=0$; VII: the Petroff line; VIII: $\bar{w}=\infty$, $q_0=0$. Curves I to VI refer to friction on the journal; curve VIII refers to friction on the bearing. $\bar{w}$=(bearing length)/(bearing perimeter); q_0=dimensionless source strength.

is that the friction coefficient for the infinitely long bearing for any given value of S represents a minimum with respect to those for bearings of finite length. Moreover the increase in coefficient becomes greater as the bearing length becomes smaller and as the source strength increases. The physical basis for these results obviously lies in the fact that the eccentricities for the finite length bearings, for given values of S, exceed that for the infinitely long bearing, as shown in Fig. 3. For as the journal load, journal speed, and lubricant viscosity are kept fixed, that is, S is fixed, it is to be expected that the resultant friction will be higher for systems of higher eccentricity or smaller minimum film thickness.

Because of the nature of the approximation method used here it is impossible to treat systems of high eccentricities or very low values of S. This explains the chopping off of the friction coefficient curves to values of S of the order of 0.1, which corresponds to maximal values for the eccentricities of $\frac{1}{2}$. From Fig. 3 it will be clear that this value of η corresponds to increasingly larger values of S as the source strength increases or the bearing length decreases.

In the region of large values of S there are no limitations upon the validity of the analysis. For from Eq. (23) it follows that large values of S imply that $\alpha\sim\pi/2$, as long as q_0 is finite. Eq. (22) then shows that η becomes vanishingly small. From Eq. (27) it therefore follows that for large S the friction coefficient asymptotically approaches the Petroff line:

$$rf/c=2\pi^2S, \tag{29}$$

regardless of the bearing length or source strength.[7] Moreover, this asymptotic limit will be approached both by the friction coefficient on the journal and that on the bearing, although the latter will always be smaller than the former, since α will be limited to the first quadrant as long as the lubricant source is set at the crown of the bearing. However, for moderate or large source strengths the absolute values of the friction coefficients on the bearing will also approach the Petroff line from above, in contrast to the case of the infinitely long bearing where the friction coefficients on the bearing lie on a curve below the Petroff line.

Before turning to a discussion of systems where the lubricant source is at the base of the bearing, it should be noted that the results developed above correspond very closely to those found in the first paper of this series[1] where it was assumed that the lubricant source was always maintained 90° in advance of the

[7] Equation (29) also remains valid regardless of the position of the lubricant source. And, as shown in the first paper[1] of this series, the asymptotic approach of the rf/c *vs.* S curve to a straight line through the origin holds even for partial journal bearings, although in such cases the slope $2\pi^2$ of Eq. (29) will be replaced by quantities depending on the bearing arc and its attitude with respect to the load.

maximum film thickness ($\alpha=\pi/2$). While in principle such a restriction is quite artificial, it turns out that even when the angle α is allowed to vary, it will still be limited, by the requirements of equilibrium between the forces due to the lubricant source and the journal rotation, to values exceeding 70° except for high journal eccentricities. The variability in the angle α has permitted an extension of the friction coefficient curves to smaller values of S, but over the same range of variables the results given here agree with those previously developed in everything except quantitative detail.

Source at Base of Bearing

Since the source is to be taken here at the base of the bearing, the geometric system will correspond to that shown in Fig. 6, at least as long as

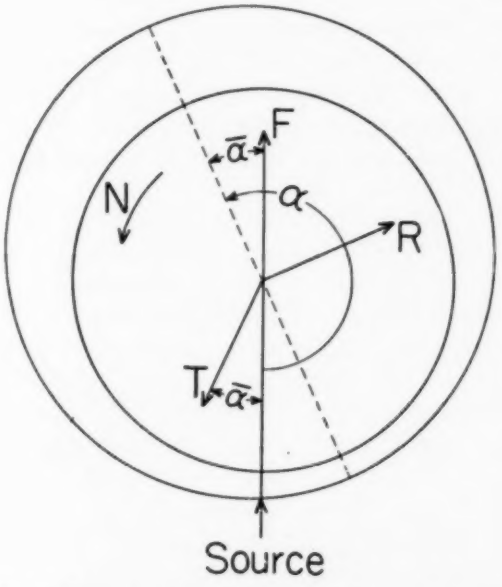

FIG. 6. Forces acting on the journal because of pressure distribution in the lubricating film when the lubricant source is at the base of the bearing and has a strength less than the "critical."

the rotational effects are the predominating elements in determining the journal displacement.

The conditions to be imposed upon the load components of Eqs. (17) and (18) for the present case will therefore be:

$$P_n=0; \quad P_p=W. \tag{30}$$

Upon eliminating β from the resulting equations,

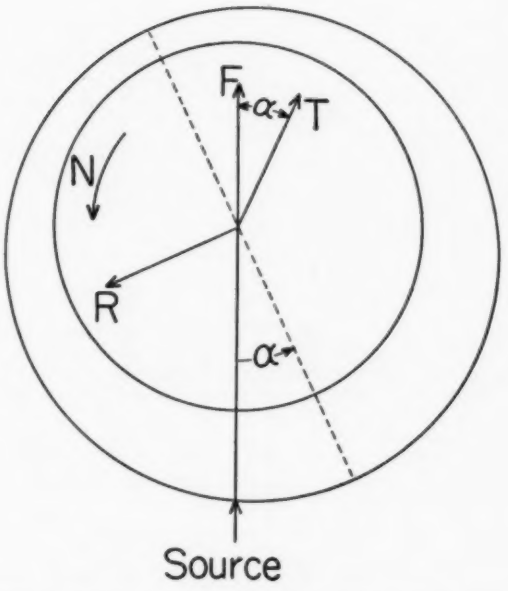

FIG. 7. Forces acting on the journal because of pressure distribution in the lubricating film when the lubricant source is at the base of the bearing and its strength exceeds the critical value.

one obtains an expression involving q_0, α, and η which is identical with Eq. (22), except for a change in sign on the right side. In solving this equation for α as a function of q_0, it is found that here the behavior of the system will depend primarily upon the magnitude of the dimensionless flux strength q_0. For small values of q_0 the forces resulting from the pressures in the film will be as shown in Fig. 6, with α lying between π and $3\pi/2$. When q_0 has the critical value given by: $1/4\pi(1-2e^{-w_0})$, the force F will be great enough to support the journal without any assistance from R. The journal will then become concentric with the bearing and the friction coefficient will be given by the Petroff line (Eq. (29)) *for all values of* S. And when q_0 exceeds this critical value the journal will rise above its central position, and α will fall to values less than $\pi/2$, as shown in Fig. 7.

To calculate the values of the Sommerfeld variable for the present case one may use exactly the same formula as when the source is at the crown of the bearing, namely, Eq. (23).

The previously discussed effect of the strength of the lubricant source on the position of the center of the journal is shown graphically in Fig. 8(a) for $\bar{w}=1$ and $S=0.05$. The arrow indi-

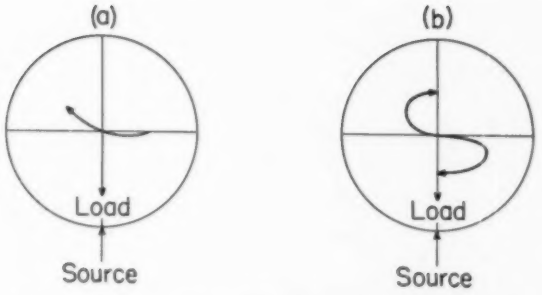

FIG. 8. (a) The motion of the journal center with increasing source strength (direction of the arrow) when the lubricant source is at the base of the bearing and $S=0.05$. (b) The motion of the journal center with fixed source strength but varying Sommerfeld variable when the lubricant source is at the base of the bearing. For segment directed to the right $q_0=0.025$; for segment directed to the left $q_0=0.20$. Arrows indicate decreasing values of S. Bearing length = bearing perimeter.

cates the motion of the center of the journal with increasing values of q_0, the extremity to the right of the curve referring to the zero value of q_0.

For a system of fixed source strength but variable S, the motion of the center of the journal is shown in Fig. 8(b). The arrows here indicate the direction of motion as S is decreased, the segments of both curves beginning at the centers of the circles, i.e., at $\eta=0$ corresponding to $S\sim\infty$, and ending on the vertical axis for $S=0$. The segment directed downward refers to the value of $q_0=0.025$, which is less than the critical value. The segment directed upward was calculated for $q_0=0.20$, which exceeds the critical value. The radically different behavior of the center of the journal under the conditions where the source strength is less or greater than the critical values will be obvious from this diagram.

The variation of the journal eccentricity with the Sommerfeld variable for fixed values of source strength q_0 is shown in Fig. 9 for $\bar{w}=1$. The solid curves refer to values of source strength less than the critical, and the dotted curves to cases where q_0 exceeds the critical values. For purposes of comparison the Sommerfeld curve of η *vs.* S is indicated by the curve marked $q_0=0$; $\bar{w}=\infty$. The line coincident with the S axis refers to the critical value of q_0, at which $\eta=0$, for all values of S.

While the general trend of the curves at the larger values of S is the same as found previously for the case where the source is at the crown of the bearing, their relative positions for different values of q_0 depend upon whether or not q_0 exceeds the critical value. Thus for fixed S, increasing values of q_0 lead to smaller eccentricities until the critical values of q_0 are reached, after which the situation reverses. This behavior clearly corresponds to that indicated in Fig. 8(a). Moreover, as actually shown for the cases where $q_0=0.05$, 0.10, and 0.15, the curves will show maxima at the small values of S, and ultimately drop off again as S approaches zero. This behavior will be followed by all the curves excepting that for $q_0=0$, the absence of the maxima for $q_0=0.01$ and $q_0=0.25$ in Fig. 9 simply indicating that these maxima and the η axis intercepts will be found for values of η exceeding 0.5 when q_0 is very small or very large. The existence of the η axis intercepts less than one means that, as previously suggested, the lubricant source alone will be able to support the load even when there is no journal rotation ($S=0$) when the source is set at the base of the bearing. The journal center will then lie, of course, along the load line, and will assume positions below or above the center of the bearing as q_0 is less or greater than the critical value. While these limiting cases of zero

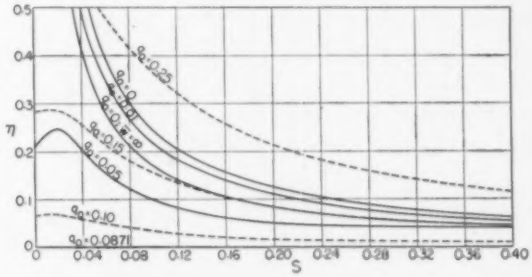

FIG. 9. The variation of the journal eccentricity, η, with S for journal bearings fed at the base of the bearing. For dotted curves q_0 exceeds the critical value; $\bar{w}=1$ except for the Sommerfeld curve: $q_0=0$, $\bar{w}=\infty$.

journal speed do not represent situations of journal bearing lubrication from a practical point of view, it is of interest that the analytical theory gives a physical description of such cases by the continuous variation of the fundamental parameter S in approaching zero.

The relative load-carrying capacities of the journal bearings with source at the base of the bearing may be obtained as in the case of Fig. 4 by simply taking the ratios of the abscissae of the Sommerfeld curve in Fig. 9 to those of the

finite length bearing curves for the same values of η. The relative load-carrying capacities will be either less or greater than that for the infinitely long bearing, depending upon the values of η and q_0. In general, parts of curves in Fig. 9 lying to the right and above the Sommerfeld curve correspond to load-carrying capacities less than that for the Sommerfeld bearing, the converse being true in the region below and to the left of the Sommerfeld curve. In the regions near the maxima of the η *vs.* S curves the load-carrying capacities will be double valued functions of the journal eccentricity, the two values corresponding, of course, to different values of S.

The general variation of the load-carrying capacity with the journal eccentricity and source strength, such as shown in Fig. 4 and as would follow from Fig. 9, may be contrasted to that heretofore assumed to obtain for finite length journal bearings. Thus under the common assumption that the axial pressure distribution falls in a parabolic manner from that around the central circumference (which is assumed to have the Sommerfeld form) to atmospheric at the ends, one finds that the relative load-carrying capacity would be $\frac{2}{3}$ of the Sommerfeld bearing for all values of bearing length. And if this axial pressure distribution follows a cosine law, the resultant values of the relative load-carrying capacity will be $2/\pi$, again independently of the actual bearing length. Moreover in both cases the ratio is independent of η. Yet it follows directly from Fig. 4 for the case where the source is at the crown of the bearing, and also from additional calculations such as given here ($\bar{w}=1$) for bearings of other lengths with the source at the base of the bearing, that actually the relative load-carrying capacities vary markedly with the bearing length. Moreover they are not independent of η. Finally they are greatly affected by the lubricant source strength and its position, which are factors that are entirely omitted in the summary representation of uniform azimuth-free variations in the axial pressure distribution by always beginning with the Sommerfeld distribution at the bearing center.

The calculation of the friction coefficients for the case where the lubricant source is at the base of the bearing follows again from the application

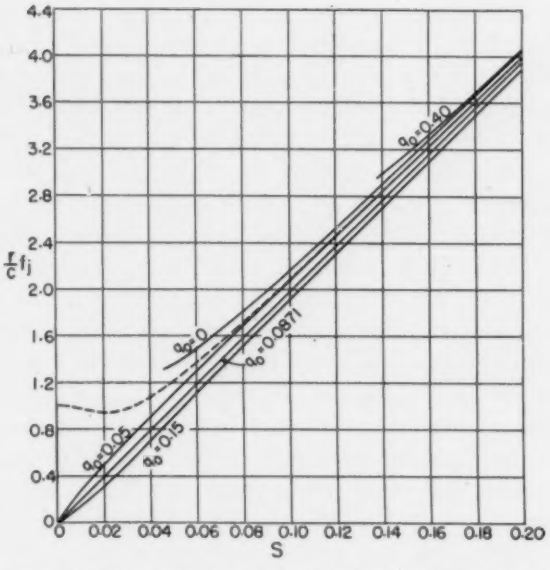

FIG. 10. The variation of the friction coefficient on the journal with S for a finite length journal bearing ($\bar{w}=1$) fed at the base of the bearing. Dotted curve represents Sommerfeld theory variation ($\bar{w}=\infty$).

of the special condition given in Eq. (30) to the general relation of Eq. (27). We thus find that

$$\frac{r}{c}f=\frac{2\pi^2 S}{(1-\eta^2)^{\frac{1}{2}}}\mp\frac{\eta}{2}\sin\alpha, \qquad (31)$$

where again the upper sign refers to the friction on the journal and the lower to that on the bearing.

Without any numerical analysis one may note from Eq. (31) that whereas for source strengths less than the critical, the friction on the journal will exceed that on the bearing ($\alpha\geqq\pi/2$), as in the case when the lubricant source is at the crown of the bearing, this situation is reversed for source strengths exceeding the critical ($\alpha\leqq\pi/2$). This inversion follows, of course, directly from the fact that the couple balancing the difference in torque moments between the journal and bearing, and which is given according to Eq. (27) by

$$\frac{r}{c}(f_j-f_b)=\eta\left(\frac{P_n}{W}\cos\alpha-\frac{P_p}{W}\sin\alpha\right), \qquad (32)$$

changes sign as the source strength exceeds the critical value and the journal displacement reverses direction in passing through the bearing center.

Several curves for the friction coefficients on the journal for $\bar{w}=1$ are shown in Fig. 10. Curves for values of q_0 between 0.15 and 0.40 were not plotted because they would fall on those for the smaller values of q_0 and make the reading of the curves too difficult. The dotted curve in Fig. 10 represents that given by the Sommerfeld theory for the infinitely long bearing. While at large values of S all the curves asymptotically approach the Petroff line (Eq. (29)), just as in the case where the source is at the crown of the bearing, very significant differences appear at the low values of S. Thus, for example, for the critical value of q_0 the friction coefficient curve becomes identical throughout with the Petroff line, since as we have seen, $\eta=0$ at the critical value. But more than that, all the curves, except that for $q_0=0$, will come down and ultimately pass through the origin as S is made vanishingly small, in contrast to the ordinate intercept of unity given by the Sommerfeld curve. This behavior is caused, as indicated above, by the fact that as long as q_0 is nonvanishing, the lubricant source will be able to support the journal without any rotation whatever provided the journal assumes the proper eccentricity along the line of the load. For values of q_0 less than the critical this eccentricity will leave the journal center below the bearing center, whereas for flux strengths exceeding the critical the journal will come to rest with the center above the center of the bearing. Thus in the case of journal bearings of finite length provided with a lubricant source in the loaded part of the bearing there will be no minima whatever in the curves that would even be suggestive of a thin film type of lubrication. The failure of the curve for $q_0=0.40$ to pass through the origin is simply due to the fact that the very low values of S, and ultimately the resting position of the journal, correspond to eccentricities greater than $\frac{1}{2}$, for which the present approximation theory would not give results that are quantitatively accurate. The same would be true for curves representing values of q_0 appreciably less than 0.05.

As to the variation of the friction coefficient with the source strength, Fig. 10 shows that the friction coefficient on the journal first decreases with increasing q_0 until values of q_0 somewhat

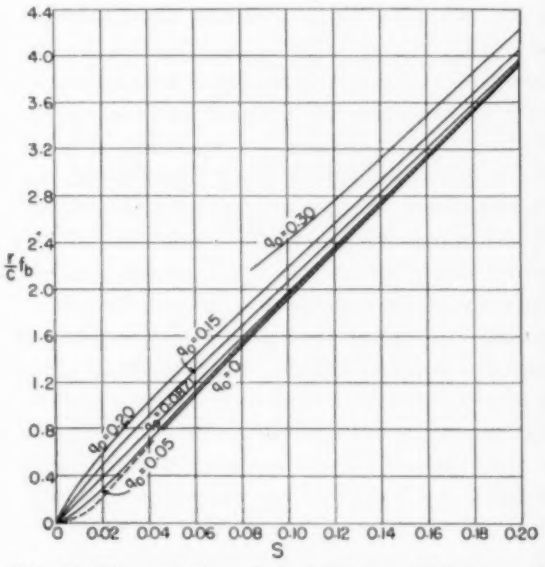

FIG. 11. The variation of the friction coefficient on the bearing with S for a finite length journal bearing ($\bar{w}=1$) fed at the base of the bearing. Dotted curve represents Sommerfeld theory variation ($\bar{w}=\infty$).

greater than 0.15 are reached. For still greater values of q_0 the friction coefficient begins to rise and ultimately exceeds that for $q_0=0$ by the time that $q_0=0.40$. Moreover, when $q_0=0$ the friction coefficients are higher than those for the infinitely long bearing. The physical basis for these features clearly lies in the η *vs.* S curves in Fig. 9, and needs no further discussion.

In the case of the friction coefficient on the bearing, all the curves again go through the origin, as shown in Fig. 11. Here, however, the contrast with the infinitely long bearing theory is not so marked, as the latter also gives a curve passing through the origin. Only the lower portion of this curve—dotted—has been included in Fig. 11, since the remainder would lie too close to the curves for $q_0=0$ and 0.05 to show up clearly. The variation with the source strength is, however, given by a monotonic rise in the friction coefficient with increasing source strength, the curve for the critical value again coinciding exactly with the Petroff line.

Since we now have what should be in principle a complete theory for the pressure distribution and lubricating properties of journal bearings of finite length, except for the necessary limitation to the thick film region, it is of interest to consider again the question of the negative film pressures predicted by the Sommerfeld theory.

As the ability of a liquid film to withstand pressures less than atmospheric is subject to some question, we shall base our considerations upon the more definite and physical question referring to the leakage of air into the film at the bearing ends. For if the negative pressures in the interior of the film should result in gradients at the bearing ends directed inward, air will be sucked into the film and the film will be broken, unless the bearing is flooded, even though it should be able to withstand a certain degree of tension. Restricting ourselves for simplicity to relatively long bearings and small eccentricities, it follows from Eqs. (7) and (10) that the axial pressure gradient at the ends of the bearing will be given by

$$\partial p/\partial w = -\beta\eta \sin(\theta-\alpha) - q + \beta\eta^2 \sin 2(\theta-\alpha) - 3\eta q \cos\alpha. \quad (33)$$

The condition that there be no air sucked in the film is, then, that this quantity be negative for all values of θ. To a good approximation this condition may be expressed as

$$q_0 \gtrsim 3S\eta/\bar{w}. \quad (34)$$

Now for a fixed S and $\bar{w}$, η as well as α is determined by q_0. If, then, the associated values of q_0, S and η turn out to satisfy the inequality of Eq. (34) all the gradients at the ends of the bearing will be outward and no air will be sucked into the film. This, of course, implies that the added pressure distribution due to the lubricant source has overcome the negative pressures due to the journal rotation, which represented the source of much concern and controversy in the discussions of the Sommerfeld theory of the infinitely long bearing.

As the relation between η, S and q_0 depends upon the position of the lubricant source, the different positions must be treated separately. Upon carrying through the necessary calculations it is then found that when the lubricant source is at the crown or unloaded side of the bearing, Eq. (34) will not be satisfied unless q_0 is of the order of, or greater than, $\frac{1}{2}$, for $\bar{w}=1$. In particular, for large values of S, Eq. (34) may be transformed into

$$q_0 \geqq \frac{1}{2\pi[\pi\bar{w} - \tanh \pi\bar{w} - 2 + 4\exp(-\pi\bar{w})]}, \quad (35)$$

the right side of which has a value of 0.506 for $\bar{w}=1$. For smaller values of S the necessary value for q_0 increases somewhat, and for $S=1.0$, q_0 must equal 0.63 in order to avoid leakage of air into the bearing.

When the lubricant source is set at the base of the bearing, the results are radically different. Here it is found that values of q_0 even as low as 0.04 will suffice to prevent leakage of air into the bearing. Moreover the necessary values for q_0 increase with increasing S. Thus for $S=0.05$, q_0 must equal 0.037, whereas for $S=0.2$, q_0 must equal or exceed 0.041. However, even though S becomes arbitrarily large, the critical value of $q_0=0.0871$ (for $\bar{w}=1$) will suffice to prevent air leakage into the bearing.

The interpretation of this marked difference between the necessary values of source strength required to prevent air leakage into the bearing when the source is at the crown or base of the bearing is to be found in the different effects of the two positions of the source upon the position of the journal. Thus when the source is placed at the crown of the bearing, its effect in increasing the journal eccentricity tends to accentuate the negative pressures caused by the journal rotation so that high values of source strength are necessary to insure that there will be no leakage of air into the bearing. However, when the source is located at the base of the bearing, the negative pressures to be overcome are lessened because of the decreased eccentricities resulting from the action of the source, and quite small source strengths will suffice to overcome the inward pressure gradients tending to suck air into the bearing. And in the limiting case where the source at the base of the bearing has the critical strength, and the journal rotates concentrically in the bearing, the pressure variation caused by the journal rotation is completely eliminated, and the resultant distribution is entirely that due to the source which is, of course, everywhere positive and outward toward the ends.

With regard to the accuracy of the calculations presented in this paper, the limitations involve only the magnitudes of the dimensionless bearing length $\bar{w}$, and of the journal eccentricity η. As to the former, it will be recalled that quantities of the order of $\exp(-2\pi\bar{w})$ were dropped throughout the analysis. It is therefore felt that the

analytical formulas and calculations should be reasonably accurate as long as $\bar{w}$ is not appreciably less than $\frac{1}{2}$. With respect to the journal eccentricity η, terms of the order of $\beta\eta^4$ and $q\eta^3$ or higher have been dropped. It is difficult to formulate an exact expression for the numerical errors involved by this approximation, as these errors depend upon the values of both $\bar{w}$ and q_0. A check of the actual numerical calculations with Eq. (22) which underlies all the subsequent computations shows, however, that while the higher order terms become of importance at the larger values of q_0 (>0.25), they do not contribute appreciably to the results even for $\eta=0.5$ when q_0 is relatively small.

Finally it should be observed that the theory developed here provides for the direct calculation of the actual feed pressure from a knowledge of the dimensionless flux strength q_0. Thus to the order of η^2 and e^{-2w_0}, it is found from Eqs. (7) and (10) that the value of the feed pressure above atmospheric is given by:

$$\frac{p-1}{W}=\frac{-3\pi S\eta\sin\alpha}{w_0}\times[1-2e^{-w_0}+\eta\cos\alpha(-\tfrac{3}{2}+2e^{-w_0})]+\frac{q_0}{(1+\eta\cos\alpha)^3}[w_0-2\log\bar{r}+3\eta\cos\alpha(w_0+2-\log 16)], \quad (36)$$

where $\bar{r}$ is the ratio of the actual radius of the source to the radius of the journal. And in the special case where q_0 has the critical value, a complete and rigorous solution for all values of w_0 gives:

$$\left.\begin{aligned} p-1&=\frac{W(1+\operatorname{ctnh}^2(w_0/2))}{8\pi}\left[w_0-2\log\bar{r}-4\sum_1^\infty\frac{1}{n(1+e^{2nw_0})}\right],\\ q_0&=\frac{1+\operatorname{ctnh}^2(w_0/2)}{8\pi}. \end{aligned}\right\} \quad (37)$$

There has therefore been no loss in generality in considering q_0 in place of the feed pressure as a fundamental independent parameter, on a par with S and w_0.

Summary

Summarizing the above developments and discussions, it appears that we now have available a fairly complete hydrodynamic theory for the thick film lubrication of journal bearings of length equal to or exceeding half the bearing perimeters. For greater bearing lengths the theory goes over continuously into the Sommerfeld theory for the infinitely long bearing. For bearings of moderate length significant differences appear. These arise, first, from the requirement that the pressure distributions in the film must fall to atmospheric at the ends of the bearings, and second, that with bearings of finite length one must provide sources for the lubricant flow into and leakage out of the bearing.

As a whole, a lubricant source placed at the base or loaded portion of the bearing will lead to higher load-carrying capacities and will be more effective in preventing the entry of air into the bearing. From a practical point of view, however, it must be recognized that such a position for the source will require that relatively high pressures be available for forcing in the lubricant, which may not always be feasible, especially if the loads are particularly high.

While the final results for the friction coefficients derived here for journal bearings of finite length do not differ greatly from those predicted by the Sommerfeld theory at large values of the Sommerfeld variable, the deviations become appreciable as the thin film region is approached. This is particularly true when the lubricant source is set at the base of the bearing. In such cases the theory developed here provides a complete description of the friction coefficient curves even in the so-called thin film region, except for very low or high values of source strength. Thus for the friction coefficients on the bearing it is found that all the curves give uniformly decreasing friction coefficients as the Sommerfeld variable decreases, as is also predicted by the infinitely long bearing theory. However, the magnitudes of the friction coefficients for values of the Sommerfeld variable which are usually considered to represent the thin film region may exceed the Sommerfeld values by more than 100 percent, depending upon the absolute value of the source strength. In the case of the friction coeffi-

cients on the journal, the differences are still more marked since the finite bearing theory predicts that here, too, the coefficients will go to zero as the Sommerfeld variable vanishes, whereas the Sommerfeld theory predicts friction coefficient axis intercepts equal to unity. Thus even here there is no suggestion of minima in the friction coefficient curves and ultimate rises in the thin film region, as might be inferred from the Sommerfeld theory. In fact, the present theory shows that unless the dimensionless source strength q_0 is extremely small or very large, there will be no thin film region at all in the ordinary physical sense. For even though the Sommerfeld variable should be vanishingly small the lubricant source, when placed at the base of the bearing, should prevent metallic contact and even permit the journal to come to absolute rest with values of the eccentricity that are appreciably less than one. That is, as far as the actual film thickness is concerned, it will not become arbitrarily small as the Sommerfeld variable approaches zero, but its minimum value will approach a definite nonvanishing limit determined by the magnitude of the source strength. The sharp rises in the friction coefficient which have been observed in the thin film region with bearings fed with lubricant at their bases, must therefore reflect sources of friction that are radically different from the hydrodynamic viscosity effects in a lubricating film.

The authors are indebted to Mr. M. W. Meres of this Laboratory for carrying through the numerical calculations reported here and for the preparation of the diagrams and to Dr. Paul D. Foote, Executive Vice President, Gulf Research & Development Company, for permission to publish this paper.

The Structural Characteristics of Certain Silver Films

SANFORD F. ESSIG
Thwing-Albert Instrument Company, Philadelphia, Pennsylvania
(Received September 21, 1938)

The structural characteristics of three types of silver films which have found general use as photocathode bases in television image analyzers and similar electronic devices are discussed. They are classified as mosaics and translucent films. Two types of mosaics are discussed, (1) the reduced oxide dust film, and (2) the agglomerated sputtered or evaporated film. A characteristic of the first is a wide range in particle size (<1–30μ in films photographed), those below 3 microns being greatest in number. A critical temperature, approx. 600°C, is observed in reduction of the oxide films above which there is a distinct liquid phase in the silver-silver oxide system resulting in a radical change in the final film structure.

The process of agglomeration is traced from the continuous through the mosaic state in the second type film. The characteristics are a smaller and more uniform particle size than the reduced oxide type. Particle size and spacing is readily controlled and reproduced. The range in initial thickness of films investigated is approximately 0.01–0.2 microns.

The third type or translucent film is a composite consisting of a silver mosaic superposed on an electrically conducting film of relatively high light transmission. Platinum is chosen as the most suitable metal for this subfilm and is protected from destructive forces such as oxidation and alloying with the silver mosaic by an intermediate film of silica or aluminum oxide.

INTRODUCTION

AMONG the various types of photocathodes which have been described there are several which have found somewhat general application in television image analyzers[1, 2] and the image converters widely described in the last few years.[3–5] They are thin silver films, the base of the $X-X_2O-Ag$ type alkali-metal composite photosurfaces. Those to be described in this paper may be classified in two groups, *viz.* (1) the mosaic, a discontinuous film composed of separated silver particles on an electrically insulating substrate (in this case mica), and (2) the translucent type, a composite consisting of a silver mosaic or discontinuous network superposed upon an electrically conducting metallic film of relatively high light transmission. Three types of films will be discussed, *viz.* (1) the reduced oxide-dust film, (2) the agglomerated* continuous

[1] Zworykin, J. Frank. Inst. **217**, 8–20 (1934).
[2] Zworykin, Morton, Flory, Proc. I.R.E. **25**, 1071 (1937).
[3] Kluge; Schaffernicht, Zeits. f. Physik **93**, 762, and 789 (1935).
[4] Coeterier and Teves, Physica **3**, 960 (1936).
[5] Zworykin and Morton, J. Opt. Soc. Am. **26**, 181 (1936).

* I.e., initially continuous. The term *agglomerate* (and its derivatives) is used in the broad sense and will apply

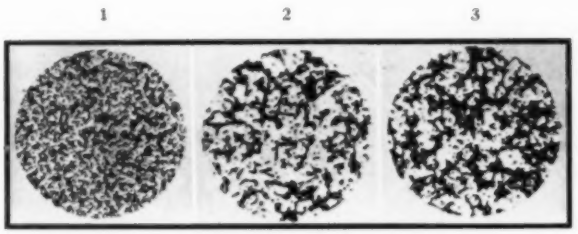

FIG. 1* (*T*) Mag. = 82.

film, and (3) the translucent or composite film. Discussion will be confined largely to the physical structure of the base films rather than to the films in their photosensitized state.

Among the requirements imposed on the mosaic type film to afford satisfactory operation of the iconoscope or similar electronic device are: (1) Relatively high capacity of the silver particle to the signal plate (a common conductor on the opposite surface of the substrate), (2) Medium to high volume resistance of the substrate, (3) Minimum interparticle capacity, (4) Maximum interparticle resistance, (5) Particle size sufficiently small so as not to limit picture resolution or quality of the same, (6) Maximum photoactive area, (7) Mechanical strength of the substrate and resistance of the same to thermal shock, (8) Resistance of the substrate to the alkali metal vapors. These requirements define both the substrate and the film. The specifications for the substrate are best fulfilled by a sheet of hard mica (muscovite) preferably of the Indian or Brazilian Ruby variety, 25–50 microns in thickness. This must be selected for flatness and freedom from discontinuous laminae, openings between laminae and stains. The film must be a mosaic of silver particles well separated and reasonably uniform in size and spacing. The maximum particle size is fixed by the picture resolution and should be preferably less than a tenth the size of the electron scanning spot. The fractional coverage of the substrate by the film may be 30–40 percent.

to the complete process of conversion of the continuous film into the beaded state, i.e., the drawing up of the metal into droplets.

* Microphotographs by incident illumination are designated $-I$, by transmitted illumination-T. Those of the first group (I) were made on a Bausch & Lomb Routine Metallograph.

1. Reduced Oxide Dust Film

This type film (first described by the writer in British patent No. 407,521)* consists of a heat reduced film of silver oxide dust deposited on the mica substrate preferably by air settling. Silver oxide is selected in preferance to other possible, silver compounds because of characteristics, to be discussed shortly, which lend themselves to the formation of a satisfactory mosaic at a temperature which will not destroy the mica substrate. Muscovite calcines at a temperature well below the melting point of silver, 800°C being about the maximum temperature at which it may be held for short periods without impairment of the structure. Some grades bubble at this or even lower temperature, i.e., bubbles of trapped or dissolved gases make their appearance and separate the laminae at the points of emission.

The temperature at which reduction of silver oxide (Ag_2O) is observed, usually given as 250°–300°C, and the speed of reaction is dependent on the purity of the compound.[6] Indications of reduction have been observed at temperatures of 100°C and lower but G. N. Lewis found that after ten hours heating at 340°C the yield of oxygen was only 0.017 cc per minute. However at the end of thirteen hours the yield was more than double this value and at the end of eighteen hours had risen to a maximum of two cc per minute or one hundred seventeen times the yield at the end of the tenth hour. The reduced oxide, i.e., the finely divided silver, scattered throughout the oxide acts as a catalyzer to speed the reaction—the phenomenon commonly known as autocatalysis. The speed of reaction has been found to be proportional to the amount of the silver and the oxide present so that it rises to a maximum, then falls to zero when reduction is complete. Manganese dioxide, platinum and many other compounds act as catalytic agents and in most cases lower the temperature of decomposition. The speed of reduction of thin films of the oxide is apparently slower than in bulk for at 400°C the reduction is quite slow.

The oxide films are most conveniently formed on the mica substrate by settling from a cloud of the air-floated particles in a closed chamber.

* Issued Mar. 22, 1934.

[6] Mellor, *Inorganic and Theoretical Chemistry* (Longmans Green and Company, 1923), Vol. 3, p. 373.

Details regarding this will be given later. The first particles to become attached to the mica surface act as anchors for those falling later from the turbulent atmosphere so that there is an acceleration in the film growth about these initial nuclei resulting in a characteristic spotty appearance of the settled film. Along any surface irregularities, such as scratches or the boundaries of discontinuous laminae, an increased accumulation of the oxide particles may always be observed. The phenomenon is not unlike the accumulation and drifting of a light snow falling in a flat, open field.

Structure of films reduced at low temperatures

Reduced by heating in air at some temperature below 550°C the silver film consists of a network of interconnected particles, porous or mossy in structure, and very lightly attached to the mica surface so that the film is readily removed by drawing a finger across it. The arrangement of the silver particles in the film is almost identical to that of the oxide particles before reduction, no appreciable displacement having occurred except for a slight matting down and slow sintering together of the silver particles. After reduction is complete, the film may be exposed for short periods (10 sec.) to any temperature below the normal melting point of silver (961°C) with but very little change in physical structure. Here, however, the network breaks and is reduced to a mosaic of well separated spherical droplets. Unfortunately, at these elevated temperatures, calcination of the mica renders the end product of no practical value. Over extended periods, especially at the higher temperatures, there is an appreciable redistribution of the silver in the network with accumulation at certain points. Essentially the same phenomenon is observed in the sintering of a quantity of silver dust or the "cold welding" of two silver surfaces in intimate contact at temperatures far below the melting point.

By varying the oxide particle size, air velocity, and thickness of the dust film, a variety of structures of any desired coverage is readily obtained. Fig. 1 shows characteristic films reduced at 500°C.

Structure of films reduced at higher temperatures

If an oxide dust film is reduced by abrupt exposure to a temperature of 700°–800°C so that the reaction is completed in a few seconds, the structure of the resulting film is distinctly different from that just described. Instead of a loosely attached network, the film now consists of a mosaic of silver beads of considerable size range, but well separated and so firmly attached to the mica surface that they are removed with difficulty. At a reducing temperature of 800°C, the beads are approximately spherical in shape while at temperatures approaching 600°C, they are more irregular and not as well separated. Fig. 2, Plate 1, is the front and Plate 2 the rear view of a film reduced at 750°C. Plate 2 is of particular interest. Here are seen the contact surfaces of the beads which wet the substrate, thus accounting for their firm connection to it. The channels through the contact areas are the result of oxygen emission during the liquid phase and the fusing together of smaller beads on repeated dusting and firing. A film of the network structure, i.e., one reduced at low temperature may if redusted and reheated at 700°–800°C be converted into one of the mosaic type. The final particles will, however, be more irregular in shape, particularly if the initial network is heavy.

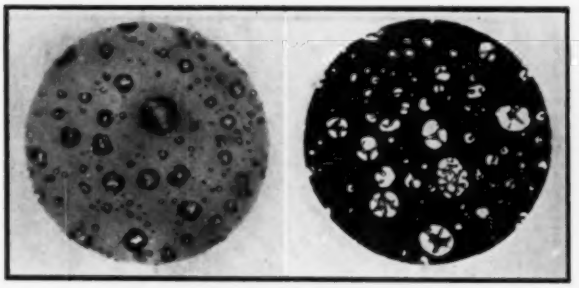

1 2

FIG. 2. (*I*) Mag. = 250.

The critical temperature at which beading or a distinct flow of the reducing metal begins is none too well defined, being influenced by such factors as oxide film thickness and heat capacity of the substrate, so that a value of 600°C is only approximately correct. The reaction is endothermic, and, as mentioned previously, the agglomeration during short periods of heating is almost nil until near the normal melting point so that we must look elsewhere for an explanation to the phenomenon. Since the beading occurs during the process of reduction, and dissolving of the oxide or atomic oxygen by silver with accompanying reduction in melting point is known to exist[7, 8] the explanation seems evident. Allen[9]

[7] Steacie and Johnson, Proc. Roy. Soc. **A112**, 542 (1926).
[8] Keyes and Hara, J. Am. Chem. Soc. **44**, 479 (1922).
[9] Allen, J. Inst. of Metals **49**, 317 (1932).

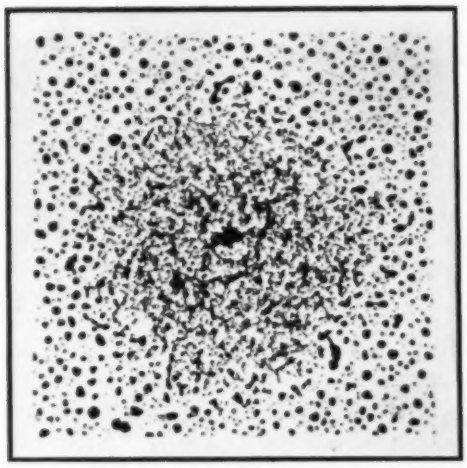

FIG. 3. (*T*) Mag. = 122.

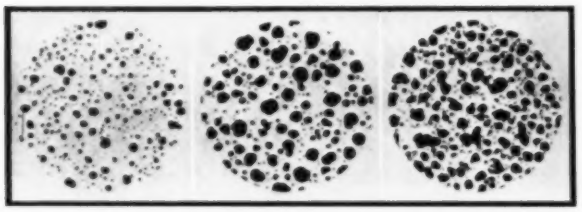

1 2 3

FIG. 4. (*T*) Mag. = 82.

obtained an eutectic of silver-silver oxide at approximately the critical temperature observed by providing sufficient pressure (400–1000 atmos.) to prevent dissociation of the oxide. To obtain any quantitative data in an unstable system such as we have here, where the content of a component in the system changes from zero to one hundred percent or vice versa in a few seconds, is impossible, so we are forced to be content with data of a more or less qualitative nature. We have observed what appears to be a reduction in the melting point of silver or the silver-oxygen system of 300°–350°C and this at atmospheric pressure.

If the speed of reaction is sufficiently accelerated by provision of a suitable catalyst, the depression in melting point is decreased to where the dust film no longer beads on reduction even at the highest temperatures permissible. The structure of the resulting film is essentially identical to one reduced at a low temperature. Carbonaceous matter, such as particles of lint, in contact with the oxide film, on heating, exert such a catalytic action as to prevent beading in the local areas surrounding the foreign material.

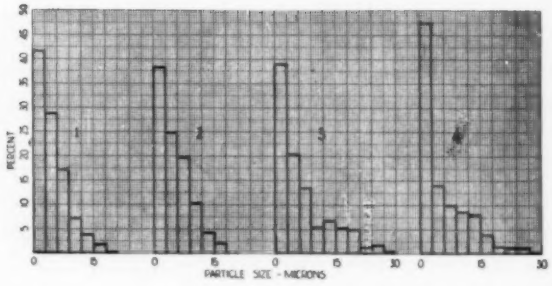

FIG. 5.

Outside the area, the beading will be entirely normal. The size of the circle of influence about the foreign material will depend on its nature and magnitude. Fig. 3 shows one of these areas in an otherwise normally beaded screen, the location of the foreign material being well defined. If an oxide film reducing at 400°–500°C be observed, these accelerated areas stand out in good contrast on the brown silver oxide background. This provides a simple and useful test for the presence of such foreign matter.

Particle size and distribution

The size and distribution of the beads over the surface of the substrate will naturally follow that of the oxide particles, the size ranging from the reduced individual grain to the reduced maximum grain cluster. Fig. 4, Plates 1, 2 and 3 are microphotographs of silver films repeatedly dusted and reduced, illustrating the increase in irregularity with particle growth. Particle size distribution in four of these films was determined by enlarging microphotographs of the same to a total magnification of 1400 times and measuring the areas of approximately 500 particles in each sample. The areas were reduced to diameters of equivalent circles. Resulting data appears in Table I and Fig. 5, the screen number of the sample indicating the number of successive dustings and reductions. The oxide used on these samples was ball-milled 10 hours in ether, then

TABLE I.

Screen No.	Size range (microns)					Max. dimension of any particle (microns)	% Coverage
	0–3	0–10	0–15	0–20	0–25		
1	40.6	90.7	97.5	99.6		28.3	18.0
2	38.3	87.3	97.7	99.8		24.9	22.7
3	39.4	75.0	85.8	93.5	97.9	39.7	30.0
4	47.5	77.5	90.7	95.7	98.2	43.1	35.5

dried and screened through a 400/inch mesh gauze. No effort was made to grade the oxide particles or determine the range in size of the same.

From the data obtained it is seen that the greatest number of particles in any sample film are below 3 microns in size; however, the smallest particles contribute least to the area covered. The size range for the singly coated film is 0–20 microns and 0–30 microns for any multiply coated one.

Apparatus

To facilitate the application and reduction of the dust films and to minimize the necessary amount of handling in the open room which could not be made dust free, the following machine was designed. (Fig. 6.) It consists of three sections, *A*, the reducing muffle which is a commercial 2.6-kw resistance furnace; *B*, the viewing and cooling compartment where the screen may be examined through a window in door *E*, and *C*, the dusting compartment. The sheet of mica to be screened is carried on *G*, which is a heavier mica (phlogopite—which is more heat resistant than muscovite) sheet in turn carried by the truck *H* on the monorail *I*. Motion of the truck and mica spade *G* is effected by the handwheel *K* through the cord *J*. The opening to the muffle is made as small as possible to minimize temperature drop on opening door *D*. Door *D* and sections *F* and *B* are water cooled to prevent heating of the machine and consequent convection air currents in the settling chamber *L*. Without this, satisfactory dusting is all but impossible. Provisions are made for locating the mica sheet with respect to a mask which constitutes the cover to compartment *C*.

The ground and screened oxide is carried in the upper section of the glass settling chamber *L*. A current of dry air from a series of jets located in the bottom of this upper section agitates the dust. The resulting dust cloud descends through the vertical neck of the conical section into which it expands. Any of the heavy oxide particle clusters finding their way into the expansion chamber are caught by *M*. Maintaining the oxide dust in a dry state minimizes the formation of these heavy clusters and permits flotation of the particles at a lower air pressure. Periodically *L* is closed and

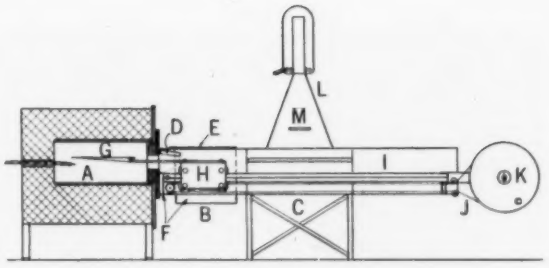

FIG. 6.

inverted and dust collected in pan *M* and on the walls of the chamber is loosened with a few sharp raps on *L* and shaken back into the upper dust reservoir. The machine must be opened periodically if for no other reason than for inserting and removing the screens. Lint from the atmosphere is sure to enter, and unless means are provided for preventing its collection by the mica sheet, no end of trouble will be experienced in obtaining a screen free from the spots described earlier. During the reduction process the mica sheet takes on an electrostatic charge so that on withdrawal into the cooling compartment, any lint particles present are immediately attracted. If, however, a humid atmosphere is maintained in section *B*, the mica sheet is readily discharged and the difficulty eliminated.

2. Agglomerated Film

This type already described by Lepeshinskaia[10] is a silver film, initially continuous, deposited on the substrate by any one of the three methods, *viz.*, evaporation, cathodic sputtering, or chemical reduction. On heat treatment of such a film of correct thickness it may be reduced to the discontinuous state, the end product being a mosaic of minute, uniform and evenly distributed particles. This type of mosaic has perhaps not been used as generally as the reduced dust type. It has, however, some desirable characteristics not possessed by the latter and it is possible and not impractical to produce it following assembly of the substrate in the electronic device and exhausting the envelope. The films described here have been deposited by evaporation in high vacuum or sputtering in argon. Details regarding this procedure are omitted due to the general knowledge of the art.

[10] Lepeshinskaia, Investia Elektroprom. Slab Toka **3**, 28–37 (1935).

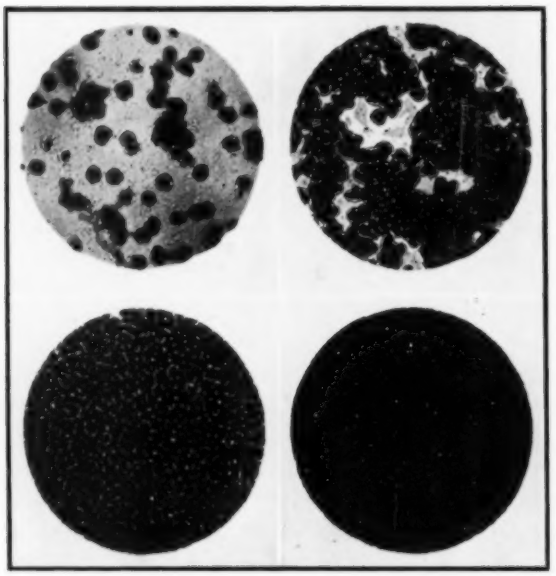

FIG. 7. (*I*) Mag. = 250.

Film structure

The behavior and progressive change in structure of a silver film of thickness of the order of 10^{-5} cm evaporated on a clean but otherwise untreated glass or mica receiver at room temperature when heated in vacuum at 400°–500°C is best illustrated by reference to Fig. 7. The plates are numbered with respect to the film thickness, Plate 1 being the heaviest and Plate 4 the lightest. Shaded areas in Plates 1 and 2 may be disregarded, these being due to sulfide stains which appeared during storage of the film sample prior to photographing.

The effects of three distinct forces may be observed in the heated film: (1) pressure at the interface of the film and substrate due to release of absorbed or dissolved gases; (2) differential expansion of the film and substrate; (3) surface tension. Another force not so evident in this series of microphotographs is (4) crystal orientation and growth by atomic migration. Gas emission and differential expansion is primarily responsible for the initial ruptures in these films, particularly the heavier ones. At a multitude of points over the surface the film is lifted from the surface of the substrate over small areas and broken. The metal in these miniature blisters flows back to the line of contact with the substrate forming a rim of accumulated metal bounding the window or opening. The process is progressive so that new fractures continually occur during the early part of the heating period and the film is rapidly reduced to a filamentary network. Crystal growth and surface tension produce a redistribution of the metal in the filaments and accumulation at points along them with the result that fractures occur. The elongated particles on continued heating tend to become spherical so that the final state is a uniform mosaic of approximately spherical droplets. The speed of agglomeration is inversely proportional to the film thickness as seen in the above plates (Fig. 7), the process being completed in the thinnest portion of the sample with little evidence of progress in the heaviest. This will be discussed later.

If the film is evaporated on an outgassed and heated receiver, gas emission as a factor in the agglomeration process is eliminated with the result that the final structure is distinctly different from the type just described. On cooling, differential contraction produces a maze of interconnected and relatively narrow (0.3–0.7μ) channels breaking up the film into particles of irregular shape and size, as illustrated in Fig. 8 (Plate 1 is the heavier film). The sample was evaporated with the mica receiver at 500°C, then cooled rapidly. The appearance by reflected light is a satiny white, almost iridescent, in contrast to the matte of the agglomerated film desposited on the cool receiver.

The characteristics of the agglomerated sputtered silver film are also different. Much of the adsorbed gas and water vapor is knocked off the surface of the substrate by ionic bombardment early in the sputtering process so that the deposited film is in very intimate contact with it and

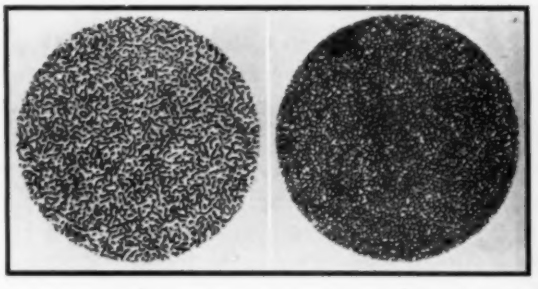

FIG. 8. (*I*) Mag. = 250.

on heating is less readily torn loose. Differential expansion here also probably plays a greater part than gas emission in breaking up this type of film. Fig. 9, Plates 1 and 2 are microphotographs of a sputtered film 0.107 in thickness heated to 220°C (36 min.) and 280°C (90 min.), respectively. The initial openings in the film probably produced by emitted gas are here of the order of a few hundredths the size of those in the evaporated film (Fig. 7, Plate 1). On continued heating these approximately circular openings do not increase appreciably in area, but more make their appearance and connect with those which appeared earlier so that the film is eventually cut through by a network of relatively narrow channels. The separated silver areas, particularly at higher temperatures, shrink in size and become less irregular in shape but never spherical, even at elevated temperatures (750°C). Irregularity of the particles, which are distinctly flakes rather than beads, and an increased size range of the same are characteristic of the agglomerated sputtered film. An evaporated film of similar structure is obtained if the surface gases are sputtered off the substrate prior to evaporation, heat treatment being the same.

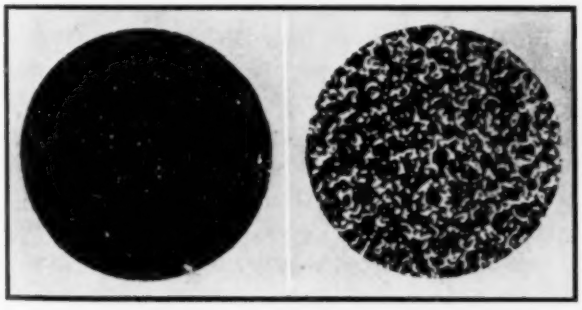

1 2

FIG. 9. (*T*) Mag. = 1125.

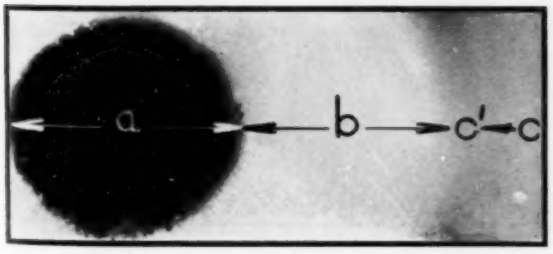

FIG. 10.

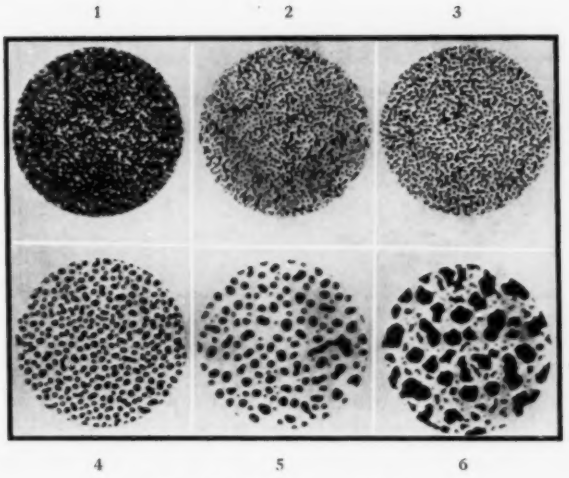

1 2 3

4 5 6

FIG. 11. (*T*) Mag. = 1025.

Film structure *vs.* film thickness

To observe the effect of initial film thickness on the final structure after heating, a number of samples were made by evaporating the film from a small source located relatively near the receiver so as to obtain in one sample a large range in thickness. The samples were heated in vacuum in the same tubes in which they were evaporated. Fig. 10 is a photograph of one of these samples after heating. It may be divided into a series of zones: *a*- the central opaque circle followed by *b*- a zone of white translucent matte, this followed by a relatively narrow zone *c'*- practically invisible by reflected, but very discernible by transmitted light. The boundaries of this zone, particularly the outer, which is multicolored by reflected light, are poorly defined. The *c* zone, relatively large, is distinctly amber in color by transmitted light, except for a narrow purple subzone at the boundary (green-amber by reflected light).

Zone *a*, well back from the boundary is essentially continuous except for an occasional opening which does not increase in size, at least appreciably, on continued heating. The film thickness here is of the same order of magnitude as the opening so that surface tension forces, in the wall of the opening, tend to oppose rather than aid its growth as is the case in the thinner portion. Near the boundary of the specular area, the number of openings per unit area increase rapidly, the boundary being defined by an open to covered ratio of unity. A short distance out from the *a*/*b*

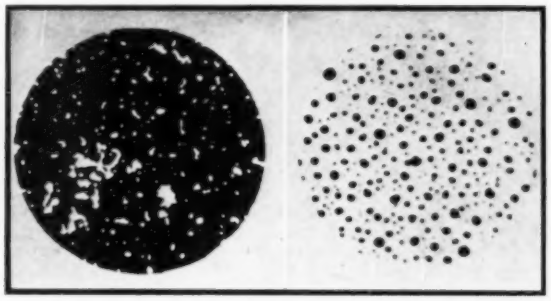

1 2

FIG. 12. (*T*) Mag. = 1095.

boundary is the beginning of the mosaic area in which we are particularly interested. Proceeding out from the center, the particles continue to decrease in size and are no longer spherical. Fig. 11 is characteristic of the particle arrangement here. No distinct changes in structure are observed on the c' boundaries. Incidentally, this zone particularly near the b/c' boundary corresponds to a film thickness correct for maximum light scattering. This is discussed in detail by Swamy.[11] In the c, or amber, zone where the effects of crystallization are more apparent, the film appears to be largely continuous with a multitude of crystal aggregates or dendrites superimposed upon it (Fig. 11, Plate 1). The metal by atomic migration is transferred to those centers with a corresponding thinning down of the surrounding areas. Gas emission here has little, if any, modifying effect on the film because of its open structure. The structure of silver films of thickness corresponding to this zone is well covered in the literature of the past five years.[12]

Initial film thicknesses were determined by two methods, both depending on the increase in weight of an aluminum foil receiver, the silver deposited simultaneously on this and the test sample. In one, the silver deposit on the samples was of uniform thickness (this was used mostly on the sputtered films), in the other the distribution followed an inverse square relationship so that if the thickness were determined for one point, say the central point of maximum thickness, the thickness at any other point would be known.

Results indicate a mean value of 0.1 micron for the thickness at the a/b boundary for silver films heated in vacuum at 450°C until agglomeration is completed. A wider range of values is obtained for the c'/c boundary because of its poor definition with a mean of 0.015 micron. If the film is heated in air these values, particularly the a/b are higher. A film sufficiently heavy to just break into particles when heated in air, remains continuous if heated in vacuum. Fig. 12 shows two samples taken from the same sputtered film and heated at 450°C, one in vacuum (Plate 1), the other in air (Plate 2). Exposure of the film to mercury vapor prior to heating also increases the boundary values.

Particle size and spacing

The relation of particle size and spacing to film thickness for sputtered silver films heated in air may be seen in Fig. 11. Data appear in Table II. With a decrease in film thickness and a consequent increase in the light transmission of the particles or heavier portions of the film, the contrast becomes increasingly poor so that microphotographs of the amber zone contain little detail. With critical illumination, photographing on Eastman M plates, developing for maximum contrast and printing on the hardest paper, Plate 1 represents about the best definition obtained in this zone.

From the available data it may be concluded that for maximum particle separation in the mosaic zone, the initial film thickness of an evaporated film (heated in vacuum) should be 0.8–0.9 micron, while for sputtered films (heated in air) it is approximately 1.0–1.2 microns. Irregularity in particle size and shape increases above these dimensions while below 0.05 micron the separation is distinctly poorer, more of the particles being connected together in chains.

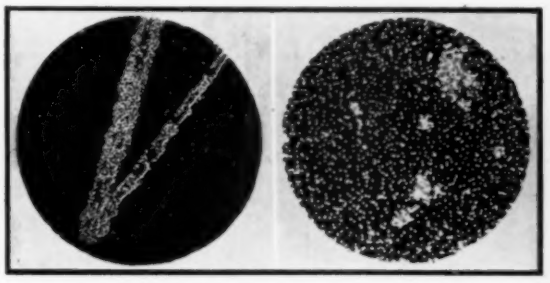

1 2

FIG. 13. (*T*).

[11] Swamy, Proc. Indian Acad. Sci. **1**, 347 (1937).
[12] Andradae Martindale, Phil. Trans. Roy. Soc. **235**, 69 (1935).

Film structure *vs.* temperature and time of heating

Summarizing the data with respect to temperature and time of heating, the following conclusions may be drawn: (1) Evaporated films (0.1μ) on nonoutgassed substrates, heated in vacuum, bead reapidly at 450°C, little change in the structure of the mosaic area occurring after two hours heating. (2) Sputtered films of similar thickness, because of better contact with the substrate, bead less rapidly at this temperature so that there is generally a reduction in the particle size observed on continued heating. (3) At 750°C the final structure is reached in a few seconds. (4) Films 0.2μ and heavier show little change in structure on prolonged heating.

Characteristics

Among the interesting characteristics of the agglomerated type of film is the effect of the substrate surface on the agglomeration process and the final structure. A thin film deposited on a surface with abrupt though minute irregularities, such as light scratches, is weakened along these lines so that agglomeration is evident first in these areas. Thus in a film of such average thickness as to develop few fractures on heating, there will be ordinarily, numerous small areas where the process has progressed almost to completion. (Fig. 13; Fig. 14).

Because of the large amount of work done in the field of x-ray and electron diffraction, the literature of the past few years is replete with information and data regarding the crystal structure of thin films and the effect exerted by the substrate on crystal orientation. The silver crystal, a face-centered cube is, according to literature, almost invariably oriented with the 111 plane parallel to the surface of a glass or mica substrate. There are critical temperatures, dependent on the substrate, at which orientation in a film occurs and

TABLE II.

SAMPLE (FIG. PL.)	INITIAL THICKNESS	TEMP. C	MEAN PART. SIZE	PARTICLES PER MM²
11/1	0.012 micron	750	—	—
11/2	0.028	"	0.36 micron	2.4×10^6
11/3	0.039	"	0.44	1.7
11/4	0.082	"	0.73	0.80
11/5	0.107	"	1.0	0.39
11/6	0.193	450 (8 hr.)	—	0.30 (8.8×10^4 Large)

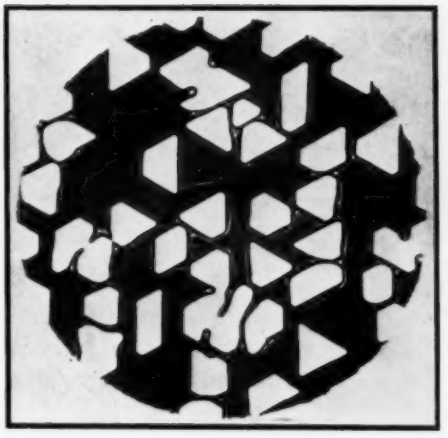

FIG. 14. (*T*) Mag. = 880.

it is interesting to note that according to Rudiger[13] silver on mica shows signs of orientation at room temperature and complete orientation at 150°C regardless of the film thickness. In contrast, natural quartz effects no orientation in silver while on fused quartz the process begins at 550°C, this applying to films 10–100 mμ in thickness.

An interesting case of crystal orientation by the substrate was observed in one sample silver film evaporated on mica at room temperature and heated in vacuum at 450°C for 4 hours. Ordinarily, the boundaries of the windows appearing in the continuous film show no tendency to regularity; in this sample, all were straight lines parallel to the hexagonal axes of the substrate. (Fig. 14). Departure from straight lines is to be observed mostly where the boundaries are especially near one another, and there is a general rounding off of corners as the windows enlarge and merge. Occasionally, one or more windows similar to these has been observed in the heavier portions of a sample film, but this was the only sample in which this general regularity appeared.

3. TRANSLUCENT FILM

This type of film, designed for rear illumination of the sensitized silver surface, is a composite of three films: (1) an electrically conducting film of high light transmission; (2) a protecting coating for the same; and (3) the silver film. The subfilm

[13] Rudiger, Ann. d. Physik **30**, 502–526 (1937).

1 2 3

FIG. 15. (*T*) Mag. = 1290.

is necessitated because of agglomeration of the thin silver film on heating, a primary requirement being electrical connection to all the silver particles.

The composite therefore, consists essentially of a silver mosaic of fine structure superimposed upon a stable transparent film serving as the common conductor to the separated silver particles.

The silver film

The thickness of the silver film for maximum efficiency of the composite has not been definitely determined but it is probable that it is that thickness associated with maximum light scattering, *viz.*, 0.01–0.02 micron. The heavier mosaics have a low fractional coverage and the light losses in the networks or the beginning of the continuous zone is excessive. Details regarding this section of the composite are omitted here having been discussed at length under *the agglomerated film*.

If the silver film be applied directly to the transparent conducting film, in this case platinum, two effects are observed: (1) low photosensitivity of the treated film and (2) electrical discontinuity of the platinum film on continued heating. The cause is found in the alloying of the two metals and a consequent lowering of the melting point of the subfilm. As a result of this lowering in melting point there is a distinct increase in the tendency of the film to agglomerate and therefore become discontinuous.

The second effect is well illustrated by Fig. 15. If heated at as high as 600°–700°C for a period of 15–30 seconds, or a proportionately longer time at lower temperature, the film is found to be covered with a great number of small openings the order of a few tenths micron in width. (Plate 1). On continued heating these elongate and interconnect (Plate 2) with the final state—a mosaic of vermicular particles of wide range of magnitude most of them long and multibranched (Plate 3).

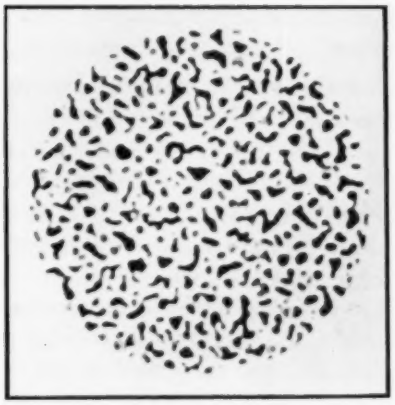

FIG. 16. (*T*) Mag. = 2000.

The intermediate film

If prior to application of the silver film, a thin protective and electrically conducting coating be applied to the platinum, adhesion and alloying of the two films may be prevented. On heating the composite to a temperature of 400°C, the silver film breaks up readily and the platinum remains conducting. Fig. 16 shows such a composite, the intermediate film here being aluminum oxide. After sputtering the platinum onto the glass receiver, and aging, sufficient aluminum was evaporated on to show a distinct decrease in the film resistance. Air was then admitted to oxidize the aluminum deposit (indicated by an increase in film resistance to approximately the initial value) after which the silver film which in this case was relatively heavy, was applied by evaporation. It will be observed that the silver particles are for the most part elongated and irregular in shape and size. This is characteristic of heated silver films deposited on a roughened substrate such as etched glass or mica or a film of cryolite deposited by evaporation and in no way militates against the successful operation of this type of film.

Of a variety of materials which may be used for this protective or intermediate film, silica is perhaps superior and may be evaporated from a tungsten filament. If the silica is in the form of a thin tube covering the filament, evaporation of the tungsten onto the receiver is minimized, if not entirely eliminated. The film to be effective may

be sufficiently thin to show no interference fringes.

Another use of the intermediate film-coating is in preventing oxidation of the conducting film so that it is possible by applying it before exposure of the latter to air, to use a thinner and consequently more transparent film.[4] With metals more susceptible to oxidation this procedure is a necessity; with platinum, an increase of 10–15 percent in transmission is possible.

The conducting film

The requirements imposed on the conducting film reduce the number of possible metals to a very small group. The film must not only remain continuous on heating in vacuum and on exposure to air, but must resist an oxygen glow discharge and the alkali metal vapors. The tendency of films to agglomerate decreases in metals of higher melting point, with a resulting increase in the optical transmissivity-electrical conductivity ratio,[4] so that optically, tungsten would be ideal. However, tungsten, tantalum and molybdenum oxidize so readily, that thin films lose their electrical conductivity on exposure to air. Elimination of these, leads to the choice of platinum, which experience indicates is entirely satisfactory and most practical. Suitable films of this metal are readily deposited by either evaporation or sputtering.

The structure of thin ($10^{-6}-10^{-7}$ cm) platinum films and their characteristics is a subject so well covered in literature that little more than a summary is called for here. The electrical characteristics are of particular interest and application.

The modifying forces common to all films, *viz.*, gas emission, differential expansion, tension, and crystallization have a pronounced effect on the electrical conductivity of these films. A sputtered platinum film exhibits the phenomenon of aging, which is an irreversible decrease in resistance with time, due to the modification in structure. Crystal orientation associated with a transformation temperature dependent on the substrate, and growth with heating also produces this aging so that with increasing temperature, the resistance falls to a minimum value. The temperature coefficients of the thinnest films are always negative, but may according to Bartlett[14] be zero, or slightly positive for the heavier. With light currents, Ohm's law is obeyed,[15] heavy currents producing aging.[14]

Change in resistance of a freshly sputtered film may be effected by exposure to the atmosphere. Curves (characteristic of the heavier films) given by Koller[16] show that the normal aging in vacuum is stopped by admission of air, the resistance rising slightly to a constant value. On re-evacuating, the process again begins, proceeding until interrupted by re-admission of air or until a final constant value is reached. Decrease in resistance may also be produced by exposure of the freshly sputtered film to air. Table III gives initial and final resistance values after exposure of platinum films to air, following sputtering and cooling. The samples were sputtered in argon on smooth but not optically polished 2″ Pyrex glass disks equipped with terminals located on opposite sides of the circumference.

TABLE III.

SAMPLE NO.	R(MEGS)	R'(MEGS)	LIGHT TRANS. %
1	0.200	0.200	71.0
2	0.500	0.200	64.0
3	0.278	0.191	68.6
4	1.000	0.310	60.5
5	4.100	1.000	68.2
6	11.000	12.100	79.6
7	19.000	9.500	72.3
8	2.750	2.800	79.0

Samples 1, 6 and 7 which had the highest light transmission and showed either zero or a small increase in resistance on admission of air were films sputtered on new disks; the remainder were on disks which had previously been sputtered with platinum. All the disks were carefully cleaned and dried prior to sputtering. It is impossible to say here whether the decrease in resistance of these samples can be entirely assigned to the previous sputtering of the disks with platinum, but probably not. However, permanent sensitization of the substrate so as to effect the behavior of the deposited film regardless of care exercised in cleaning has been observed by a number of investigators.[12, 17]

Among other interesting characteristics, which incidentally have no application to the particular problem, is the catalytic action of these thin

[14] Bartlett, Phil. Mag. **5**, 848–859 (1928).
[15] Perucca, Ann. d. Physik **4**, 252–272 (1936).
[16] Koller, Phys. Rev. **18**, 221–235 (1921).
[17] Starkey, Phil. Mag. **18**, (57), 241–256 (1934).

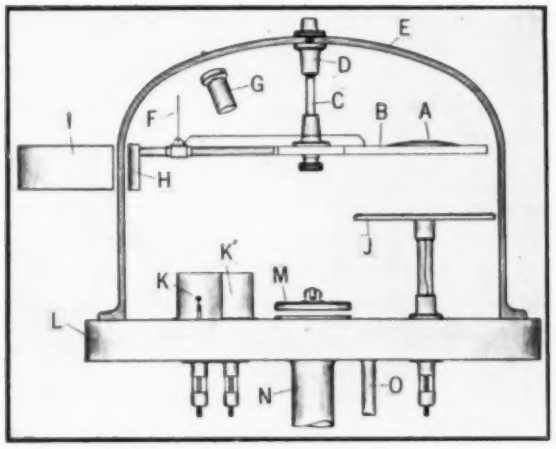

FIG. 17.

platinum films. The structure is essentially the same as chemically prepared platinum black[18] with similar effects on combustible gas mixtures such as hydrogen and air.[16]

Apparatus

For production of these experimental translucent films on 90-mm watch glasses, the device illustrated by Fig. 17 was used. As previously stated, in order to use a platinum film of minimum thickness so as to obtain maximum light transmission, it is necessary to apply the protective intermediate film prior to exposure of the platinum film to the atmosphere. With the device to be described the three films are applied consecutively and the composite completed before admitting air to the sputtering and evaporating chamber.

The cleaned watch glass *A* is mounted in the holder *B* which is free to turn about the vertical support rod *C*. This whole assembly may be removed from the fitting *D* which is sealed through the roof of the bell-jar *E*. This is a convenience in mounting and removing the watch glasses and makes cleaning of the bell-jar easier. Leads connecting through spring clips to terminals located opposite each other on the circumference of the watch glass terminate, one on the holder so as to make connection to the outside through fitting *D*, the other to a thin tungsten "whisker" *F* which is insulated from the holder, but by rotation of the holder about *C*, contacts with terminal *G* which also serves as a sputtering anode. Motion of the holder is effected from outside the bell-jar by attraction of the armature *H* by the magnet *I*. By rotation of the holder, the watch glass may be brought directly over the platinum sputtering cathode *J* or a number of evaporating positions *K*, *K'*—etc., all located on the circumference of a circle whose center coincides with the axis of the support rod *C*. The evaporators are located vertically so as to coincide with the center of curvature of the watch glass when located directly overhead. Cylindrical shields prevent transferal of material from one evaporator onto another or onto the sputtering cathode.

The bell-jar is waxed to the pump-plate *L* with Apiezon-Q wax. The vacuum system, consisting of mechanical and diffusion pumps, cold trap, etc., is entirely conventional except for the valve *M* which consists of two flat and lapped surfaces located within the bell-jar immediately at the end of the pump tube. The valve is actuated through a sylphon bellows from beneath the pump plate. (The actuating mechanism is omitted from the diagram.) *O* is the valve by-pass and gas inlet.

The thickness of the sputtered platinum film is determined by successive resistance measurements between terminals *D* and *G* and the sputtering continued until the correct resistance value is obtained. Following application of the platinum film, the chamber is exhausted to a high vacuum, the watch glass is moved over the position *K* where the intermediate film is applied, then over *K'* where it is completed on application of the silver film. Beading of the silver film takes place automatically on baking the assembled tube prior to photosensitizing the film.

CONCLUSION

In conclusion it should be stated that the greatest portion of the work reported in this paper was conducted in the vacuum tube laboratory of the Philco Radio & Television Corporation. The writer wishes to express due appreciation to all assistants and associates who in any way contributed to the work and to Mr. Crebbin of the Bausch & Lomb Optical Co. who very kindly lent the writer optical equipment.

[18] Fery, Proc. Phys. Soc. **49** Extra Part (Aug. 31, 1937).

Electrical and Luminescent Properties of Phosphors Under Electron Bombardment

WAYNE B. NOTTINGHAM*
Research Laboratory, General Electric Company, Schenectady, New York
(Received September 16, 1938)

A tube using a cathode-ray type of electron gun has been used to study the properties of five phosphor samples using four different materials. These were (1) zinc-orthosilicate (2) calcium-tungstate (3) zinc-sulfide: cadmium-sulfide and (4) zinc-sulfide. The first three showed saturation effects with current density definitely greater than the last, and the first two have maximum potentials as limited by secondary emission of 6500 and 5000 volts respectively. For these, the light output per unit electron current increased with the square of the voltage, while it increased with the 2.8 power of the voltage for the zinc-sulfide. A simple power law does not hold for the zinc-sulfide: cadmium-sulfide which shows a maximum light output at 8000 volts. All of the sulfides had such good secondary emission properties that the maximum limiting potential was well above 10,000 volts.

INTRODUCTION

THE electrical and luminescent properties of willemite under electron bombardment were investigated and reported in this Journal.[1] Those results were preliminary in the sense that definite improvements in technique were suggested which would make the conclusions drawn more certain. Although at the time there was no immediate prospect of continuing the work, this has been done with the result that the present paper not only applies to willemite but a number of other phosphors as well.

The results of the earlier study may be summarized very briefly. An investigation of the screen potential showed that, under normal conditions, it remained very slightly negative with respect to the most positive anode of the tube up to a value of voltage of the order of 6500 volts. No higher potential could be obtained with the willemite samples studied, because at this voltage one secondary electron was produced for each primary arriving at the phosphor. The light output was determined as a function of the bombarding current and found to be perfectly linear and directly proportional to the current for densities less than about two microamperes per sq. cm, but for current densities of the order of ten milliamperes per sq. cm the light output per unit current was observed to be only two percent of that found for the lower intensities. This saturation effect was found to be very nearly independent of the bombarding voltage but depended only on the current density. At low current densities the light output was proportional to the square of the electron energy, except when the grain size of the willemite was so small that penetration through the individual grains was possible. Willemite held in position by binder showed an increase in light intensity with voltage which was more rapid than the second power at low voltages. Under these conditions the empirical formula incorporating the concept of "dead voltage" again indicated the applicability of a formula involving the square of the screen potential.

Two difficulties were present in the previous study: (1) Secondary emission from the first anode sometimes made the determination of the true screen potential difficult and also influenced the determination of the current density. (2) The current density measurements could not be obtained directly but had to be computed after making certain allowances which could not be tested rigorously. The design of the tube to be described below permitted the elimination of these two sources of uncertainty. Also it was considered important to investigate other materials and to determine the light output as a function of the time the electron beam is applied to the phosphor. Developments have been made to permit investigation of this aspect of the problem, but the results have not been completed, and therefore the present discussion must be confined to the investigation of the light output as a func-

* On leave of absence from Massachusetts Institute of Technology.
[1] W. B. Nottingham, J. App. Phys. **8**, 762 (1937).

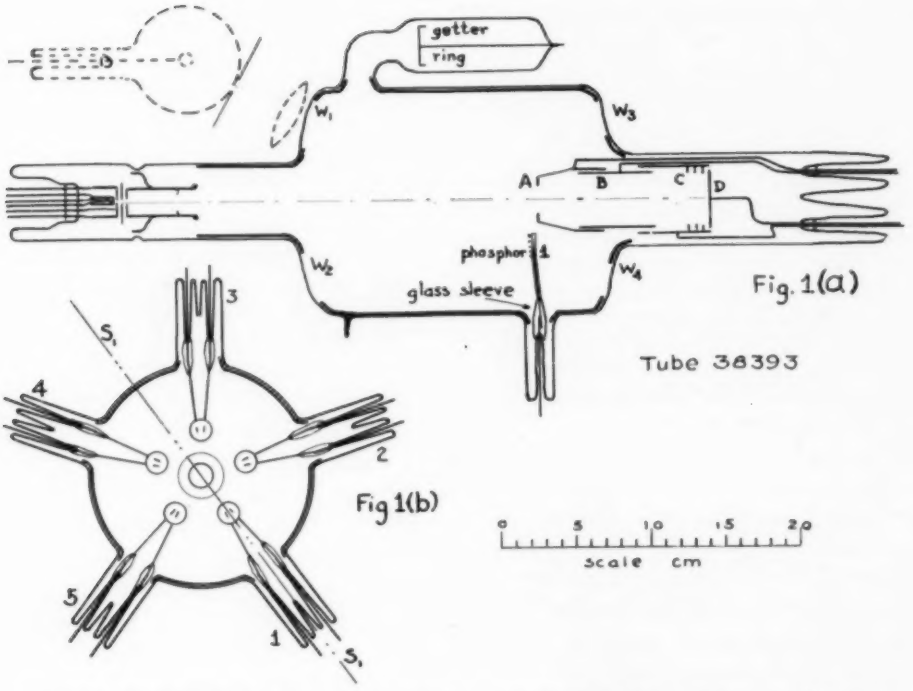

FIG. 1(a). Scale drawing of tube showing only one of the five phosphor mounts. (b) Section perpendicular to tube axis through plane of phosphor mounts.

tion of the current density and voltage with a stationary beam applied continuously to the sample.

DESIGN AND CONSTRUCTION OF THE TUBE

A standard vacuum tube blank, made of Nonex glass, designated by T-48-El, was utilized as the starting point for the experimental tube shown in Figs. 1(a) and 1(b). Although these drawings are made to scale, they are not mechanical drawings in the sense that all of the details which could be seen are given. Fig. 1(a) shows the section in the plane defined by the tube axis and the line S_1-S_1 of Fig. 1(b). This shows only one of the five phosphor mounts, since an attempt to show others would only make the picture more difficult to understand. Fig. 1(b) is a section taken through the plane of the phosphor mounts perpendicular to the tube axis. The heavy line drawn as on the inside wall of the glass blank represents, in schematic, the gold coating applied to the inside wall of the tube to serve as the "second" anode and collector of the electrons. Openings about an inch in diameter are shown as breaks in the heavy line at W_1, W_2, W_3 and W_4. There were ten of these altogether which served as windows through which the light emitted by the phosphors was measured and viewed. For example, when phosphor (1) (the only one shown in Fig. 1(a)) was being studied, a lens and photoelectric cell were located at W_1 as shown by dotted lines, and the light taken from the sample was focused on an aperture attached to the cell. This arrangement was used in order to reduce the amount of light received by the cell from phosphors not being studied, but nevertheless slightly excited by secondary electrons from the bombarded sample. The tube was mounted at the two ends on a wooden frame so arranged that the tube could be rotated about its axis. This made it unnecessary to rearrange the optical system and the photoelectric cell as different samples were investigated. All of the connecting leads to the tube were made sufficiently flexible so that it could be rotated without disconnecting any wires.

An RCA 912 cathode-ray tube gun was used as the source of electrons, and was mounted on the axis of the main tube as shown in the figure. After

having sealed the gun onto the tube, it was cracked off and remounted in an auxiliary tube for outgassing purposes. The metal parts were then heated by high frequency induction to the maximum temperature thought permissible, with the coils arranged so as not to overheat the cathode. The object in this preheating was to remove all of the easily vaporized material from the gun, so that during the final exhaust of the tube the adulteration of the surfaces of the phosphor samples would be reduced to a minimum.

A four-element electron collector was mounted on the axis of the tube directly in line with the gun, with the entrance opening practically in the same plane as the mounts supporting the phosphors being investigated. The circular opening of this electron collector was equal in diameter to that of the phosphor mounts to be described below. The object in building an electron collector as shown in the figure was to make it possible to measure the primary beam current and to determine whether or not any appreciable fraction of the beam was made up of secondary electrons from one or more of the elements of the electron gun. Furthermore, it was considered undesirable to place any of the samples on the axis of the tube, since some adulteration might come from the cathode, either by direct evaporation or as negative ion emission.

The samples were mounted on disks of 705-AO glass which were formed as shown in Fig. 1 by building up a sphere 1.5 cm in diameter on the end of two 60-mil Fernico rods which had been previously covered with a coating of this glass except for a short length used for welding. Each sphere of glass was ground and polished, leaving a disk 1.5 cm in diameter on one surface of which were exposed the two Fernico wires separated by a distance of about 4 mm. The tube blank, with its five side arms and four single lead stems used for mounting the electron collector, was connected to the vacuum system and baked for about 12 hours at 500°C. After this was done, the five side arms were cracked off and the phosphor mounts welded to the leads, with movable glass sleeves arranged so that after the welding was completed the sleeves could be put into place and melted down so as to hold them firmly. These sleeves served to eliminate the possibility that any electrons, except those which arrived there by flowing through the phosphor itself, could be collected on these leads. The conductivity of one of these mounts was measured before the application of the phosphor in a specially constructed evacuated tube, so that the resistance of the phosphor could be determined later. The conductivity, as a function of the temperature, was found to obey the equation

$$K = 130\, e^{-11,900/T}\ (\text{ohm})^{-1}.$$

The resistance between probe wires was measured after the evacuation of the tube, and the results are tabulated in Table I. It is at once apparent that although the resistances, as shown, are low enough to make the measurement of the phosphor potential easily possible, they are many orders of magnitude higher than those previously reported.[1] The exact reason for this difference is not apparent unless it is due to the fact that the thickness of the phosphor was probably less in the present case than for the previous study of willemite. It is also possible that the acetone previously used may have left a residue which altered the conductivity.

After the construction work was finished, the five sample mounts were coated with the phosphors under investigation. These included two samples of zinc-sulfide, silver activated, which were chosen in order to get a little check on the question of reproducibility; one sample of calcium-tungstate; one of zinc-orthosilicate, manganese activated (willemite); and one of zinc-sulfide: cadmium-sulfide, silver activated. The phosphors were all ground fine enough so that they would not fall out of suspension in acetone in less than a few minutes. This size particle

TABLE I.

Sample No.	1	2	3	4	5	Glass
Phosphor	ZnS	ZnS	ZnS; CdS	$2(ZnO)SiO_2$	CaW	No coating
Resistance at room temperature	2.1	1.9	1.8	1.8	0.194	17×10^{14} ohms

seems to be about ideal for study, since the particle size is large enough to prohibit the complete transmission through individual grains by the electrons, and yet small enough to permit application to the mount without the use of binder. The powdered phosphors were put in acetone and, after agitation, were applied to the mounts as drops of suspended material in the liquid. By keeping the mount in motion during the time that the acetone was evaporating, it was possible to cause the phosphor to adhere to the glass plate with considerable thickness and reasonable uniformity.

Experiment showed that when the getter was mounted on the electron gun structure, as is usually done, a sufficiently thick layer of material was deposited on the phosphors to alter seriously their electrical properties. For this reason an appendix was connected to the main tube and a getter ring was mounted, as shown in the figure, using eight pellets of the King Laboratory barium-aluminum getter. During the final exhaust of the tube this ring was held at a dull red heat for a period of time sufficient to outgas it, so that when the getter was finally flashed a half an hour before sealing off the tube, very little additional gas was liberated.

After about 16 hours of baking at 480°C, the metal parts of the assembled tube were heated by high frequency until the vacuum, with these parts hot, was better than 10^{-7} mm of mercury. At this stage the cathode was activated and operated for sixteen hours with the first grid at +9 volts and the cathode heating current ten percent above normal. Then the seal-off constriction was preheated, and the getter flashed. After sealing off the tube the cathode was further aged by drawing a current to the first grid with a potential of ten volts applied. Tests were made to try to detect the presence of positive ions by maintaining the electron collector system, that is, parts *A*, *B*, *C* and *D*, 20 volts negative with respect to the cathode, while the electron beam was shot down the tube to the second anode with an applied potential of 5000 volts. Even with a beam current of 100 microamperes, no ion current could be detected, although the galvanometer used would have responded to a current as small as 10^{-9} ampere. The conventional method of measuring the ion current to the first grid of the electron gun also showed none that could be detected. After two months of operation the tube was again tested in this way and found to be free from detectable ion current.

Circuits

The circuit used is shown in Fig. 2, in which the three sources of d.c. power, P_{a1}, P_{a2}, P_{ag}, were very well filtered rectifier units operated from a regulated a.c. line. The voltages were read by measuring the current flowing through calibrated wire-wound resistances. The method of measurement usually involved the setting of V_{a2} (the potential on the second anode relative to the cathode) at some arbitrary value and the adjustment of V_{a1} to approximately one-tenth of this value, since for this adjustment of V_{a1} the diameter of the beam at the plane of the samples was about 1.2 cm and very nearly perfectly round and quite uniform. With this arrangement the phosphor under investigation was bombarded over nearly its entire cross section. Two permanent bar magnets served to create the magnetic field required to deflect the beam from the axis of the tube to the sample being studied. After having adjusted the potentials V_{a1} and V_{a2}, the current in the beam was controlled by varying the potential V_{g1} on the first grid. The light output was measured as a function of the current on one of a number of different photoelectric cells used in this work. Only in the case of the zinc-sulfide phosphor was there any difference in the results obtained with different photoelectric cells. A potassium photoelectric cell was used for some of the work, and found to give identical results with those obtained with a barium and a caesium cell, used with and without filters, for all phosphors except zinc-sulfide. In this case the potassium cell gave anomalous results which indicated that some slight change in the quality of the light probably took place for this phosphor.

At each value of current, the potential V_{ag} was adjusted to give zero current through the electrometer connected to the probe wire of the phosphor under investigation. This served as a direct measure of the difference in potential between the phosphor and the second anode. By subtracting V_{ag} from V_{a2}, the true potential of the phosphor relative to the cathode was determined. The results obtained are given below in

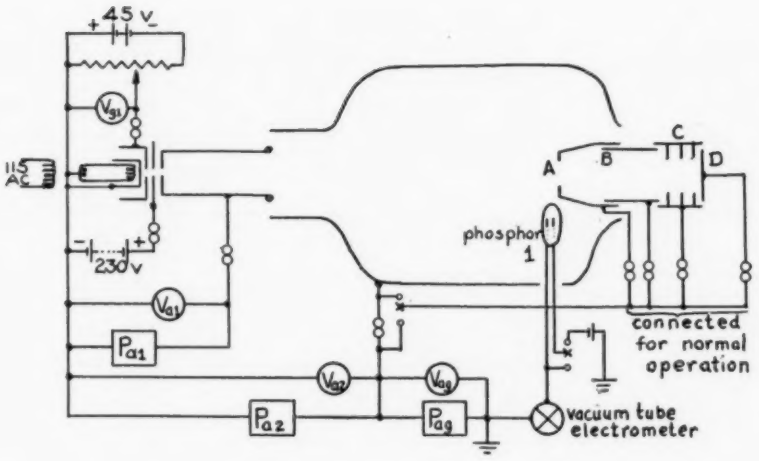

FIG. 2. Circuit diagram.

connection with the discussion of each individual phosphor studied. During these measurements all four electrodes of the electron collector were connected to the gold coating which served as the second anode, and the current measured at this electrode served as a direct measure of the primary beam current. The fact that the beam current could be measured in this direct way was proved by adjusting the magnetic field so that the beam, instead of striking either the gold coating wall or one of the phosphors, went directly through the opening of the electron collector at A of Figs. 1 and 2. In this case the current collected on the second anode proper fell to one percent of the value observed when the beam impinged either on one of the phosphors or on the wall of the tube. When the electron beam was being measured, the first electrode (A) was maintained at the second anode potential. The second one (B) was maintained 100 to 300 volts negative with respect to (A), while (C) and (D) were kept positive with respect to (A). All electrons, except for a very small fraction, were collected on (C) and (D). There was a very small current flow in the (B) circuit, indicating the escape of a small electron current, and the current measured at (A) showed that a small number of electrons were received there. This number happened to be almost exactly equal to the electrons leaving (B). In all cases these two currents were of the order of one or two percent of the primary beam current. These measurements were taken to indicate that an error of not more than two or three percent would be introduced by assuming that the measured second anode current was equal to the primary beam current bombarding the sample.

In order to measure the currents in any part of the circuit, disregarding the potential of that part of the circuit relative to the ground, a galvanometer was set up on a single wire suspension to eliminate building vibrations[2] and enclosed completely in a conducting shield. The connecting wires and also the Ayrton shunt were enclosed in shielding. All of these shields were connected to the "battery side" of the galvanometer, so that the instrument and its surroundings were always at the same potential. This method of mounting made it possible to insert the galvanometer into any part of the circuit and have a negligible background current caused by corona discharge and other leakages. The galvanometer was connected to a plug on an insulated handle and every lead connecting to the tube had series jacks and a shunt switch (shown by the two small circles in each lead of Fig. 2), so that the galvanometer could be plugged into any lead and with the shunt open was available for reading the current.

A vacuum-tube electrometer was used to measure the small photoelectric current produced. Since in certain cases currents as small as 10^{-13} ampere were measured, polarization currents would have been objectionable were not all of the high voltage leads enclosed within a shield, and the photoelectric cell and its connections shielded

[2] R. P. Johnson and W. B. Nottingham, Rev. Sci. Inst. **5**, 191 (1934).

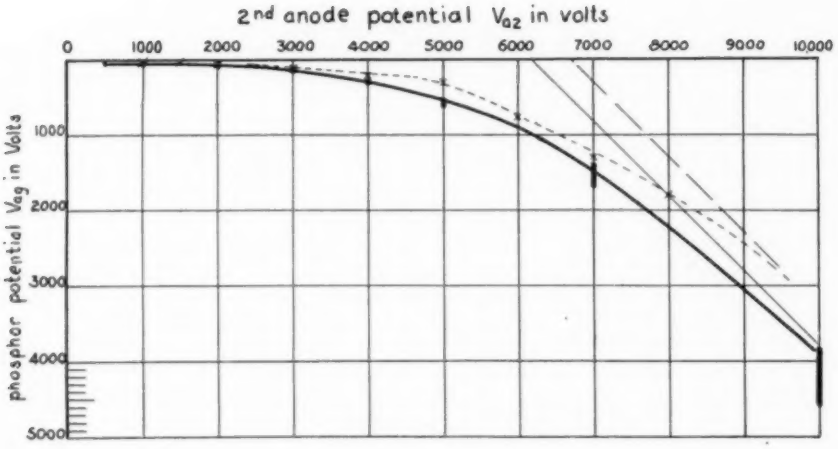

FIG. 3. Anode to phosphor potential as a function of the second anode potential. Solid line present data; dotted line previous data taken from reference 1. Heavy vertical lines show range of potential change with current density.

as well as possible. This precaution of using double shielding was necessary since neither of these two circuits could be shielded alone with the required degree of perfection to eliminate polarization currents completely. The system as a whole was also shielded to eliminate stray light and external electrical disturbances. The amplifiers used for these measurements were constructed to operate within a vacuum housing and used the DuBridge-Brown[3] circuit with FP-54 vacuum tubes.

EXPERIMENTAL RESULTS

Properties of willemite

Measurements made, according to the methods described above, on the sample of willemite showed that the screen potential remained slightly negative with respect to the second anode over the entire range of voltage from 500 to 5000. For applied potentials above 5000 the difference in potential between the screen and the second anode increased very rapidly, indicating that the maximum potential obtainable for this sample of willemite was about 6200 volts. These data are shown in Fig. 3, along with the curve (dotted) observed in the previous investigation.[1] The fact that the agreement in these two cases is so close, is a strong indication that the results are significant. If the secondary emission properties of a given phosphor sample are perfectly uniform, the observed potential difference between the sample and the second anode should be independent of the current density. Below 5000 volts a change in observed potential of only a few volts was found with a change in current density of over a thousandfold, while with 10,000 volts applied, the difference in potential between the sample and the anode changed from 3800 to 4600 volts as the current density was increased to about 100 microamperes per sq. cm. In all cases the difference in potential increased with increasing current density, and the extent of this change is shown by the vertical lines of Fig. 3. Although the detailed explanation of this effect is not understood, it seems reasonable to attribute it to nonuniformities of the secondary emission properties, caused either by surface contamination or a difference in the emission of certain grain facets as compared with others, depending on the crystallographic orientation of the various exposed surface planes. All of the phosphors exhibited this effect to a certain extent, although it was most prominent in the case of willemite.

In Fig. 4 typical data are shown giving the light output as a function of the current with 7000 volts applied. The heavy line of the figure which agrees very well with the present observed data shown by circles, is a reproduction of the curve taken from my earlier publication.[1] The fact that some of the points observed at current densities above 80 microamperes per sq. cm fall below the curve may be due to the heating of the sample under electron bombardment, since the beam was allowed to bombard the sample con-

[3] L. A. DuBridge and H. Brown, Rev. Sci. Inst. **4**, 532 (1933).

tinuously during the time required to take the last seven points. In spite of this objection to the experimental technique, these data have been used since they extend to somewhat higher current densities than the other data taken. Curves just like this in form were obtained at other applied voltages between 500 and 10,000 volts. The light output, as read from each curve at one microampere per sq. cm, has been plotted as a function of the voltage in Fig. 5. It is clear from inspection that the light is quite accurately proportional to the square of the energy of the bombarding electrons. A comparison of these new data with those of the earlier publication indicates a quantitative agreement throughout, in spite of the fact that the tube structures used in these two cases were entirely different, and that the sample of willemite was obtained from the same source (RCA Manufacturing Company, Harrison) with a year intervening.

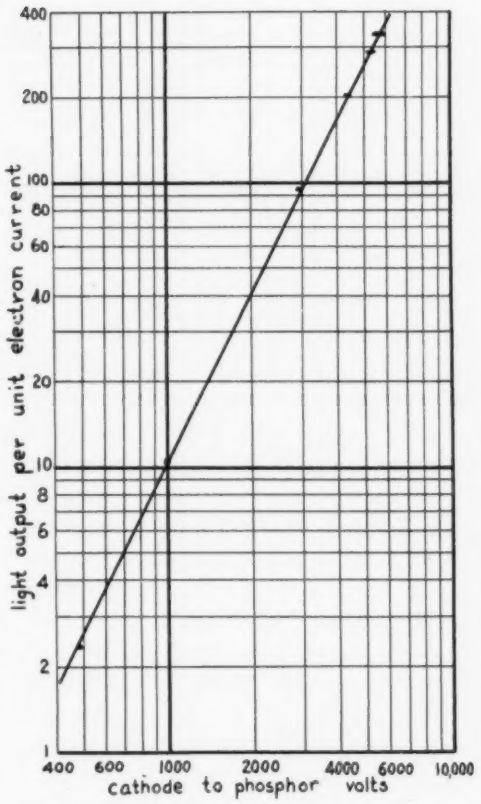

FIG. 5. Light output as a function of the phosphor potential for the willemite sample. Straight line drawn with a slope of two.

Properties of calcium-tungstate

The sample of calcium-tungstate was studied over the range of 500 to 5000 volts. Curve *A* of Fig. 6 shows the results of the determination of the phosphor potential relative to the second anode. Although the data are not sufficiently complete to make possible the drawing of the limiting line with certainty, the one shown terminating at 5000 volts cannot be far off. After about two months additional operation of the tube, Dr. R. B. Nelson made a redetermination of this curve and obtained the one shown as *B* of Fig. 6. There can be no question but that the limiting line has shifted to about 7500 volts, which indicates that in spite of all of the precautions which were taken to reduce the surface contamination to a minimum, the secondary emission from the calcium-tungstate altered very definitely in the favorable direction as judged from the practical point of view. There were two possible sources of contamination which were either the cathode or the zinc-sulfide sample number 1 which was adjacent to the calcium-tungstate number 5. Although it is not certain, it seems that the latter was the more likely source, since in the course of the experiments it was severely bombarded and may have evaporated over to the calcium-tungstate sample enough to modify its secondary emission since,

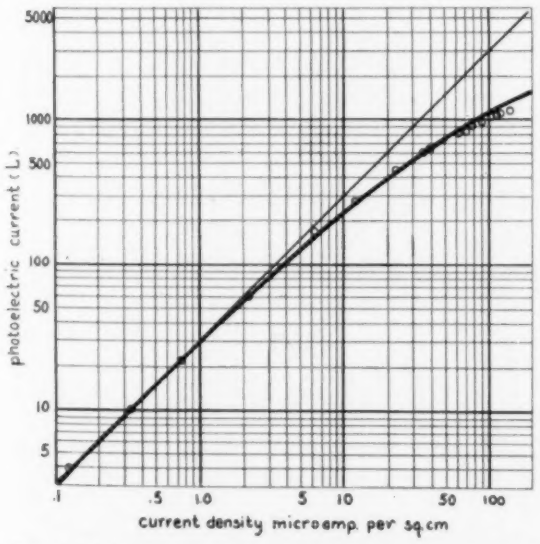

FIG. 4. Light output as a function of the current density for the willemite sample. Second anode potential 7000 volts, phosphor potential 5500 volts. Heavy line represents results of previous study. (Reference 1).

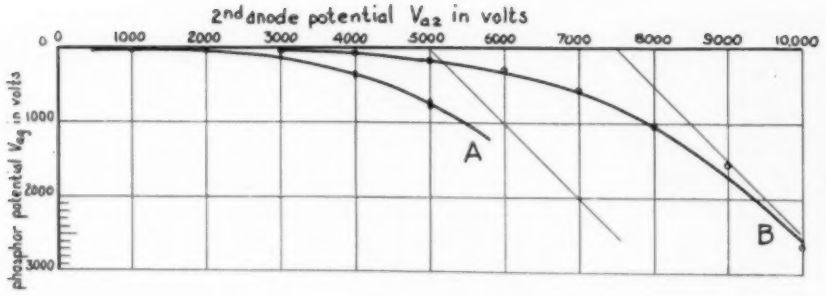

FIG. 6. Anode to phosphor potential as a function of the second anode potential. Curve *A* for calcium-tungstate before extended use of the tube; curve *B* after sufficient tube use to cause some contamination of surface.

as will be shown below, the sulfides studied were superior from the standpoint of secondary emission properties at high voltages.

The light output as a function of the current is shown in Fig. 7. From this it is seen that there was a small saturation effect which became noticeable above 20 microamperes per sq. cm. The dashed curve represents the willemite data, and has been drawn in to facilitate ready comparison. Curves representing data taken at other voltages were of the same form as the one shown, again indicating that the saturation effect depends primarily on the current density and only very slightly, if at all, on the bombarding voltage.

The circles of Fig. 8 show the light output per unit electron current as observed. These do not fall on a straight line, but, if a "dead voltage" of 100 volts is assumed and subtracted from each of the "cathode to phosphor" voltage readings, then a straight line, with a slope of two, results as indicated by the crosses.

Properties of zinc-sulfide: cadmium-sulfide; silver activated

The sample of zinc-sulfide : cadmium-sulfide was investigated over the same current and voltage range as described above. In view of the fact that so very little seems to be known about the secondary emission properties of the sulfides, it was very interesting to observe that the potential difference between this sample and the second anode remained small, even with 10,000 volts applied. In fact, here the difference in potential was found to be about 100 volts, depending slightly on the current density and location of the beam on the sample when focused. As will be mentioned below, the two samples of zinc-sulfide also showed this favorable property of giving good secondary emission up to 10,000 volts. It would be interesting and important to determine the maximum potential which could be used with the sulfides, but with the apparatus and time available, it was not possible to carry on these tests. The light output as a function of the current was accurately linear for current densities less than one microampere per sq. cm. Above this the light output per unit current decreased to almost exactly the same extent as was found for willemite. The dashed line of Fig. 9 represents the willemite data. As is shown, there was a drop in output of about 50 percent at about 100 microamperes per sq. cm, which was practically independent of the anode voltage. Another very unexpected effect is illustrated in Fig. 10, in which the light output is shown as a function of the voltage. At very low voltages, the light increased with the square of the voltage, but, as the curve shows, this rate of increase did not continue. In fact, above 4000 volts the in-

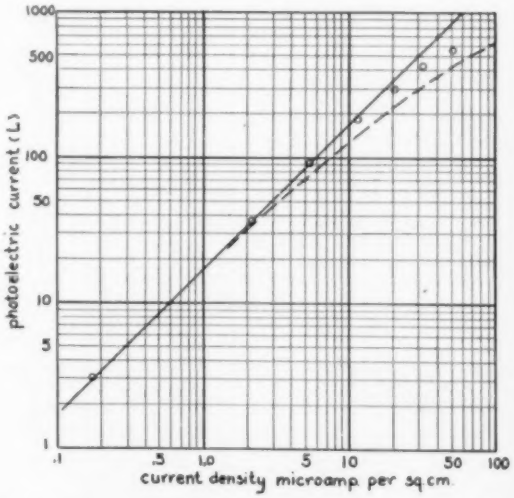

FIG. 7. Light output as a function of current density for the calcium-tungstate sample taken at 5000 volts applied. Phosphor potential 4300 volts to cathode. Dashed line willemite curve for comparison.

crease is even less than the first power.* This type of curve is particularly interesting in that it shows that if one were to use the rate of increase of light intensity with voltage as an indirect measure of the potential of the phosphor, the deductions on this basis would be decidedly in error, since direct measurements indicated that the potential of the phosphor throughout the entire observable range differed very little from that of the anode, and yet the rate at which the light output increased with voltage might be taken mistakenly as an indication that the potential of the phosphor had remained fixed at some relatively low voltage.

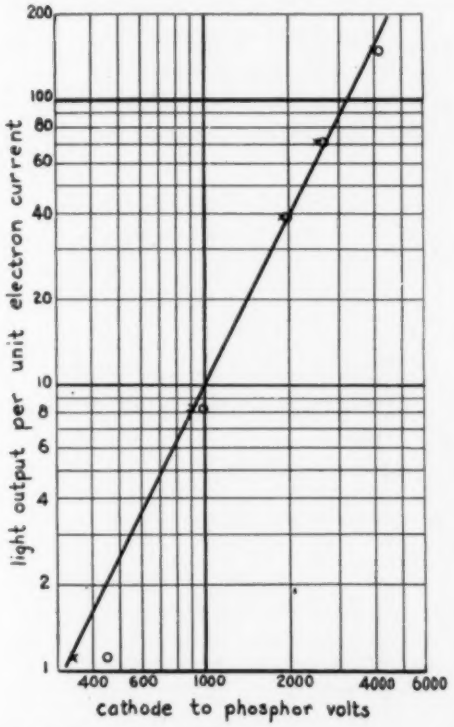

FIG. 8. Circles show light output per unit electron current as a function of the phosphor potential for calcium-tungstate. Crosses assuming a "dead voltage" of 100 volts. Straight line drawn with slope of two.

Properties of zinc-sulfide; silver activated

Silver activated zinc-sulfide was deposited on two of the test plates. These two samples were

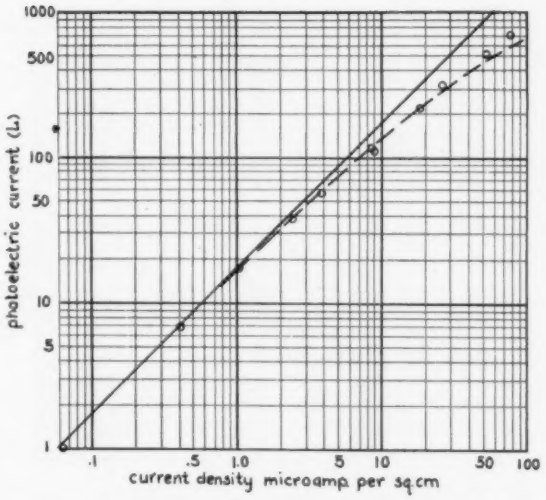

FIG. 9. Light output as a function of current density for the zinc-sulfide: cadmium-sulfide sample taken with 5000 volts applied. Phosphor potential 4970 volts. Dashed line is willemite curve for comparison.

similar in their behavior in all respects, and again showed that sulfides are good secondary emittors up to 10,000 volts and are probably able to go to much higher voltages than this. Another important property of these two samples of zinc-sulfide was that the light output per unit area was directly proportional to the current density to much higher values than for any other phosphor examined in this study. There was no detectable saturation effect up to 100 microamperes per sq. cm. At 3000 volts and with a sharply focused beam giving a current density of about ten milliamperes per sq. cm, the light output dropped to 40 percent of that expected on the assumption of perfect linearity between light output per unit area and current density. With this current density, willemite delivered only two percent of the expected light. Very extensive data were taken on these two phosphors because it was noticed that nearly all curves plotted showing the logarithm of the light output as a function of the logarithm of the current were good straight lines with a slope slightly in excess of unity. Some data showed an excess of as much as five or six percent. Since this was most noticeable with the lower anode voltages, where on account of the weakness of the light the errors are greatest, it must be assumed for the present that this apparent increase in light output above that expected was too near the limit set

* Dr. F. Seitz has suggested that this effect may be due to the excitation of x-ray levels in the cadmium atoms, with the resultant loss in electron energy, and therefore a decrease in the light-producing efficiency with increased voltage.

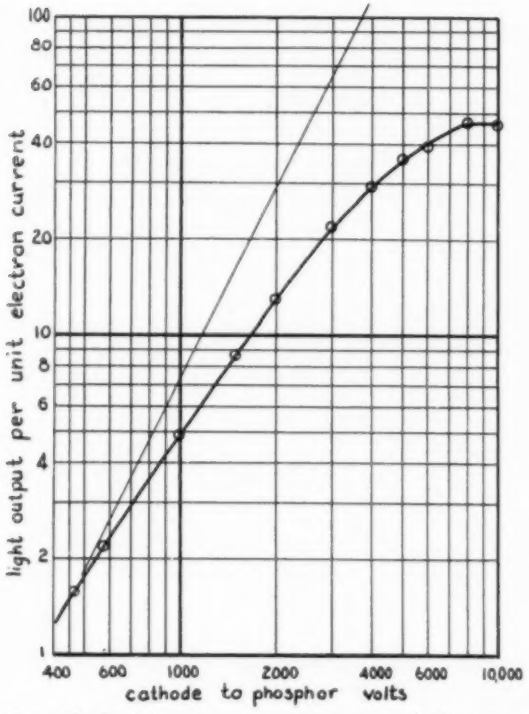

FIG. 10. Light output as a function of the electron energy for the zinc-sulfide: cadmium-sulfide sample. Straight line drawn with a slope of two.

by errors of measurement to be established without additional experiments.

Figure 11 shows the logarithm of the light output at constant current as a function of the logarithm of the electron energy in volts. The results obtained on both samples are shown, and, as is indicated, the slope observed on sample No. 1 was 2.8 while that for No. 2 was 2.9. These results were indeed surprising and can be taken as an indication that there must be some fundamental difference in the excitation process for zinc-sulfide as compared with willemite and calcium-tungstate. As long as the actual efficiency of the process in terms of watts input and light energy output is small, an increase in light output with the square of the voltage can be interpreted as showing that the number of excited centers produced per unit path length of the primary electron is independent of the electron energy, and therefore the light output is proportional to the penetration which, according to Leverenz,[4] is proportional to the square of the electron energy. A light output increasing more rapidly than the square of the voltage may perhaps be an indication that excited centers are produced more efficiently by a high energy electron for each unit of path length.

[4] H. W. Leverenz, J. Opt. Soc. Am. **27**, 25 (1937).

SUMMARY OF RESULTS

As a result of these studies, the following conclusions seem to be justified.

(1) For low current densities the light output per unit area is accurately proportional to the current density. This is the equivalent of stating that for low current densities the light per unit of current is *constant*.

(2) With increased current density the light per unit current at constant voltage falls by an amount which depends primarily on the current density. The function representing this relation is nearly independent of the bombarding voltage. The slight dependence seems to be in the direc-

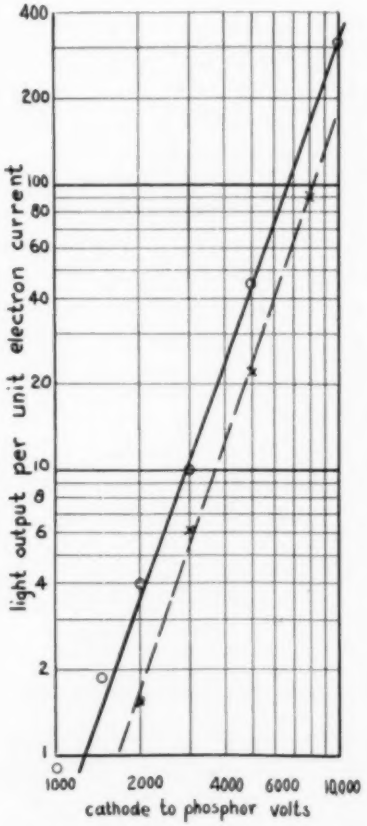

FIG. 11. Light output as a function of the electron energy for two samples of zinc-sulfide. Solid line for No. 1 and dashed line for No. 2. Straight lines drawn with slopes of 2.8 and 2.9. (The vertical separation is not significant.)

tion of a smaller saturation effect as the voltage is increased. A twenty percent loss in light per unit current was observed at the current densities given in Table II for the various phosphors.

(3) Except for the zinc-sulfide : cadmium-sulfide phosphor, the light per unit current at low densities, as a function of the electron energy V, was well represented by the empirical equation $(L/i)=A(V-V_0)^n$, where L/i is the light per unit current, A a constant, V_0 the so-called "dead voltage," generally zero, and n an exponent characteristic of the phosphor, tabulated in column three of Table II.

(4) Secondary emission properties of insulated phosphors operated in high vacuum determine the maximum useful operating voltage as discussed at length in the previous paper.[1] For conditions which are thought to correspond to the uncontaminated state of the materials, the upper limits of potential are given in column four of Table II.

TABLE II.

PHOSPHOR		MICROAMP. PER SQ. CM FOR 20% LOSS IN LIGHT	"n," POWER OF VOLTAGE FACTOR	MAXIMUM LIMITING VOLTAGE
CRYSTAL	ACTIVATOR			
$2(ZnO)SiO_2$	Mn	10	2	6500
ZnS; CdS	Ag	10	variable	>10,000
$CaWO_4$		30	2	5000
ZnS	Ag	200	2.8	>10,000

For the opportunity to carry through the experiments upon which this paper is based, I am indebted to both the Massachusetts Institute of Technology and to the Research Laboratory of the General Electric Company, and, in particular, to Drs. W. D. Coolidge, S. Dushman and A. W. Hull. I owe much for the able assistance rendered by the various service departments, and especially the glass-blowing department under the direction of Mr. William Ruggles. I am also indebted for the valuable technical help given by Messrs. A. B. White and James Hocker. The phosphors studied were furnished in suitable form for immediate use through the kind cooperation of the late John C. Warner of the RCA Manufacturing Company at Harrison.

X-Ray Study of Menthol

S. S. SIDHU
The Cooperative X-Ray Laboratory, University of Pittsburgh, Pittsburgh, Pennsylvania
(Received August 18, 1938)

The stable α-form of menthol crystallizes in the hexagonal form with an axial ratio of 1.635; $a_0=11.82\pm0.02$A; number of molecules per unit cell is eight and the calculated specific gravity is 0.885. The diffraction data presented here should be useful in the study of inversion phenomena in menthol by x-ray methods.

I. INTRODUCTION

MENTION is made by Wright[1] that the crystal form of menthol is hexagonal, but no references are found in the literature concerning its lattice parameters or diffraction data. Such data were obtained, though not reported, during an x-ray investigation of the form of acetylsalicylic acid in certain sugars.[2] They may, however, be of considerable interest both to crystallographer and to the physical chemist because of the wide use of menthol, and because menthol appears in four different forms, α, β, γ and δ, the last three bearing monotropic relations to the stable α-form. The application of x-ray analysis to the study of inversion phenomena of this kind promises a deeper insight into the mechanics of such phenomena and the results described here may be quite useful in such a study.

[1] F. E. Wright, "The Crystallization of Menthol," J. Am. Chem. Soc., **39**, 1515 (1917).
[2] S. S. Sidhu, J. App. Phys. **9**, 546 (1938).

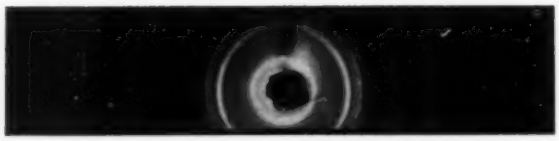

FIG. 1. Powder photograph of menthol.

II. EXPERIMENTAL PROCEDURE

The sample used in this study was of U.S. Pharmacopoeia grade. A portion of it, ground to a fine powder, was packed into a 19-gauge stainless steel hypodermic needle tubing with internal diameter of 0.7 millimeter, compressed with a plunger, and finally extruded as a compact cylinder of the same diameter. The steel tubing was then mounted in a cylindrical camera of 57.3 millimeters of effective diameter in such a way that only the extruded part of the specimen appeared in the x-ray beam.

Collodion, which was used in the preparation of the samples of other substances as a binding material, could not be used in this case as it dissolved menthol practically instantaneously. It was found, however, that no binding material was necessary. Finely powdered menthol under compression forms a compact mass well suited for specimens.

The x-ray powder photograms were made by the usual Debye-Scherrer-Hull method. Filtered characteristic copper and chromium x-rays were employed. The lattice constants were determined from several carefully calibrated patterns with sodium chloride as the reference standard.

TABLE I. *Interplanar spacings for menthol.*

OBSERVED SPACING A	ESTIMATED RELATIVE INTENSITIES*	CALCULATED SPACING A	CALCULATED INDICES
10.25	V.S.	10.22	(100)
5.92	M	5.90	(110)
5.11	V.S.	5.11	(200)
4.36	S	4.36	(104)
4.00	S	4.00	(203)
3.40	W	3.41	(300)
3.04	M	3.02	(124)
2.67	M	2.66	(107)
2.42	W	2.41	(008), 2.43(207)
2.18	W	2.18	(208)
1.98	M	1.98	(137) (209)
1.88	W	1.88	(129), 1.87(228), 1.90(236)
1.77	W	1.79	(237) (245)
1.64	W	1.64	(148), 1.63(250)
1.27	V.W.	1.28	(800)
1.17	V.W.	1.20	(180)
1.09	V.W.	1.08	(190)

* V = very; S = strong; M = medium; W = weak.

III. RESULTS

In Fig. 1 is shown the diffraction pattern of menthol. The interplanar spacings corresponding to the diffraction angles measured on the photogram were calculated, and indexed by the chart method of Hull and Davey.[3] The spacings were found to fit best on the chart for a closed packed hexagonal lattice with axial ratio $c_0/a_0 = 1.635$. Values of a_0 were calculated from all of the stronger lines for various values of the axial ratio in the neighborhood of 1.64. The a_0 values for $c_0/a_0 = 1.635$ were the most uniform, and the corresponding average value of a_0 is 11.82 ± 0.02A. The observed interplanar spacings and relative visual intensities obtained from the photogram together with calculated interplanar spacings and the indices of the diffraction planes are given in Table I.

Taking the value of specific gravity from International Critical Tables as 0.884, one obtains the number of molecules per unit cell:

$$n = PV/Mm = 7.99,$$

where P is the specific gravity, V is the volume, M is the molecular weight of menthol and m is one-sixteenth the mass of an oxygen atom.

SUMMARY

The stable α-form of menthol is shown to possess hexagonal symmetry with a unit cell containing 8 molecules;

$$a_0 = 11.82 \pm 0.02\text{A}, \quad c_0/a_0 = 1.635.$$

The theoretical value of specific gravity is 0.885, compared with 0.884 for the experimental value.

ACKNOWLEDGMENT

The writer wishes to express his appreciation to Westinghouse X-Ray Company for the gift of certain apparatus which made this work possible.

[3] A. W. Hull and W. P. Davey, Phys. Rev. **17**, 549 (1921).

Wratten Light Filters

for Photography, Photomicrography, Spectroscopy, Photometry, and Astronomy

WRATTEN LIGHT FILTERS are universally used in widely separated fields of scientific research.

The Wratten list includes filters for use with all types of color-sensitive films and plates. Over one hundred different filters are available.

Complete spectrophotometric data are given in the Eastman publication, *Wratten Light Filters*. The price of this 96-page booklet is 50 cents.

A price list of filters will be furnished free on request.

EASTMAN KODAK COMPANY

Research Laboratories **ROCHESTER, N. Y.**

Just Published

REICH'S

THEORY AND APPLICATIONS OF ELECTRON TUBES

By HERBERT J. REICH

Associate Professor of Electrical Engineering
University of Illinois

651 pages, 6 x 9, illustrated. $5.00

THE purpose of this important new book is to give the student a sufficiently thorough grounding in the fundamental principles of electron tubes and associated circuits to enable him to apply electron tubes to the solution of new problems. The book is exceptionally complete, including a wealth of material assembled and coordinated in a uniquely logical presentation. Unusually comprehensive treatments of the following topics are given: series expansion for plate current; graphical methods of analysis in the practical handling of vacuum tube problems; equivalent circuits; oscillators; theory of electrical conduction in gases; thyratrons; etc.

Send for a copy on approval

McGRAW-HILL BOOK COMPANY, INC.

330 West 42nd Street **New York, N. Y.**

Please mention this journal when writing to advertisers

Innovations in Instruments

Thermocouple Potentiometer

The Leeds & Northrup Company has recently announced a new Wenner-type potentiometer for the measurement of thermocouple and other voltages. This instrument has a higher accuracy than most other wide range potentiometers. It is useful for measurements in the range between 0 to 0.11111 volt. A booklet has been issued showing the basic principle of the Wenner-type potentiometer and showing its construction. A copy of this booklet may be obtained from the company at 4907 Stenton Avenue, Philadelphia, Pennsylvania.

Jumbo Six-in-One Meter

The Hickok Electrical Instrument Company of Cleveland, Ohio, announces a jumbo six-in-one meter. This meter has a scale which is more than 7 inches long. The following ranges are provided: a.c. and d.c. volts, 0/10/50/250/500/2500; d.c. microamperes, 0/500; d.c. milliamperes, 0/5/50/500; resistance to 10 megohms; decibels, −10 to +15.

Duplicates of 16-mm Kodachrome

Users of 16-mm motion picture cameras, either silent or sound, can now have their Kodachrome reels duplicated in full color, and in a quality comparing favorably with the originals, the Eastman Kodak Company announces from Rochester, New York.

Technical details of the duplicating process have been worked out at the Kodak laboratories in Rochester, and for the present all duplicates will be made there. Modestly priced, the duplicates will cost only a fraction more than an equivalent length of unexposed 16-mm Kodachrome film.

Advantages of duplicating Kodachrome movie reels in the full color of the original will be apparent in many fields. Heretofore, a Kodachrome movie has been limited to the color original and black-and-white duplicates. Now, a valuable original reel can be duplicated and stored, the full-color duplicate being used for everyday projection.

Any number of duplicates can be made from a chosen Kodachrome reel. This facility will be of particular value in the production of commercial and educational motion pictures, where a number of copies of one film must be available for widespread, simultaneous distribution. Use of duplicates makes this possible at small cost, and at the same time eliminates risk of damage to the original, which often could not be retaken.

Measurement of Electrical Impulses

The time during which an a.c. circuit is energized is shown directly on a meter scale in a new instrument known as the RayTimeR manufactured by the Raytheon Manufacturing Company. It may be calibrated in either cycles or seconds and covers with equal precision excitation periods from 1/120 of a second to 30 seconds, the accuracy being plus or minus 5 percent. It is a simple electronic device with no moving parts except the indicating pointer and no maintenance other than the occasional replacement of the vacuum tube. This is a standard type used in radio receiving sets and easily obtainable. The illustration shows a double unit having two RayTimeRs assembled in one container for convenience in measuring two different impulses simultaneously. Single unit RayTimeRs are also made. The RayTimeR has a wide field of usefulness including checking welder and x-ray exposure timing, measuring the closing and opening time of relays and contactors, measuring time periods and operating speeds of mechanisms having electrically actuated sequences.

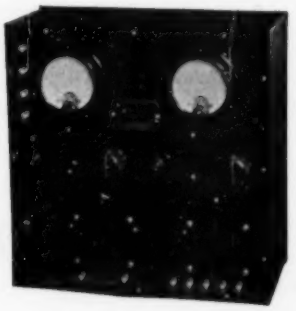

Spectrometer L234-HT

Universal

QUARTZ SPECTROMETER and MONOCHROMATOR

Calibrated from 1850 Å to 25000 Å

Versatility, accuracy, and high transmission are outstanding characteristics of this instrument, which serves equally well as spectrometer, spectrograph, or monochromator over the entire transmission range of quartz. Uses include irradiation, vitamin determination, spectrophotometry, identification of elements, calibration of light sources and of photocells, etc. A full line of accessories is available.

Many laboratories find that one of these instruments deals successfully with all of their spectroscopic problems

Write for Catalog L2 describing this and other spectroscopic equipment.

THE GAERTNER SCIENTIFIC CORPORATION

1212 Wrightwood Avenue, Chicago, Illinois, U.S.A.

A Reference Book for Science Libraries

HACKH—Chemical Dictionary (2d Edition)

Thoroughly Revised, Many New Diagrams, Tables, Etc.
100 Illus. 1020 pages. Washable Fabric Covers $12.00
By I. W. D. HACKH, A.M., F.A.I.C., F.R.S.A. (San Francisco)
With Collaboration of JULIUS GRANT, PH.D., F.I.C. (Lond.)

The new edition of this dictionary is a valuable inventory of present-day facts and terminology of chemistry and the allied sciences. Definitions have been prepared in the light of modern concepts of matter and energy. The pronunciation is given and many practical reference tables of unique value to educators have been prepared especially for this work.

A New Book for Rheologists

BLAIR—Introduction to Industrial Rheology

20 Illus. Glossary, Bibliography. Washable Fabric $2.25
By G. W. SCOTT BLAIR, PH.D., A.I.C., Univ. of Reading (Eng.)

This new book, the first of its kind, surveys and summarizes the vast number of important physical and chemical principles involved in the study of materials which "flow."

P. BLAKISTON'S SON & CO., Inc., Philadelphia, Pa.

RCA Television Transmitter

The RCA Manufacturing Company has recently announced that it will make available television transmitting equipment for sale to stations desiring to enter this field of service. This apparatus includes studio equipment, transmitters and television test equipment.

The RCA 1-kw television transmitter is the first medium-powered television transmitter to be made available by RCA. It is believed that the power of this transmitter is sufficient to enable experimental stations to render a satisfactory service over a reasonable area without too great an initial expense in starting television service. The transmitter conforms fully with the recently established RMA standards and is designed for d.c. transmission with negative modulation. The video response of the transmitter extends well beyond the range required for present-day, 441-line pictures with equal horizontal and vertical detail, thus providing for future requirements as to frequency response. The transmitter includes many circuits specially developed by RCA engineers to provide for good quality picture transmission.

The transmitter employs a long line controlled oscillator with an invar rod (which is unaffected by changes in temperature) to maintain the carrier frequency at a stable value. Because of the relatively high power output from the oscillator, only two buffer amplifier stages are necessary in order to drive the final power amplifier stage. Lines are employed instead of conventional tank circuits in the radio-frequency amplifiers. A special modulator circuit is employed with the plates of the modulators directly connected to the grids of the power amplifier tubes in order to provide for carrier control during picture transmission. Rectifier and filter circuits have been specially designed to avoid reaction and to provide an extremely low impedance at all video frequencies. The transmitter includes provision for inserting the d.c. component during the picture transmission which provides for variable carrier output in accordance with the light and shade tones of the picture.

The transmitter is arranged for disassembly if necessary in transporting it into buildings since in some cases the transmitter may be located near the roof to be adjacent to the antenna system.

RCA's program of television transmitter development has been carried forward for the last five years in order to

The RCA 1-kw television transmitter, the first medium powered television transmitter to be made available by RCA. It is believed that the power of this transmitter is sufficient to enable experimental stations to render a satisfactory service without too great an initial expense. The video response of the transmitter extends well beyond the range required for present-day 441-line pictures, thus providing for future requirements as to frequency response.

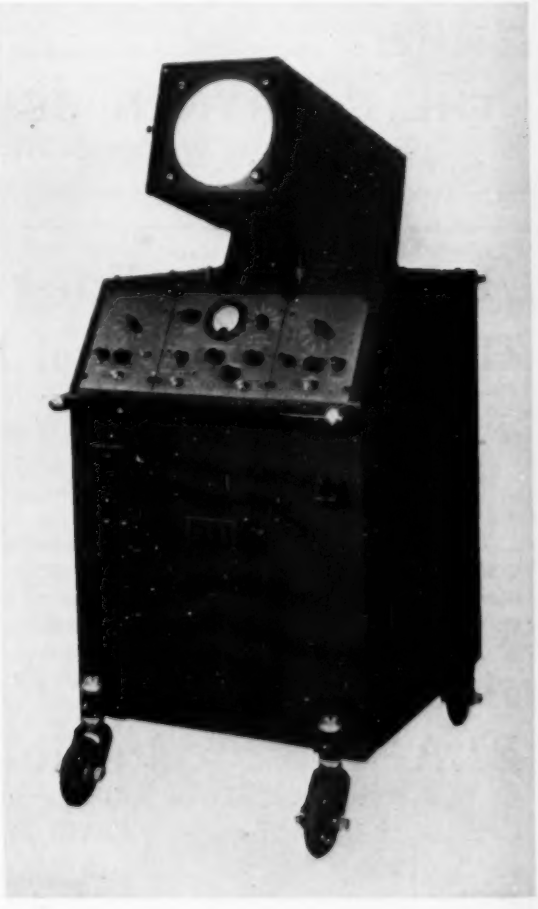

The RCA 136-B special cathode-ray oscillograph, provided with amplifiers extending over the entire video band of 30 cycles to two million cycles. Few, if any, cathode-ray oscillographs have been able to amplify over such a wide band. With it, it is possible to examine the wave form of minute impulses and to produce a large image for photographic purposes.

DUO-SEAL TWO STAGE VACUUM PUMP

This Vacuum Pump, although smaller than the 1405 which has made such phenomenal service and endurance records, has the same internal vane movements and other important mechanical features.

No. 1400

FIVE SPECIAL FEATURES

1. The proper pump speed is approximately 475 R.P.M., which produces a free air capacity of nineteen liters per minute.
2. Each pump is tested on our certified McLeod gauges to less than 0.1 micron (.0001 mm Hg) and many register less than .07 micron.
3. The mechanical action is unusually quiet for a vacuum pump.
4. The exhaust chamber is arranged for the collection of gases where this is desired.
5. The oil level is visible and the oil can be conveniently drained. Positive oil seal—no oil can back up.

No. 1400—Price complete as illustrated and described with pulley but without belt, motor or base.....Only $60.00

No. 1400B—DUO SEAL VACUUM PUMP, Motor driven. Mounted on a cast iron base with 1/6 H.P. 110 volt A.C. motor and V belt with belt tightening device.....Each, $85.00

WELCH

Catalog lists over 10,000 items for Science Laboratories.

WRITE FOR IT

Includes many new and interesting pieces.

W. M. WELCH SCIENTIFIC COMPANY

Established 1880

1518 Sedgwick Street Chicago, Illinois, U. S. A.

FINE WIRES

TAYLOR PROCESS

THE TAYLOR PROCESS is a method for making wires from substances which lack ductility. The elements or alloys, because the drawing is done in glass or quartz, are in a very pure state. Lengths of more than a few feet cannot be obtained. The wires may be had with or without the glass insulation. We make Taylor Process wire of Pt, Pd, Rh, Au, Ag, Cu, Fe, Co, Zn, Cd, Pb, Sb, Bi, Sn, Se, Te, Tl, Ga, and In, Constantan, Bi-Sn, Cd-Sb (used where large E.M.F. is desired) and many other alloys. Our wires are packed in containers holding one foot and, with few exceptions, the sizes are from one *mm* to one micron. We manufacture, too, fine wire by the Wollaston Method, by extrusion and by bare drawing.

WE ARE SPECIALISTS IN PLATINUM AND CAN SUPPLY IT IN WHATEVER FORM YOU REQUIRE

BAKER & CO., INC.

113 Astor Street, Newark, New Jersey

A NEW SHALLCROSS INSTRUMENT

The No. 835 Decade Potentiometer is a precision voltage divider and can be employed as an auxiliary to the laboratory precision potentiometer.

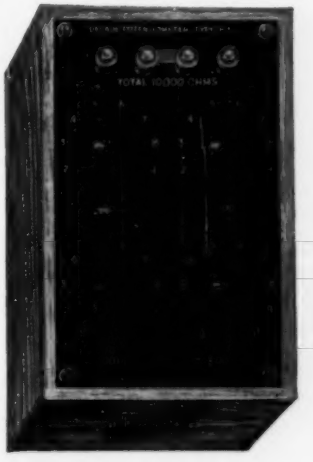

Provides Voltage Ratios of 0.0001 to 1.0

Schools and colleges will find it ideal for student instruction and industrial laboratories will also use it for calibration of galvanometers and voltmeters. Send for Bulletin 835–AH describing this new instrument.

Shallcross Mfg. Co., Collingdale, Penna.

New RCA square wave generator. Early in the program of RCA's television research, it was discovered that by transmitting a square wave through the apparatus instead of the conventional sine wave, engineers could observe the wave shape of the impulse at the output of the equipment and could tell the deficiencies in the equipment by the difference in the two forms. For example, if the amplifier being tested lacks high frequency response, the wave would not be reproduced with square corners but would be rounded. If phase shift occurs in the amplifier, other distortions would take place which would be readily recognized. The RCA instrument produces square waves having exceedingly straight sides, at several convenient frequencies over the video band. It also possesses the property of making square waves out of sine waves which are fed into it.

provide satisfactory apparatus at reasonable prices. It is felt that the 1-kw television transmitter will provide apparatus which may be used by television stations in the initial period of service and encourage operation on an economical basis.

New Slide Projector

A new projector for 2″×2″ and 3¼″×4″ color slides has been announced by Spencer Lens Company of Buffalo, New York. It is said to project a 2″×2″ slide with greater brilliance than does the usual 1000-watt auditorium lantern slide projector with a 3¼″×4″ slide. So much illumination is available that an iris diaphragm is sometimes needed to control the light on the screen when using thin slides or projecting to small gatherings. For dense slides or large magnifications the full intensity of the illumination can be utilized.

This projector will be offered three ways: for 2″×2″ slides only, for 3¼″×4″ slides only and for 2″×2″ and 3¼″×4″ slides. The only difference is in the optical units which can be exchanged in a few seconds.

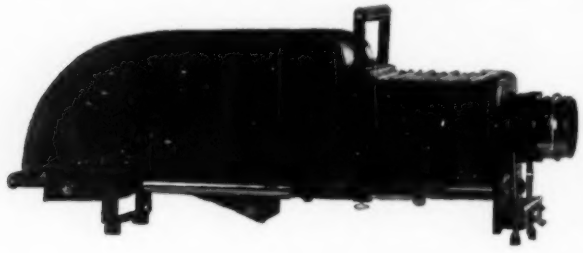

The new projector is equipped with a 750-watt lamp, cooling fan, three element condensing system with heat filter and projection lens. Lenses range from 6½″ (*f*: 2.75) to 10″ (*f*: 4.23). It weighs 21 pounds and measures 21 inches in length, 7½ inches in width and 8¾ inches in height.

Light Measuring Instrument

A sensitive light measuring instrument called the Photrix Universal Photometer, Model A, is announced by F. Loewenberg, 10 East 40 Street, New York City. This instrument consists of a wooden case with carrying strap containing a galvanometer and a photoelectric element. The latter is connected to the instrument by means of a flexible cable and rests in a compartment of the case when the instrument is not in use. The instrument is calibrated in footcandles, i.e., the illumination prevailing at a 1-foot distance from a light source which has a light intensity of 1 candlepower. The scale comprises four measuring ranges. Changing from one range to the other is accomplished by means of a 4-point switch operating a series of shunt resistances. In the lowest, i.e., most sensitive measuring range, the instrument has a full-scale deflection of 2.5 footcandles, each division thus representing 0.05 footcandles.

Television at World's Fair

Visitors to General Electric's building at the New York World's Fair next year will not only see, but will participate in television programs. In addition to its other attractions, which will include man-made bolts of lightning rated at ten million volts, and a swiftly paced presentation of current developments in science and research, the company will establish in its building a studio with a number of television receivers, cameras, and transmitting equipment, according to a joint announcement by Dr. W. R. G. Baker, managing engineer of the General Electric radio division, and Chester H. Lang, advertising manager. The receivers, of the latest design, will be available for the reception of all television programs broadcast by transmitters in the New York area during the fair. In between times, a permanent program director will initiate visitors into the experience of acting before the television camera, for the amusement of friends and others in the audience.

New Officers

The Board of Directors of the Roller-Smith Company announce the election of the following Officers of the Company whose appointment becomes effective at once: Mr. J. D. Wood, President, Mr. G. L. Crosby, Vice President and General Sales Manager, Mr. W. J. Schuhmann, Treasurer.

ULTRAVIOLET AND INFRARED OPTICS

The Harshaw Chemical Company is producing optical crystals of:

LITHIUM FLUORIDE
SYNTHETIC ROCK SALT
POTASSIUM BROMIDE

Prices and specifications will be furnished on request

The HARSHAW CHEMICAL CO.
SPECIAL PRODUCTS DIVISION
CLEVELAND, OHIO

PORTABLE POTENTIOMETERS

Rubicon portable potentiometers are available in a variety of single and double range models suitable for thermocouple, pH and instrument calibration work. Guaranteed accuracy to .1%.

These sturdy, self-contained instruments are built to give years of satisfactory service under all conditions encountered in the laboratory, shop or field. They are outstanding values in their class.

Ask for Bulletin 270.

RUBICON COMPANY
Electrical Instrument Makers
29 North Sixth Street Philadelphia, Pa.

PHOTRIX UNIVERSAL PHOTOMETER

UNEQUALLED SENSITIVITY
PERMANENT STABILITY

MODEL A:
4 measuring ranges
With single cell:
0-2.5, 0-10, 0-50, 0-250 ft. cdl.
With double cell:
0-0.25, 0-1, 0-5, 0-25 ft. cdl.

MODEL B:
3 measuring ranges
0-12, 0-60, 0-1000 ft. cdl.

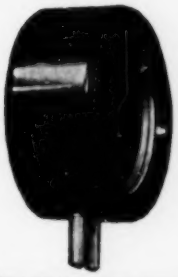

ALSO INDIVIDUAL PHOTOCELLS:

ELECTROCELL
SELF-GENERATING PHOTO-ELECTRIC ELEMENTS
(Barrier Layer Cells)
Great variety of sizes and shapes.
Round cells from ½" to 2½" diam.
Unmounted or mounted.

DR. F. LOEWENBERG
116 East 40th St. New York City

"POINTOLITE" *Lamps*

BRILLIANT—
CONCENTRATED—
STEADY—WHITE

When an evenly distributed field of illumination is needed . . . or a light source of constant intensity . . . or one that will remain in a fixed position . . . use Pointolite Lamps. Let us tell you more about these highly concentrated sources of white light and their various applications.

Bulletin 1530-R lists sizes from 30 to 1000 c.p. for direct current, and 150 c.p. for alternating current, as well as auxiliary control devices. . . . Write for a copy.

JAMES G. BIDDLE CO.
ELECTRICAL INSTRUMENTS
1211-13 ARCH STREET PHILADELPHIA, PA.

INDEX TO ADVERTISERS

Name	Page
BAKER & CO., INC. — Platinum crucibles, dishes, triangles, filter cones, anodes, cathodes, electrodes, platinum tipped crucible tongs, fine wires and bismuth foil.	ix
JAMES G. BIDDLE COMPANY — "Jagabi" Rheostats; Adam Hilger and Kipp & Zonen Optical Instruments; "Pointolite" Lamps; Electrical Testing and Speed-measuring Instruments.	xi
P. BLAKISTON'S SON & CO., INC.	vii
CAMBRIDGE UNIVERSITY PRESS	iv
CENTRAL SCIENTIFIC COMPANY — Manufacturers of Cenco Physical Apparatus and Instruments to meet all requirements of University, College and High School Physics Laboratories—Educational Distributors of Leeds and Northrup Electrical Measuring Instruments, Weston Electric Meters, Paulin Barometers, etc.	Cover 4
EASTMAN KODAK COMPANY — Purified Organic Chemicals for research purposes; Plates for Photography, Photomicrography, Spectroscopy, Photometry, Astronomy; Wratten Light Filters; Cameras and Films.	v
THE EPPLEY LABORATORY, INC. — Standards of e.m.f. (standard cells). Precision electrical instruments; potentiometers, bridges, temperature bridges, volt boxes. Thermopiles and pyrheliometers.	ii
GAERTNER SCIENTIFIC CORP. — Spectroscopes, Spectrometers, Spectrographs, Spectrophotometers, Heliostats, Measuring Microscopes, Comparators, Cathetometers, Reading Telescopes, Interferometers, Chronographs, Dividing Machines, etc.	vii
GENERAL RADIO COMPANY — Pioneer designers and manufacturers of apparatus for the general applications of electric communications technique.	Cover 3
HARSHAW CHEMICAL CO. — Optical Lithium Fluoride grown in single crystal to predetermined size. Industrial Chemicals.	xi
INTERNATIONAL RESISTANCE COMPANY — Manufacturers of metallized and wirewound fixed and variable Resistors including high voltage and high frequency types.	iii
LEEDS & NORTHRUP COMPANY — Manufacturers of Galvanometers, Resistors, Bridges, Condensers, Inductances, Potentiometers, Testing Sets; Temperature Measuring, Recording and Controlling Apparatus; Instruments for Measuring and Controlling Conductivity of Electrolytes and Hydrogen Ion Concentrations.	i
LOEWENBERG, DR. F. — Light measuring instruments, single and double cell types. Self-generating photo-electric elements, wide variety of electrocells.	xi
MACMILLAN COMPANY	iv
MCGRAW-HILL BOOK CO., INC.	v
POLARIZING INSTRUMENT COMPANY — Polaroid Desk Lamp. Polarizing Microscope Attachment, Polarizing Projection Equipment. Polaroid Film.	ii
RUBICON COMPANY — Galvanometers, electrometers, potentiometers, Wheatstone and Kelvin bridges, resistance boxes, hydrogen ion and conductivity apparatus.	xi
SHALLCROSS MFG. COMPANY — Taylor High Voltage Resistors for Voltmeter Multipliers. High resistance and high Wattage Decade Boxes and other laboratory instruments. Super Akra Ohm wire wound, non-inductive and accurate resistors. Special resistors for special purposes.	ix

INDEX—*Continued*

Name	Page
W. M. WELCH SCIENTIFIC CO. — Scientific instruments—laboratory apparatus. Catalog lists 10,000 items.	ix

PRODUCTS ADVERTISED

	Page
Daylight Lamp, High Light Output	Cover 4
Electrocells	xi
Fine Wires, Taylor Process	ix
Insulation-Resistance Test Set	i
Monochromator	vii
Photometer, Photrix Universal	xi
Pointolite Lamps	xi
Polaroid Desk Lamp	ii
Potentiometer, Decade Type	ix
Potentiometers, Portable	xi
Quartz Spectrometer	vii
Resistors for High Voltage	iii
Student Cell, Cadmium	ii
Synthetic Optical Crystals	xi
Vacuum Pump, Duo-Seal Two Stage	ix
Wave Analyzer, Heterodyne Type	Cover 3
Wratten Light Filters	v

Books and Publications

Chemical Dictionary—Hackh	vii
Electron Tubes, Theory and Applications of Reich	v
Industrial Rheology, Introduction to—Blair	vii
Mechanics, Problems in—Karelitz, Ormondroyd and Garrelts	iv
Mechanics of Solids, Contributions to the	iv

Back Issues

of these journals are available.

	Single Copy
Journal of Applied Physics	**$ .70**
Review of Scientific Instruments	**.50**
Physical Review (from July 1929)	**.75**
Same (before July 1929)	**1.50**
Reviews of Modern Physics	**1.20**
Same April 1936	**1.75**
Journal of Chemical Physics	**1.00**
Journal of the Optical Society	**.60**
Journal of the Acoustical Society	**1.80**
American Physics Teacher (from 1937)	**1.00**
Same (before 1937)	**1.50**

Special prices for complete back volumes and complete sets.

Orders may be sent to

American Institute of Physics

175 Fifth Avenue

New York, N. Y.